

PRIMORDIAL BLACK HOLES IN NON-LINEAR PERTURBATION THEORY

JUAN CARLOS HIDALGO CUELLAR

ASTRONOMY UNIT

SCHOOL OF MATHEMATICAL SCIENCES

QUEEN MARY COLLEGE

UNIVERSITY OF LONDON

UNITED KINGDOM

A DISSERTATION SUBMITTED IN CANDIDATURE FOR THE DEGREE OF DOCTOR OF PHILOSOPHY
IN THE UNIVERSITY OF LONDON

TUESDAY 14TH JULY 2009

Abstract

The thesis begins with a study of the origin of non-linear cosmological fluctuations. In particular, a class of models of multiple field inflation are considered, with specific reference to those cases in which the non-Gaussian correlation functions are large. The analysis shows that perturbations from an almost massless auxiliary field generically produce large values of the non-linear parameter f_{NL} .

Next, the effects of including non-Gaussian correlation functions in the statistics of cosmological structure are explored. For this purpose, a non-Gaussian probability distribution function (PDF) for the curvature perturbation \mathcal{R} is required. Such a PDF is derived from first principles in the context of quantum field theory, with n -point correlation functions as the only input. Under reasonable power-spectrum conditions, an explicit expression for the PDF is presented, with corrections to the Gaussian distribution from the three-point correlation function $\langle \mathcal{R}\mathcal{R}\mathcal{R} \rangle$.

The method developed for the derivation of the non-Gaussian PDF is then used to explore two important problems in the physics of primordial black holes (PBHs). First, the non-Gaussian probability is used to compute corrections to the number of PBHs generated from the primordial curvature fluctuations. Particular characteristics of such corrections are explored for a variety of inflationary models. The non-Gaussian corrections explored consist exclusively of non-vanishing three-point correlation functions.

The second application concerns new cosmological observables. The formation of PBHs is known to depend on two main physical characteristics: the strength of the gravitational field produced by the initial curvature inhomogeneity and the pressure gradient at the edge of the curvature configuration. The latter has so far been ignored in the estimation of the probability of PBH formation. We account for this by using two parameters to describe the profile: The amplitude of the inhomogeneity and its second radial derivative, both evaluated at the centre of the configuration. The method developed to derive the non-Gaussian PDF is modified to find the joint probability of these two parameters. We discuss the implications of the derived probability for the fraction of mass in the universe in the form of PBHs.

I hereby certify that this thesis, which is approximately 45,000 words in length, has been written by me, that it is the record of the work carried out by me at the Astronomy Unit, Queen Mary, University of London, and that it has not been submitted in any previous application for a higher degree.

Some of the work contained in Chapter 2 was carried out in collaboration with Dr David Seery and Dr Filippo Vernizzi and is unpublished. Chapter 3 presents a project developed in collaboration with Dr David Seery, published as an article in the Journal of Cosmology and Astroparticle Physics [Seery & Hidalgo, 2006]. The work in Chapter 4 was done by me alone and it is described in an article available on-line [Hidalgo, 2007]. The material in Chapter 5 was done in collaboration with Dr Alexander Polnarev and is published in Physical Review D [Hidalgo & Polnarev, 2009]. I made a major contribution to all the original research presented in this thesis.

Juan Carlos Hidalgo

Queen Mary, University of London

London, United Kingdom

April, 2009

Acknowledgements

I would first like to thank my parents Jesús and Lídice, and my sister Aura for their continual support, encouragement and inspiration throughout my studies.

I am grateful to my supervisor Prof Bernard Carr for his invaluable support and guidance during my PhD.

I am also very grateful to my collaborators, Dr David Seery and Dr Alexander Polnarev, for their assistance through several challenges. Special thanks also to Dr Karim Malik for his encouragement and sense of humour. (Apologies for the ‘Oscar winning’ speech).

I would like to thank all those who have helped me from the School of Mathematical Sciences and in particular, Mr William White and Prof Malcolm MacCallum.

Dr Sergio Mendoza in the Instituto de Astronomía, UNAM, has always been supportive and attentive to my academic development. I am grateful to him for many years of inspiration.

I would like to express my gratitude to my entire family and especially my grandfather Alfonso Cuéllar, my cousin Lídice Cuellar Quintero and my aunt Carmen Watson for their resolute encouragement.

Finally, I would like to thank Christine Rooks for being brave enough to join me on this journey. All friends who have stood by me: Rodrigo, Adrián, Julián, Rogelio, Gustavo and Mauricio, also to my flatmates Noèlia and Periklis. Last but not least, I would like to include Julio, Gian Paolo, Guillermo, Cesar, Rubén, Mariana, Paola and Pedro. To all of them a ‘big’ thanks.

This work was fully funded by the Mexican council for Science and Technology (CONACYT scholarship No. 179026), with complementary support from the School of Mathematical Sciences at Queen Mary, University of London. I gratefully acknowledge this support.

Publications resulting from the work in this thesis

1. D. Seery and J. C. Hidalgo,
“Non-Gaussian corrections to the probability distribution of the curvature perturbation from inflation,”
JCAP **0607** (2006) 008
[arXiv:astro-ph/0604579].
2. J. C. Hidalgo,
“The effect of non-Gaussian curvature perturbations on the formation of primordial black holes,”
arXiv:0708.3875 [astro-ph].
3. J. C. Hidalgo and A. G. Polnarev,
“Probability of primordial black hole formation and its dependence on the radial profile of initial configurations,”
Phys. Rev. D **79** (2009) 044006
arXiv:0806.2752 [astro-ph].

TO MY PARENTS,
AND TO THE LOVING MEMORY OF MY GRANDMOTHER JUANA.

Contents

Acknowledgements	4
1 Introduction	12
1.1 Cosmological observations and the Big Bang	13
1.1.1 Basic dynamics of the universe	13
1.1.2 The Big Bang model	14
1.2 Cosmological inflation	16
1.2.1 Motivation and achievements	16
1.2.2 An embarrassment of richness	19
1.3 Non-Gaussianity	19
1.4 Primordial black holes	22
1.4.1 Standard picture	22
1.4.2 Shortcomings	25
1.4.3 Alternative mechanisms of PBH formation	27
1.5 Thesis outline	29
2 Non-Gaussian curvature perturbations	31
2.1 Outline	31
2.2 Linear perturbations	32
2.2.1 Metric perturbations	33
2.2.2 Gauge freedom	35
2.2.3 Perturbations of the matter sector	37
2.2.4 Physical quantities and scales	38
2.2.5 Particular gauges	40

2.3	Evolution of perturbations and conserved quantities	43
2.3.1	Background equations	44
2.3.2	Dynamics of perturbations	47
2.4	Inflation	52
2.4.1	Inflationary field power spectrum	54
2.4.2	Observables	57
2.4.3	The δN formalism	59
2.5	Non-Gaussianity from isocurvature fields	61
2.5.1	Two-field inflation	63
2.5.2	Non-Gaussianity and nonlinear evolution	65
2.5.3	Field bispectrum	67
2.5.4	The curvaton	72
2.6	Model discrimination through observations	75
3	Statistics of non-Gaussian fluctuations	78
3.1	Introduction	78
3.2	The probability measure on the ensemble of \mathcal{R}	85
3.2.1	The generating functional of correlation functions	86
3.2.2	The probability density on the ensemble	88
3.2.3	The smoothed curvature perturbation	92
3.3	Harmonic decomposition of the curvature perturbation	94
3.3.1	Harmonic expansion of \bar{R}	94
3.3.2	The path integral measure	97
3.3.3	The total fluctuation ϱ and the spectrum $\mathcal{P}_\varrho(k)$	98
3.4	The probability density function for ϱ	99
3.4.1	The Gaussian case	100
3.4.2	The non-Gaussian case	102
3.4.3	When is perturbation theory valid?	107
3.5	The probability density function for $\mathcal{P}_\varrho(k)$	108
3.6	Summary of results	111

4	Probability of primordial black hole formation	113
4.1	Introduction	113
4.2	The non-Gaussian PDF	115
4.3	Non-Gaussian modifications to the probability of PBH formation	120
4.4	Constraints on non-Gaussian perturbations of PBH range	123
4.5	Closing remarks	126
5	Curvature profiles of large overdensities	128
5.1	Introduction	128
5.2	Probability of profile parameters of cosmological perturbations	129
5.3	The link between perturbation parameters and the curvature profiles used in numerical calculations	136
5.3.1	Initial conditions	136
5.3.2	Physical criteria for the identification of parameters	137
5.3.3	Parameter values leading to PBH formation	141
5.4	Two-parametric probability of PBH formation	143
5.5	Discussion	145
6	Conclusions and future work	147
6.1	Summary of results	148
6.2	Future research	151

List of Figures

4.1	The fractional departure from the Gaussian PDF is plotted for two types of non-Gaussian distributions \mathbb{P}_{NG} , as defined in Eq. (4.12). For the potential in Eq. (4.17), $f_{\text{NL}} > 0$ and the departure is plotted with a solid line. For the potential in Eq. (4.18), $f_{\text{NL}} < 0$ and the departure is shown by a dashed line.	123
4.2	The constraints on β_{PBH} in Table I are plotted together with the smallest value considered for each mass.	126
4.3	A subset of the constraints on $\Sigma_{\mathcal{R}}$ from overproduction of PBHs is plotted for a Gaussian and non-Gaussian correspondence between β and $\Sigma_{\mathcal{R}}$, Eqs. (4.24) and (4.27) respectively. The dashed line assumes a constant $f_{\text{NL}} = 51$ and the dotted line a value $f_{\text{NL}} = -1/\Sigma_{\mathcal{R}}^2 \approx -66$. The solid line represents the constraints for in the Gaussian case	127
5.1	(a) The top plot shows the parameter values for initial configurations which collapse to form black holes according to Polnarev & Musco [2007]. (b) In the $[\mathcal{R}(0), \mathcal{R}''(0)]$ plane three regions of integration are considered to compute the probability of PBH formation. Area I is the region enclosed by the solid curves and corresponds to the area denoted by BH in Fig. 1a. Area II is the region to the right of the grey dotted line, representing the area of integration considered in previous studies where only the amplitude is taken into account. Area III is the region above the solid line and between the dashed lines. This contains those configurations which have a smooth profile in the centre and present the amplitudes $\mathcal{R}(0)$ that are found to form PBHs in [Polnarev & Musco, 2007]. The complete description of the physical characteristics of profiles with values in this region is given in Section 5.3.	138

-
- 5.2 The curvature profile for three different families of configurations with common central amplitude $\mathcal{R}(0) = 1$. The configurations shown by the dashed lines have values of $\mathcal{R}''(0)$ larger in absolute magnitude than the parabolic one shown in black. The configurations shown by the dotted lines have values of $\mathcal{R}''(0)$ smaller than the parabolic one. All profiles satisfy conditions (5.37) and (5.39). 142
- 5.3 The logarithmic probability of PBHs for two tilts in the power spectrum ($n_s = 1.23$ on the top figure, $n_s = 1.47$ on the bottom figure), integrated for the three different regions sketched in Fig. 5.1. The integrals over Areas I and II correspond to the dashed and solid lines, respectively. The probability integrated over Area III is represented by the dotted lines in both figures. 144
- 5.4 The grey dashed line shows the ratio of the total probability β_{PBH} which results from integrating over Area I on the $[\mathcal{R}(0), \mathcal{R}''(0)]$ parameter space of Fig. 1b to the probability which results from the integrating over Area II. The black line is the ratio of the probability integrated over Area III to the probability integrated over Area II. 145

Chapter 1

Introduction

Cosmology is at the forefront of modern physics. Over the last two decades, it has moved from a predominantly theoretical discipline to a sound observational science. Today's experiments are capable of observing tiny fluctuations of a faint signal coming from the Big Bang, emitted about thirteen billion years ago. The observations of primordial inhomogeneities are a unique probe of the physical conditions in the early universe. The inflationary paradigm indicates that the inhomogeneities are the result of quantum fluctuations of the matter dominating the universe in its first moments. In this widely accepted picture the observed inhomogeneities fix the normalisation of an inflationary potential setting the energy scales for inflation to about 10^{16}GeV , the GUT scale. This is 10^6 times more than the energy of particles released by supernovae. A similar ratio arises for the energy scales to be tested by the large hadron collider (LHC). These numbers show how the geometry of the universe and its inhomogeneities constitute a unique probe of high energy physics.

Several observational parameters have been defined in cosmology in order to determine the physical conditions of the early universe. The density and nature of matter observed today, the distribution and mean amplitude of initial inhomogeneities, and most recently the non-Gaussianity of primordial fluctuations are among these parameters. The latter has received considerable attention from cosmologists but the analysis of the latest observations has not yet provided conclusive evidence for departures from Gaussian statistics. A great deal of effort is under way to reduce the detection thresholds of the non-Gaussian parameters. Even if non-Gaussianity remains undetected by future experiments, we can still constrain

theoretical models that are known to develop large non-Gaussianity.

The main objective of the present work is to study how non-Gaussian statistics, inherited from inflation, can modify the probability of primordial black hole formation. The class of models of inflation that motivate this study and the development of statistical tools to address this question are complementary projects, and both are included in the present thesis. In the rest of this chapter we provide a brief description of the state of the art in cosmology, with special attention to the open questions that motivate this thesis.

1.1 Cosmological observations and the Big Bang

It has been more than four decades since Penzias & Wilson [1965] managed to identify, for the first time, the cosmic microwave background (CMB) radiation. This was detected, almost by accident, while calibrating a large reflector at the Bell Laboratories. The uniform and isotropic radiation observed corresponds to the most perfect black-body radiation ever measured, peaking at $\lambda = 1.9$ mm, with a red-shifted temperature of $T_{\text{CMB}} = 2.725$ Kelvin [Jaffe et al., 2001].

The detection of the CMB gave decisive support to the Big Bang theory. The standard Big Bang model considers a universe dominated by uniform and isotropic matter. Its dynamics is governed by gravity, with equations prescribed by the theory of general relativity. (Gravity is the only long-range force to be considered since the universe is electrically neutral.) The conditions of isotropy and homogeneity, in this context, imply that the spacetime admitting these properties is necessarily a Friedmann-Robertson-Walker universe (FRW) (see e.g. Wald [1984]).

1.1.1 Basic dynamics of the universe

We write the FRW metric in the form of the line-element in spherical coordinates.

$$ds^2 = -dt^2 + \frac{a(t)^2}{1 - \kappa r^2} (dr^2 + r^2 [d\theta^2 + \sin^2 \theta d\phi^2]), \quad (1.1)$$

where t and κ are the coordinate time and the uniform curvature of the spatial sections respectively. The usual spherical coordinates in the spatial hypersurfaces are r, θ and ϕ .

Finally, $a(t)$ is the scale factor, with present value $a_0 = 1$. The Einstein equations of general relativity provide the dynamical relation between the matter and spacetime variables. Assuming homogeneous and isotropic matter, with density ρ and isotropic pressure p , the Einstein equations show that the evolution of the scale factor is given by

$$H^2 \equiv \left(\frac{\dot{a}}{a}\right)^2 = \frac{1}{3}\rho - \frac{\kappa}{a^2}, \quad (1.2)$$

where an over-dot is the coordinate time derivative and H is the Hubble parameter, a measure of the expansion rate. Its present value is $H_0 = 100h \text{ kms}^{-1}\text{Mpc}^{-1}$, with $h = 0.71 \pm 0.08$ [Freedman et al., 2001]. This last equation is known as the Friedmann equation. We use throughout units where $c = \hbar = 8\pi G = 1$.

The matter contents of our universe has several components and the fraction of each component relative to the critical density is called the density parameter $\Omega_i = \rho^{(i)}/3H^2$. If we denote the sum of all matter components as Ω_T , the Friedmann equation can be written simply as

$$\Omega_\kappa(t) + \Omega_T(t) = 1, \quad (1.3)$$

where $\Omega_\kappa = \kappa/(aH)^2$ is the curvature density parameter. When the matter density is equal to the critical density $3H^2$, then $\Omega_T = 1$ and the universe is flat at all times. Observations tell us that we live in a nearly flat universe ($|\Omega_\kappa| < 10^{-2}$), so we assume $\Omega_\kappa = 0$ hereafter. The energy density is dominated by two main components, a cold dark matter component ($\Omega_{\text{CDM}} \simeq 0.23$) and another component referred as dark energy ($\Omega_\Lambda \simeq 0.72$). The nature of both these components is a crucial question in cosmology and has motivated a lot of research. We will return to this point and to an analysis of the Einstein equations later in this work.

1.1.2 The Big Bang model

The hot Big Bang model is now accepted as the standard model describing the evolution of the universe. This model characterises, with impressive accuracy, the evolution after the first second. At this time, the universe was a primordial fireball with high enough temperature and pressure to dissociate any nuclei. The formation of nuclei was only possible once the

cosmic expansion reduced the average kinetic energy sufficiently. The formation of the first elements took place at temperatures of around $T \simeq 0.1$ MeV, when the universe was around 1 s old. This process involves conditions that cannot be replicated elsewhere (cf. stellar nucleosynthesis). Within the current observational limitations, the Big Bang prediction for the present abundance of light elements is confirmed remarkably by the present measurements.

Big Bang nucleosynthesis halted once matter had cooled down enough, due to the cosmic expansion. The electrical neutrality of the matter was reached at a more recent event: the so called ‘recombination’ process refers to the time when each electron was captured by a nucleus forming the first neutral atoms. Subsequently, at a temperature of around $T \approx 0.1$ eV ($\approx 10^3$ Kelvin), CMB photons decoupled from ordinary matter and have since travelled freely. These same photons reach us in the form of microwave radiation. The surface of emission of these primordial photons is called the last-scattering surface. CMB observations constitute irrefutable proof that the universe was homogeneous at early epochs and dominated by radiation when $T > 10^3$ Kelvin.

The current temperature of the CMB radiation ($T_{\text{CMB}} = 2.725$ Kelvin) is measured with such precision because its fluctuations are tiny. The first observational evidence for the CMB anisotropies came from the COBE satellite [Smoot, 1992; Bennett et al., 1996]. The results of this experiment showed that the temperature fluctuations have a mean amplitude $\delta T/T \sim 10^{-5}$. The amplitude of such deviations was predicted by Peebles & Yu [1970] and Zeldovich [1972] in terms of the matter density perturbation $\delta\rho/\rho \sim 10^{-5}$. These inhomogeneities are related through the Sachs-Wolfe formula [Sachs & Wolfe, 1967]. This prescribes that for inhomogeneities of comoving size λ ,

$$\frac{\delta T}{T} \approx -\frac{1}{2} (a_{\text{LS}} H_{\text{LS}} \lambda)^2 \delta_\rho \quad (1.4)$$

where we have defined $\delta_\rho \equiv \delta\rho/\rho$, and where a subscript LS indicates an evaluation at the last-scattering surface.

More recent experiments, such as BOOMERANG [Netterfield et al., 2002], MAXIMA [Hanany et al., 2000] and WMAP [Hinshaw et al., 2007; Komatsu et al., 2008], managed to measure the acoustic oscillations in the radiation plasma due to the small-scale density variations in the early universe. Measurements of acoustic oscillations in the CMB demon-

strated the flatness of the universe to 1% precision (i.e. $|\Omega_\kappa| < 10^{-2}$). They were also used to rule out cosmic strings as a significant contributor to structure formation and suggested ‘cosmological inflation’ as the theory of structure formation [Jaffe et al., 2001].

1.2 Cosmological inflation

1.2.1 Motivation and achievements

The observations mentioned above provided strong arguments in favor of the Big Bang model but also showed the necessity of a larger theoretical framework due to the following problems:

1. **Horizon problem.** In the Big Bang model, the distance light could have traveled up to the time of last-scattering d_{LS} is of order 180 Mpc. This is called the particle horizon and determines the radius of causally connected regions at that time. The particle horizon today is much larger, with radius $d_0 \sim 6000$ Mpc. Therefore, the measurements of CMB radiation at angular scales larger than one degree include regions that were causally disconnected at the time of the photon decoupling. The temperature at such scales is observed to be uniform up to one part in 10^5 . This means that causally disjoint patches of the universe in the past had the same thermal history. In the context of the hot Big Bang model there is no plausible explanation for this fact.
2. **Flatness problem.** The density of matter components in the universe is diluted with time due to the cosmic expansion. Conversely, if there was an initial curvature component κ , then this would rapidly dominate the matter contents. This is easily derived from Eq. (1.3), which can be written in the form

$$\Omega_{\text{T}} - 1 = \frac{\kappa}{a^2 H^2} \equiv \Omega_\kappa. \quad (1.5)$$

The product aH decreases with time in a radiation or matter dominated universe. If the universe is initially flat, then it remains flat for subsequent times, but observations show that $|\Omega_\kappa| \lesssim 10^{-2}$ today, and the Friedmann evolution demands an even smaller curvature in the past. For example, at nucleosynthesis, when the universe was around

1 s old, we require $|\Omega_\kappa| \lesssim 10^{-16}$ to be consistent with the present value. Such a small value requires an extreme fine-tuning of initial conditions Ω_T , for which a causal explanation would be desirable.

A solution to these problems is provided by the inflationary paradigm, which we will study in detail in Chapter 2. The main feature of this theory is that it changes the behaviour of the comoving cosmological horizon by considering an accelerated expansion of the universe at early times, i.e., at times prior to nucleosynthesis. In terms of the scale factor, this condition demands

$$\ddot{a} > 0 \quad \Rightarrow \quad \frac{d}{dt} \left[\frac{1}{aH} \right] < 0. \quad (1.6)$$

The shrinking of the cosmological horizon represents a ‘reverse’ evolution of spacetime which avoids the fine-tuning of initial conditions demanding homogeneity and flatness. If we consider an inhomogeneous patch of the universe when inflation starts, at an initial time t_i , the cosmic accelerated expansion brings all initial inhomogeneities out of the comoving cosmological horizon. If inflation lasts long enough, then after the inflationary period we are left with a much larger region composed of small patches of size of the cosmological horizon which are out of causal contact but with common physical characteristics. The number of e-folds of expansion required for the listed problems to be solved is

$$N = \ln \left(\frac{a(t_{\text{end}})}{a(t_i)} \right) \gtrsim 60. \quad (1.7)$$

This number is required to guarantee that the comoving scale of the current size of the universe exited the horizon at the beginning of inflation [Liddle & Lyth, 2000]. This indicates that inflation must last longer than 60 e-folds. Arguably, it was Guth [1981] who first brought these ideas together.

The theory of inflation has received important contributions from particle physics. In particular, the theory of particle creation from vacuum fluctuations [Hawking, 1982; Starobinsky, 1982] gave inflation its strongest argument: the vacuum fluctuations generated during inflation are redshifted to superhorizon scales by the action of the inflationary mechanism. At the end of inflation, the thermalisation of the inflaton false vacuum reheats the universe

and the standard hot Big Bang phase begins. In this transition, the vacuum fluctuations of the inflaton field are transformed into matter density perturbations with a prescribed amplitude. From this transition onwards, the modes re-enter the expanding comoving horizon. Thus, initial conditions of cosmological perturbations in the hot Big Bang are set by inflation. The observed mean amplitude of the temperature inhomogeneities [Smoot, 1992; Netterfield et al., 2002; Spergel et al., 2007] sets the energy scale at which the initial vacuum fluctuations were generated by tracing back the evolution of fluctuations described above. This simple explanation of the origin of the temperature fluctuations constitutes a decisive argument in favour of the inflationary scenario. It represents the greatest advantage of inflation over many other alternative extensions of the standard Big Bang scenario.

In summary, the requirements for a period of inflation are: (1) a mechanism to generate an accelerated expansion maintained for at least 60 e-folds of expansion; (2) a way of accounting for the transition to the subsequent FRW stages of evolution, thereby providing the suitable initial conditions for the Big Bang scenario; (3) quantum fluctuations of the inflationary field, generated at observable scales such that the matter density fluctuations of size λ meet the relation $(aH\lambda)\delta_\rho \simeq 10^{-5}$ and this product is almost invariant over the observed scales.

In practice, measurements of CMB anisotropies, combined with measurements of background parameters inferred from supernovae surveys [Astier et al., 2006; Riess et al., 2007], indicate that the root-mean-square (RMS) amplitude of temperature fluctuations is

$$\left(\frac{\delta T}{T}\right)_{\text{RMS}} \approx 2 \times 10^{-5}, \quad (1.8)$$

at the pivot scale with comoving size $\lambda_{\text{CMB}} = 150 \text{ Mpc}$ customarily used in CMB studies. Observations also indicate that this value does not vary significantly over the range of observed scales. In other words the mean amplitude is almost scale-invariant for angular scales larger than one degree. In Chapter 2 we show how this relates to the curvature perturbation ζ and discuss its basic properties. In particular, we will show that, in the cases which concern us, ζ is constant for scales larger than the particle horizon.

1.2.2 An embarrassment of richness

The required amount of inflation and the corresponding amplitude of the curvature perturbations determine the kind of matter and energy scale necessary to satisfy the conditions for accelerated expansion. These prerequisites have been met by several models of inflation which may or may not be motivated by more fundamental theories of physics. One of the main problems faced by the inflationary paradigm is that of richness. There are many models that meet the dynamical requirements. Most of them invoke one or more scalar fields $\{\phi_i\}$ with dynamics governed by a potential $V(\phi_i)$. There are a plethora of models, each of which corresponds to particular realisation of this potential, which satisfy the observational constraints up to the level of the observed inhomogeneities. Consequently, many of the models cannot be distinguished at the level of linear perturbation theory. This demands the formulation and experimental determination of new parameters that provide complementary information about the early universe. An important constraint on the inflationary models can be obtained by considering the statistical deviations from a Gaussian field of fluctuations. This idea has opened a new window in the study of the early universe, namely the nonlinear extension of perturbation theory and its non-Gaussian statistics.

1.3 Non-Gaussianity

By non-Gaussianity in cosmology we refer to the small deviations of observed fluctuations from the random field of linear, Gaussian, curvature perturbations $\zeta_1(t, \mathbf{x})$. $\zeta(t, \mathbf{x})$ is the curvature perturbation in the comoving gauge, that is, as measured by an observer which sees no net-momentum flux. The mathematical expression for $\zeta(t, \mathbf{x})$ in terms of the matter density perturbation is provided in Chapter 2.

Among the parameters of nonlinearity, the nonlinear coupling f_{NL} is the most useful observable for describing non-Gaussianity. Its definition comes from the second order expansion of curvature perturbations in real space, which can be written as

$$\zeta(\mathbf{x}) = \zeta_1 + \frac{1}{2}\zeta_2, \quad (1.9)$$

where ζ_1 refers to the Gaussian perturbation with variance $\Sigma_\zeta^2(x) = \zeta_{\text{RMS}}^2(x)$ and ζ_2 is the

second order perturbation parametrised by the nonlinear parameter f_{NL} in the following way

$$\zeta_2(\mathbf{x}) = -\frac{6}{5}f_{\text{NL}}(\zeta_1(\mathbf{x})^2 - \zeta_{\text{RMS}}(x)^2). \quad (1.10)$$

Note that the perturbative expansion of ζ implies also the rough definition

$$f_{\text{NL}} = -\frac{5}{6}\frac{\zeta_2(\mathbf{x})}{\zeta_1^2(\mathbf{x})}, \quad (1.11)$$

which gives an intuitive notion of this parameter. Historically, non-Gaussianity as a test of the accuracy of perturbation theory was first suggested by Allen et al. [1987]. The definition of f_{NL} used here was first introduced by Salopek & Bond [1990] in terms of the Newtonian or Bardeen potential Φ_B (defined in Chapter 2). Their initial definition has been preserved by convention [Gangui et al., 1994; Verde et al., 2000; Komatsu & Spergel, 2001], which is why the transformation to the curvature perturbation ζ_2 involves the numerical factor $-5/6$. In the context of perturbation theory, the study of dynamical equations at second order yields important information independent of the parameters of linear perturbations. Thus, in the nonlinear regime, we can discriminate different models of inflation which are degenerate at linear order. This fact has motivated the search for non-Gaussianity in the CMB and large-scale structure.

Statistically, the lowest order effect of including a non-Gaussian contribution is a non-vanishing correlator of three copies of the curvature field ζ . The three-point function in Fourier space is given by the bispectrum B , defined by

$$\langle \zeta(\mathbf{k}_1)\zeta(\mathbf{k}_2)\zeta(\mathbf{k}_3) \rangle = (2\pi)^3 B_\zeta(k_1, k_2, k_3)\delta^{(3)}(\mathbf{k}_1 + \mathbf{k}_2 + \mathbf{k}_3), \quad (1.12)$$

where $\delta^{(3)}$ is the three-dimensional Dirac delta function.

The bispectrum is directly related to the parameter f_{NL} and for each mode $k = |\mathbf{k}|$. Moreover, being a function of three momenta, the k -dependence of the bispectrum also provides valuable information which could help us to understand the physics of the early universe.

The nonlinear parameters have been investigated through the analysis of higher order correlations in the CMB anisotropies observed mostly by the WMAP satellite [Spergel et al.,

2007]. After five years of collecting data, WMAP observations give the limits $-151 < f_{\text{NL}}^{\text{equil}} < 253$ [Komatsu et al., 2008] for an equilateral triangulation of the momenta and $-4 < f_{\text{NL}}^{\text{local}} < 80$ [Smith et al., 2009] for a local triangulation. The triangulation of the bispectrum is a characteristic which arises due to the following: The momentum conservation in the three point correlation is guaranteed by the delta function in Eq. (1.12), which demands that the sum of the three vectors is zero. In consequence the three momenta represent the sides of a triangle in k -space. Two main triangulations can be distinguished: the equilateral triangulation and the isosceles or local triangulation, which are characteristic shapes of different models of inflation (see e.g. Babich et al. [2004]). An experimental detection of f_{NL} would greatly narrow the range of cosmological models which meet the observational bounds. In the near future, space telescopes, and in particular the PLANCK satellite, are expected to tighten these bounds considerably. Specifically, any signal with $|f_{\text{NL}}| \gtrsim 5$ should be observed by PLANCK [Komatsu & Spergel, 2001; Liguori et al., 2006]. This raises the exciting possibility of looking for particular signatures of inflationary models.

Another attractive observational prospect for non-Gaussianity is to look at the implications of considering primordial non-Gaussian fluctuations in the study of the statistics of galaxies and other large-scale structures (LSS) [Verde et al., 2000; Matarrese et al., 2000; LoVerde et al., 2008]. Such observations probe inhomogeneities at scales smaller than those observed in the CMB.

The effects of non-Gaussianity in the LSS can be classified into two categories, which provide distinct observational methods for detecting non-Gaussianity. The first is the bispectrum of galaxies, potentially determined by computing the three-point correlation function from redshift catalogues [Verde et al., 2001; Scoccimarro et al., 2004]. The second is the non-Gaussian correlations in the probability distribution function (PDF) which leads to modifications in the number of galaxies and other structures with respect to the Gaussian case [Verde et al., 2000; Matarrese et al., 2000].

Both methods involve delicate issues, crucial for the correct interpretation of observations. Most important is the fact that the inhomogeneities that collapse to form galaxies evolve in a nonlinear fashion at late times. This is because the primordial fluctuations enter the horizon much before they form virialised structures. Consequently, the nonlinear

evolution of fluctuations may blur the primordial non-Gaussianity of the initial statistics.

Another important problem is that there is no single way of constructing a non-Gaussian PDF from theoretical models, i.e., several non-Gaussian PDFs can be constructed with a common variance and skewness. This well known problem has been expressed pithily by Heavens [2006]: “We know what a dog is, but, what is a no-dog? A no-dog can be anything”. The effects on, say, the integrated number of galaxies may change substantially with every realisation of the PDF. This complicates the interpretation of non-Gaussian signatures.

In Chapter 3, a formalism is presented to attack this problem. We construct the PDF of the curvature perturbations with a direct input from its higher-order correlations. The formalism is then applied to compute the modification which a non-Gaussian distribution of fluctuations brings to the abundance of primordial black holes.

1.4 Primordial black holes

1.4.1 Standard picture

The idea that large amplitude matter overdensities in the universe could have collapsed through self-gravity to form primordial black holes (PBHs) was first put forward by Zel’Dovich & Novikov [1966] and then independently by Hawking [1971] and Carr & Hawking [1974] more than three decades ago. They suggested that at early times large-amplitude overdensities would overcome internal pressure forces and collapse to form black holes. The standard picture of PBH formation from initial inhomogeneities prescribes that an overdense region with size r_i will overcome pressure and collapse to form a black hole if its size is bigger than the associated Jeans length

$$r_J = 4\pi \frac{\sqrt{w}}{5 + 9w} d_H, \quad (1.13)$$

where the particle horizon d_H is of order of the Hubble radius $r_H = 1/H$. Here we assume an equation of state $p = w\rho$, where w is constant. For the case of radiation-domination, for example, $w = 1/3$.

The size of the initial inhomogeneity must also be smaller than the separate universe scale

$$r_U = \frac{1}{H} f(w), \quad (1.14)$$

where the function $f(w)$ has been derived by Harada & Carr [2005], and is of order unity. Thus, $r_J < r_i < r_U$, both limits being of order the Hubble radius. Consequently the mass of a PBH is close to the Hubble horizon mass. This gives a simple formula for the mass of a PBH forming at time t during radiation domination [Carr, 1975]:

$$M_{\text{PBH}} \simeq M_H = \frac{4}{3} \pi r_H^3 \rho = 10^{15} \left(\frac{t}{10^{-23} \text{ s}} \right) \text{ g}. \quad (1.15)$$

The PBH mass spectrum depends mainly on two characteristics of the early universe: the equation of state w , which determines how large the amplitude of initial inhomogeneities should be to halt the background expansion and recollapse, and the nature of the initial density fluctuations, which determines how likely such amplitudes are. Carr [1975] determined the threshold amplitude $\delta_{\text{th}} \equiv (\delta_\rho)_{\text{th}}$ required for the density perturbation to collapse to a PBH to be $\delta_{\text{th}} \sim w$. In this case, one needs perturbations to the FRW metric with mean amplitude of order unity to form a significant number of PBHs.

The special characteristic of PBHs is that they can form at very early epochs and have very small masses. The smallest PBHs would have formed at the end of the inflationary expansion [Carr & Lidsey, 1993], even from field fluctuations that never exited the horizon [Lyth et al., 2006; Zaballa et al., 2007]. The mass of the horizon at the end of inflation is [Zaballa et al., 2007]

$$M_H \simeq 10^{17} \text{ g} \left(\frac{10^7 \text{ GeV}}{T_{\text{RH}}} \right)^2, \quad (1.16)$$

where the reheating temperature T_{RH} depends sensitively on the model of inflation considered. In the canonical slow-roll inflationary model this temperature can be well above 10^{10} GeV [Kolb & Turner, 1990]. Taking on account the production of dark matter candidate particles in supersymmetric models, this temperature could be dropped by several orders of magnitude, however, leptogenesis does not allow the reheating scale to be smaller than

10^9 GeV [Buchmuller et al., 2005]. This in turn means that PBHs could have been produced with masses much smaller than 10^{11} g. On the other hand, PBHs that formed at 1 s have masses of order $10^5 M_\odot$ which is already in the range of masses of black holes at the centre of galaxies.

The small masses of PBHs prompted the investigation of their quantum properties. The well known result of Hawking [1974] shows that black holes radiate with a temperature

$$T \simeq 10^{-7} \left(\frac{M}{M_\odot} \right)^{-1} \text{ Kelvin} \quad (1.17)$$

and evaporate entirely on a time scale

$$t_{\text{evap}} \simeq 10^{64} \left(\frac{M}{M_\odot} \right)^3 \text{ y}, \quad (1.18)$$

where M_\odot is the solar mass. With the age of the universe estimated as $1.37 \pm 0.015 \times 10^{10}$ y [Spergel et al., 2007], we can predict that PBHs with mass $M_{\text{crit}} = 5 \times 10^{14}$ g are evaporating now. PBHs are also the only type of black holes for which the effect of Hawking evaporation could be observed. Indeed, the black holes evaporating now would be producing photons with energy 100 MeV [Page & Hawking, 1976]. The observed γ -ray background radiation at this energy implies that the density parameter of such PBHs must satisfy [Page & Hawking, 1976]

$$\Omega_{\text{PBH}}(M \sim 10^{15} \text{ g}) \lesssim 10^{-8}. \quad (1.19)$$

This bound remains the tightest constraint to the abundance of PBHs. Additional cosmological bounds to the mass fraction of PBHs are reviewed in Chapter 4.

The mass fraction of the universe turning into PBHs of mass M at the time of their formation is denoted by $\beta_{\text{PBH}}(M)$. This is equivalent to the probability of formation of PBHs of mass M . In a rough calculation, $\beta_{\text{PBH}}(M)$ is given by the Press-Schechter formalism [Press & Schechter, 1974; Carr, 1975] as the integral of the PDF over all amplitudes δ_ρ

above the threshold δ_{th} :

$$\beta_{\text{PBH}}(M) = 2 \int_{\delta_{\text{th}}}^{\infty} \mathbb{P}(\delta_{\rho}) d\delta_{\rho}, \quad (1.20)$$

where the factor two has been added to account for the half volume of the universe that is necessarily underdense. With this factor the Press-Schechter formula gives a good fit to the results of N-body simulations for the case of galactic haloes [Peebles, 1980]. For the case of PBHs, an upper limit of integration is formally required. This is the amplitude of an inhomogeneity for which the total mass would form a separate closed universe. However, the contribution of higher values to the probability is almost negligible and we do not include an upper limit here. For the case of a Gaussian PDF with variance $\Sigma_{\rho}(M)$ this integral is approximated by [Carr, 1975]

$$\beta_{\text{PBH}}(M) \approx \delta_{\text{th}} \exp\left(-\frac{\delta_{\text{th}}^2}{2\Sigma_{\rho}^2(M)}\right). \quad (1.21)$$

This equation demonstrates the sensitive dependence of the probability of PBH formation with δ_{th} . The above integral is expected to be small due to the exponential dependence on the threshold value δ_{th} . β_{PBH} is also known to be small because it is related to the current density parameter Ω_{PBH} of PBHs formed at time t and with mass M by

$$\Omega_{\text{PBH}} = \beta_{\text{PBH}} \Omega_{\text{R}} \left(\frac{a_0}{a(t)}\right) \simeq 10^6 \beta_{\text{PBH}} \left(\frac{t}{1 \text{ s}}\right)^{-1/2} \simeq 10^{18} \beta_{\text{PBH}} \left(\frac{M}{10^{15} \text{ g}}\right)^{-1/2}, \quad (1.22)$$

where $\Omega_{\text{R}} = 8 \times 10^{-5}$. The factor a^{-1} arises because PBHs form mostly during the radiation-dominated era but PBH density scales as a^{-3} , while radiation scales as a^{-4} . From this relation we see that any limit on Ω_{PBH} places a direct constraint on β_{PBH} . For example, from the bound in Eq. (1.19), we infer that $\beta_{\text{PBH}}(M = 10^{15} \text{ g})$ can only have a small value of order 10^{-26} .

1.4.2 Shortcomings

The simple picture of PBH formation described above has several shortcomings

1. In the radiation era the inhomogeneities forming PBHs must have a large amplitude when they enter the horizon and they must be bigger than the horizon for a considerable period of their evolution. As we will show in Chapter 2, the inhomogeneities at superhorizon scales are best described in terms of curvature perturbations because they are constant in this regime. The curvature perturbation has already been used in the more recent numerical simulations of PBH formation [Shibata & Sasaki, 1999; Niemeyer & Jedamzik, 1999; Polnarev & Musco, 2007]. Here, as in several other recent works on the subject [Yokoyama, 1999; Green et al., 2004; Zaballa et al., 2007; Josan et al., 2009], we compute the probability of formation of PBHs from the statistics of the curvature perturbations. This has the advantage of relating the formation of PBHs directly to the initial perturbation spectrum. Additionally, it avoids the gauge anomaly associated to the matter density fluctuation.
2. In the calculation of the probability of PBH formation, one could argue that the Press-Schechter formula in Eq. (1.20) is only an empirical approximation. Alternative approaches have therefore considered the theory of peaks [Green et al., 2004]. However, this does not render significant corrections to the Press-Schechter result. Moreover, the Press-Schechter formula can be used to calculate the probabilities of large-scale structure formation from non-Gaussian PDFs [Matarrese et al., 2000]. Indeed, the latest numerical simulations confirm that it is a good approximation even in this case [Grossi et al., 2009]. This justifies our choice of the Press-Schechter formalism to explore new aspects of the probability of PBH formation.
3. A severe oversimplification of the usual calculation of the probability of PBH formation is the assumption of Gaussianity. The exponential decay of the Gaussian PDF is preserved after its integration in the Press-Schechter formula (1.21). The fact that the mass fraction involves an integration over the tail of the normal distribution, where the probability density is small, leads us to consider that a slight variation on the profile of the PDF might modify this picture significantly. Indeed, non-Gaussian probability distributions have been considered in studies of the probability of PBH formation by Bullock & Primack [1997] and Ivanov [1998]. The discrepancy in their results and the large departures from the Gaussian case make this problem worth revisiting. One main

objective of this thesis is to derive the modifications that non-Gaussian PDFs bring to the probability of PBH formation in the most general cases. We explore for the first time the modifications that a non-Gaussian PDF may bring for the bounds on the amplitude of fluctuations and the higher order statistics parameter f_{NL} on the cosmological scales relevant to PBH formation.

4. The last important problem in the calculation of β_{PBH} is the determination of the precise value of the threshold amplitude δ_{th} or ζ_{th} for the density or the curvature inhomogeneity. This approximation of β_{PBH} prompted several studies of PBH formation to determine the precise value of the threshold amplitude. Early numerical simulations of gravitational collapse, however, already showed that this value depends sensitively on the shape and profile of the initial configuration $\delta_{\rho}(\mathbf{x})$ [Nadezhin et al., 1978]. This dependence indicates that the lower limit of the integral (1.20) is not uniquely prescribed for all configurations collapsing to form PBHs. The problem then is how to differentiate profiles of initial inhomogeneities in the calculation of the probability of PBH formation. This is another problem we address in this thesis. We calculate the probability of PBH formation by taking into account the radial profiles of initial curvature inhomogeneities. This represents a first attempt to incorporate profiles into the calculation of β_{PBH} and allow for a more precise estimation of the probability of PBH formation.

1.4.3 Alternative mechanisms of PBH formation

The formation of PBHs is not limited to the collapse of overdensities. PBHs may also form at the phase transitions expected in the early universe. Let us here briefly review other known mechanisms of PBH formation.

- PBHs may form at early phase transitions where the equation of state is soft for a small period of time. In such transitions, the effective pressure in the universe is reduced due to the formation of non-relativistic particles. Hydrodynamical simulations show that at such a phase transition the value of δ_{th} is reduced below the value pertaining to the radiation era. This mechanism enhances the probability of PBH formation at a

mass scale of the order of the horizon mass at that time [Khlopov & Polnarev, 1980; Jedamzik, 1997].

- Loops of cosmic strings can collapse to form PBHs. Cosmic strings are topological defects formed at the phase transitions in the very early universe. Closed loops can be formed from string self-intersection. The scale of a loop will be larger than the Schwarzschild radius by a factor $(G\mu)^{-1}$, where μ is the string mass per unit length, a free parameter in the theory. In the cosmic string scenario, these loops are responsible for the formation of cosmological structures if $(G\mu)$ is of order 10^{-6} . In this scenario, there is always a small probability that particular configurations, in which all the loop dimensions lie within its Schwarzschild radius, can collapse to form black holes. This mechanism has been discussed by many authors (see e.g. Hawking [1989]; Polnarev & Zembowicz [1991]; Garriga & Sakellariadou [1993]). However, WMAP and observations of galaxy distributions show that cosmic strings can at most contribute to 10% of the temperature anisotropy in the CMB [Wyman et al., 2005]. The mass per unit length is less constrained by the observational limits on primordial black holes [Caldwell & Casper, 1996]. Because the μ parameter is scale-invariant and its most stringent limit comes from CMB observations, we can say that the formation of PBHs from cosmic string loops is subdominant with respect to the standard picture of collapse of overdensities.
- One can also consider closed domain walls which form black holes. Domain walls are hypothetical topological defects of higher order. In a phase transition of second order, such as might be associated with inflation, sufficiently large domain walls may be produced [Crawford & Schramm, 1982]. This leads to the formation of PBHs in the lower end of the range of masses [Rubin et al., 2001].
- Recently, a mechanism to form PBHs as the result of warping cosmic necklaces has been suggested. These topological defects arise in the process of symmetry breaking in the framework of quantum strings [Matsuda, 2006].

In all these mechanisms the PBHs have mass of order the horizon mass at phase transitions in the early universe. They are also expected to produce PBHs with a Gaussian distribu-

tion. Here we are interested mostly in PBHs with a non-Gaussian distribution in order to produce constraints on models of inflation, so we do not study these alternative formation mechanisms.

1.5 Thesis outline

Chapter 2 presents a study of non-Gaussianity from inflationary scalar perturbations. It first introduces the relevant definitions and the main tools used in the study of inflationary perturbations. It then focuses on the derivation of non-Gaussian correlation functions. Specifically, the three-point correlation is studied in models where an auxiliary scalar field during inflation is responsible for the generation of non-adiabatic fluctuations. The cases in which the non-adiabatic fluctuations may generate large values of f_{NL} is considered in detail.

The method used to derive the non-Gaussian correlators requires the solution of the Klein-Gordon equation beyond linear order. This equation is solved considering a perturbative expansion of the nonlinear terms without taking on account the metric back-reaction. For the cases in which analytic solutions are possible, the derivation of the three-point correlation is presented. Finally, the observational limits on f_{NL} are used to constrain models of inflation which include a curvaton field, a special case of an isocurvature field.

Chapter 3 discusses the decomposition of the curvature perturbation \mathcal{R} into harmonics. This is a technical step, which is necessary in order to write down a path integral for the PDF $\mathbb{P}(\mathcal{R})$. We present the calculation for the Gaussian case first, in order to clearly explain our method with a minimum of technical details. This is followed by the equivalent calculation including non-Gaussian corrections which follow from a non-zero three-point function. Finally we calculate the probability $\mathbb{P}[\mathcal{R}(k)]$, which will be used to derive a non-Gaussian probability of PBH formation.

In Chapter 4 we compute the mass fraction β_{PBH} resulting from a non-Gaussian PDF of primordial curvature fluctuations \mathcal{R} . We restrict ourselves to the case in which the non-Gaussian PDF corresponds to a constant value of f_{NL} . It is first shown how to reconcile the discrepancy between two previous studies of non-Gaussian PBH formation [Bullock & Primack, 1997; Ivanov, 1998]. We then calculate the modifications to the observational bounds to β_{PBH} when a large value of f_{NL} is included.

Chapter 5 explores the probability of finding non-trivial spatial profiles for the perturbations that form PBHs. The numerical simulations show that the usual assumption of homogeneous spherically symmetric perturbations collapsing to PBHs is not appropriate. Chapter 5 provides a probabilistic analysis of the radial profiles of spherical cosmological inhomogeneities that collapse to form PBHs. Based on the methods used to construct non-Gaussian PDFs, we derive the probability distribution for the central amplitude of \mathcal{R} and for the second radial derivative $d^2\mathcal{R}/dr^2$ at the centre of the spherically symmetric inhomogeneity used to describe the radial profiles explored in studies of gravitational collapse. We then consider the joint probability of both parameters to compute the correction to β_{PBH} . The results show how much the probability of PBH formation can be reduced if we do not include all possible configurations forming PBHs.

Chapter 6 is the summary and conclusion of this thesis. We also describe future research which may follow. The key achievement of this thesis is to combine for the first time the study of two crucial probes of the early universe. The effects of nonlinear non-Gaussian inhomogeneities and primordial black hole formation.

Chapter 2

Non-Gaussian curvature perturbations

2.1 Outline

Observations of cosmological structure and CMB parameters are best interpreted in the context of cosmological perturbation theory. This is a useful tool to connect observations with models of inflation derived or motivated by high energy physics theories for which there is no other available test. Surprisingly enough, the simplest inflationary model, consisting of a single scalar field slowly rolling down a quadratic potential, motivated mainly by its simplicity, has passed all observational tests. The future of cosmology relies on the extension of experimental tests and predictions for new cosmological parameters, mostly beyond linear order. This is crucial if we want to achieve a better understanding of the physics dominating the early universe.

This is enough motivation to study the nonlinear regime of cosmological inhomogeneities. Among the observable effects, the non-Gaussianity of perturbations has been widely studied in inflationary models. Non-Gaussianity is an important observational test as it might eliminate models of inflation even for a null detection. Our goal in this chapter is to compute the nonlinear correlations of a general isocurvature field which is valid for all models.

We first introduce the theory of perturbations and then focus on the situation in which the curvature perturbation is generated by the quantum fluctuations of an isocurvature scalar field. The isocurvature or entropy perturbations are transformed into curvature inhomogeneities at the end of a period of inflation or shortly after it. We will show that only the presence of entropy fluctuations can affect the evolution of curvature fluctuations on super-

horizon scales.

At linear order, we will show under which conditions the observed power spectrum of curvature fluctuations can be attributed to the action of the isocurvature field. Subsequently we present a method of deriving such correlations from the solutions to the Klein-Gordon equation of the isocurvature field. For specific cases we are able to derive an explicit expression for the nonlinear parameter f_{NL} . The prospects of observationally testing the predictions for the models of structure formation presented here are also briefly discussed.

The introductory sections of this chapter present a review of the elements of the standard inflationary scenario, including the linear perturbation theory. We present the relevant definitions and conventions to be used, with particular attention to those results of linear perturbation theory which will be used in this and subsequent chapters. From Section 2.5 onwards, we focus on the description of the non-Gaussian correlators of an auxiliary isocurvature field χ . The expressions for the curvature perturbation three-point correlators and the f_{NL} values are presented in the last section of this chapter.

2.2 Linear perturbations

In cosmological perturbation theory, the universe is described to a lowest order by a homogeneous, isotropic background spacetime. The large-scale inhomogeneities and anisotropies observed in the real universe result from the growth of density fluctuations, the amplitudes of which are small in the early stages of the universe. (See Peebles [1980] for a textbook description of the development of perturbation theory.)

In the framework of perturbation theory, the homogeneous background spacetime is accounted for by an ansatz metric. The most useful ansatz in this case is the Friedmann-Robertson-Walker (FRW) metric:

$$g_{\mu\nu} = a^2(\eta) \begin{pmatrix} -1 & 0 \\ 0 & \gamma_{ij} \end{pmatrix}, \quad (2.1)$$

where the conformal time η is given in differential form by

$$d\eta = \frac{dt}{a(t)}, \quad (2.2)$$

a is the scale factor and γ_{ij} is the metric of the three-dimensional space. In our notation Greek indices have values 0, 1, 2, 3, while Latin ones have values 1, 2, 3. We assume throughout a flat space, relying on the observational limit $|\Omega_\kappa| < 10^{-2}$ [Komatsu et al., 2008]. The FRW metric describes the isotropic space-time expanding at a uniform rate. The expansion rate is conventionally characterised by the Hubble parameter

$$H = \frac{d\ln a}{dt} = \frac{1}{a} \frac{d\ln a}{d\eta} = \frac{1}{a} \mathcal{H}, \quad (2.3)$$

where H is defined with respect to coordinate time t and \mathcal{H} with respect to conformal time η .

2.2.1 Metric perturbations

In perturbation theory, observed anisotropies and inhomogeneities are considered as departures from the metric (2.1). For a perturbed metric, the metric tensor can be split as

$$g_{\mu\nu} = g_{\mu\nu}^{(0)} + \delta g_{\mu\nu}, \quad (2.4)$$

where $g_{\mu\nu}^{(0)}$ is the homogeneous FRW background and $\delta g_{\mu\nu}$ encodes the perturbed quantities. First order scalar perturbations of the metric are expressed in terms of the functions φ , B , ψ and E , which are defined by

$$\begin{aligned} \delta g_{00}^{(s)} &= -2a^2 \varphi(\eta, \mathbf{x}), \\ \delta g_{0i}^{(s)} &= a^2 B(\eta, \mathbf{x})_{,i}, \\ \delta g_{ij}^{(s)} &= 2a^2 (\psi(\eta, \mathbf{x}) \gamma_{ij} + E_{,ij}(\eta, \mathbf{x})), \end{aligned}$$

where the index (s) denotes scalar modes. The vector constructed from the scalar B is necessarily curl-free, i.e. $B_{,[ij]} = 0$. The pure vector contributions to the metric perturbations

are

$$\delta g_{0i}^{(v)} = -a^2 S_i, \quad \delta g_{ij}^{(v)} = 2a^2 F_{(i,j)},$$

where we demand $S_{[i,j]} \neq 0$. The symmetric derivative of the function F_i is the vector contribution to g_{ij} . To distinguish scalar and vector contributions, the vector part is forced to be divergence-free, i.e., $\gamma^{ij} S_{i,j} = 0$. (The decomposition of a vector field into curl- and divergence-free parts is formally known as Helmholtz's theorem.) The tensor contribution to the perturbation quantities is $\delta g_{ij}^{(t)} = a^2 h_{ij}$. This is constructed as a transverse, traceless tensor, which guarantees that it cannot be constructed from scalar or vector perturbations.

The perturbation functions φ , B , ψ and E , represent four degrees of freedom. The divergenceless vectors S_i and F_j each have two degrees of freedom and the transverse traceless tensor h_{ij} has two more. We therefore have 10 degrees of freedom in total. The contravariant metric tensor of the perturbed metric is constructed, to first order, from the condition, $g_{\mu\alpha} g^{\mu\beta} = \delta_\alpha^\beta$. Finally, the line element of the metric is

$$ds^2 = a^2(\eta) \left\{ - (1 + 2\varphi) d\eta^2 + 2(B_{,i} - S_i) d\eta dx^i + [(1 + 2\psi)\gamma_{ij} + 2E_{ij} + 2F_{i,j} + h_{ij}] dx^i dx^j \right\}. \quad (2.5)$$

In the present work we will study the nonlinear perturbations as the quantum fluctuations of scalar matter fields. We will establish the correspondence between scalar matter fluctuations and scalar perturbations in the metric at first and second order in perturbation hierarchy. We will then derive statistical parameters of nonlinearity.

In contrast to the scalar metric fluctuations, the vector and tensor perturbations in the metric are not sourced by scalar matter perturbations at first order. In the standard picture, they are only related at second or higher order in perturbation theory (see e.g. Lu et al. [2008]), therefore their contribution to the statistical parameters of nonlinearity are subdominant and henceforth we neglect their contributions to the perturbations in the metric.

2.2.2 Gauge freedom

In general relativity, the mathematical relations between physical quantities are manifestly independent of the coordinate choice. However, there is no covariant way of splitting background and perturbed variables. There is always an unphysical coordinate or gauge dependence associated with perturbed spacetimes. This issue of gauge ambiguity was disregarded in the initial works of perturbation theory [Lifshitz, 1946; Lifshitz & Khalatnikov, 1963]. This could lead to erroneous results which were eventually resolved in a systematic way by Bardeen [1980]. The importance of determining the gauge changes that equations and perturbations undergo leads us to look at this problem in detail. In the following we adopt a ‘passive’ approach to gauge transformations (For a recent review of these results, see Malik & Wands [2008]). Let us consider the general coordinate transformation,

$$\tilde{\eta} = \eta + \xi^0, \quad \tilde{x}^i = x^i + \xi^i + \bar{\xi}^i, \quad (2.6)$$

where $\xi^0 = \xi^0(\eta, x^i)$ is a scalar that determines the choice of constant- $\tilde{\eta}$ hypersurfaces. The scalar ξ and the divergence-free vector $\bar{\xi}^i$ are also functions of the original coordinates within these hypersurfaces.

The principle of relativity states that any physically meaningful measurement must be invariant for all observers, in particular, for observers with different coordinate systems. One of these invariants is the line element ds^2 , where coordinates enter via differentials. Such differentials and the scale factors in both coordinate systems are related in the following way:

$$\begin{aligned} d\eta &= d\tilde{\eta} - \xi^{0'} d\tilde{\eta} - \xi^0_{,i} d\tilde{x}^i, \\ dx^i &= d\tilde{x}^i - (\xi^{i'} + \bar{\xi}^{i'}) d\tilde{\eta} - (\xi^i_{,j} + \bar{\xi}^i_{,j}), \\ a(\eta) &= a(\tilde{\eta}) - \xi^0 a'(\tilde{\eta}). \end{aligned} \quad (2.7)$$

Where a $'$ is the derivative with respect to conformal time. To first order in the metric perturbations and coordinate transformations, the perturbed line element, Eq. (2.5) is written in

the ‘shifted’ coordinate system as

$$ds^2 = a^2(\tilde{\eta}) \left\{ - (1 + 2(\varphi - \mathcal{H}\xi^0 - \xi^{0'})) d\tilde{\eta}^2 + 2[(B + \xi^0 - \xi'),_i - S_i + \bar{\xi}'_i] d\tilde{\eta} d\tilde{x}^i \right. \\ \left. + [(1 + 2(\psi - \mathcal{H}\xi^0)) \gamma_{ij} + 2(E - \xi)_{,ij} + 2F_{i,j} - 2\bar{\xi}_{i,j} + h_{ij}] d\tilde{x}^j d\tilde{x}^i \right\}, \quad (2.8)$$

where, as before, $\mathcal{H} \equiv a'/a$ is the Hubble parameter in terms of conformal time. This metric can also be written using the initial definitions in terms of the ‘shifted’ coordinates:

$$ds^2 = a^2(\tilde{\eta}) \left\{ - (1 + 2\tilde{\varphi}) d\tilde{\eta}^2 + 2(\tilde{B}_{,i} - \tilde{S}_i) d\tilde{\eta} d\tilde{x}^i \right. \quad (2.9)$$

$$\left. + [(1 + 2\tilde{\psi}) \tilde{\gamma}_{ij} + 2\tilde{E}_{ij} + 2\tilde{F}_{i,j} + \tilde{h}_{ij}] d\tilde{x}^i d\tilde{x}^j \right\}. \quad (2.10)$$

This shows that the coordinate transformation Eq. (2.7) induces a transformation of the metric perturbations. Comparing Eqs. (2.5) and (2.10), the change is given to first order by

$$\tilde{\psi} = \psi - \mathcal{H}\xi^0, \quad (2.11)$$

$$\tilde{\varphi} = \varphi - \mathcal{H}\xi^0 - \xi^{0'}, \quad (2.12)$$

$$\tilde{B} = B + \xi^0 - \xi', \quad (2.13)$$

$$\tilde{E} = E - \xi. \quad (2.14)$$

It must be stressed that the gauge transformations are, in effect, a change of the correspondence between the perturbed spacetime and the unperturbed background spacetime.

A first exercise concerning gauge transformations is to find those quantities which remain invariant after a gauge transformation. To first order in perturbation variables, gauge-invariant quantities are linear combinations of the gauge-dependent quantities presented above. For scalar perturbations Bardeen [1980] shows that only two independent gauge-invariant quantities can be configured purely from the metric perturbations:

$$\Phi_B = \varphi + \mathcal{H}(B - E') + (B - E')', \quad (2.15)$$

$$\Psi_B = -\psi - \mathcal{H}(B - E'). \quad (2.16)$$

Any other gauge invariants in the metric are linear combinations of these two quantities because the gauge freedom allows only two arbitrary scalar functions ξ^0 and ξ [Malik, 2001].

The Bardeen invariants will be useful in relating curvature perturbations in different gauges, as we will show below.

2.2.3 Perturbations of the matter sector

Before displaying conservation equations for the curvature perturbations, we will discuss the perturbations of the matter sector. For a perfect fluid, that is, a fluid with no heat conduction or viscosity, the stress-energy tensor is

$$T^\mu_\nu = (p + \rho)u^\mu u_\nu + p\delta^\mu_\nu, \quad (2.17)$$

where the 4-velocity is defined with respect to proper time τ as

$$u^\mu = \frac{dx^\mu}{d\tau} \quad (2.18)$$

and is subject to the normalisation $u^\mu u_\mu = -1$. Anisotropic stresses would be encoded in a stress tensor $\Pi_{\mu\nu}$, but are absent for perfect fluids and for scalar fields minimally coupled to gravity. These are precisely the kinds of matter considered here, so we ignore the tensor $\Pi_{\mu\nu}$ in the subsequent analyses.

Using the normalisation $u^\mu u_\mu = -1$, the perturbed velocity has components

$$u^0 = \frac{1}{a}(1 - \varphi), \quad u^i = \frac{1}{a}(v^{,i} + v^i), \quad (2.19)$$

$$u_0 = -a(1 + \varphi), \quad u_i = -a(v_i + v_{,i} + B_{,i} - S_i), \quad (2.20)$$

where the spatial parts are written in terms of the gradient of a scalar $v_{,i}$ and a (solenoidal) vector v_i . The perturbed energy-momentum tensor is:

$$T^0_0 = -(\rho_0 + \delta\rho), \quad (2.21)$$

$$T^0_i = (\rho_0 + p_0)(B_{,i} + v_{,i} + v_i - S_i), \quad T^i_0 = -(\rho_0 + p_0)(v^{,i} + v^i), \quad (2.22)$$

$$T^i_j = (p_0 + \delta)p\delta^i_j, \quad (2.23)$$

where p_0 and ρ_0 represent the uniform pressure and matter density. In general our scalar

stress-energy components can be written as $f(\eta, x^i) = f_0(\eta) + \delta f(\eta, x^i)$, with the subscript 0 denoting the background homogeneous part. As in the case of metric perturbations, coordinate transformations will affect the matter perturbations. This means that the matter density, velocity and pressure perturbations are gauge dependent. Under the transformation Eq. (2.6), perturbed scalar functions of the form are thus transformed as

$$\widetilde{\delta f} = \delta f - f'_0 \xi^0. \quad (2.24)$$

The vector perturbations are derived either from a potential, which will transform with the shift ξ^i , or from a pure divergence-free vector, whose transformation depends on ξ^i . In particular, the velocity potential v transforms as:

$$\tilde{v} = v + \xi^i, \quad (2.25)$$

and the vector function v^i is transformed as

$$\tilde{v}^i = v^i + \bar{\xi}^{i'}. \quad (2.26)$$

2.2.4 Physical quantities and scales

Before addressing the characteristics and governing equations of the perturbed spacetime, let us define the physical scales and the quantities that determine of the size and age of the universe.

The time-like 4-vector field

$$N_\mu = -a(1 + \varphi)\delta_\mu^0, \quad (2.27)$$

defines the direction perpendicular to the hypersurfaces of constant time. In consequence, this vector field defines a coordinate system. This vector is unitary ($N^\nu N_\nu = -1$) and the contravariant vector $N^\nu = g^{\nu\mu} N_\mu$ has components

$$N^0 = \frac{1}{a}(1 - \varphi), \quad N^i = \frac{1}{a}(S^i - B^i). \quad (2.28)$$

The expansion rate of the spatial hypersurfaces with respect to the proper time of observers with 4-velocity N^μ is $\theta = N^\mu_{;\mu}$. Considering only scalar perturbations, this is given by

$$\theta = 3\frac{a'}{a^2}(1 - \varphi) + 3\frac{1}{a}\psi' - \frac{1}{a}\nabla^2(B - E'), \quad (2.29)$$

where the operator ∇ denotes the usual three-dimensional gradient.

By looking at the relation between proper and coordinate time, $d\tau = (1 + \varphi) dt$, we extract the expansion with respect to coordinate time from the above expression by writing

$$\theta_{(t)} = (1 + \varphi)\theta = 3H + 3\dot{\psi} + \nabla^2\sigma_{(t)}, \quad (2.30)$$

where the Hubble parameter, $H = \dot{a}/a$ is the background uniform expansion rate with respect to the coordinate time. The shear scalar in coordinate time is $\sigma_{(t)} = (\dot{E} - B/a)$.

For the sake of completeness, we include here the definition of some useful scales. A comoving observer is one moving with the expansion of the universe, i.e., one who measures zero net momentum density. The distance of a comoving point from our location (taken to be at the origin of coordinates), is given by $r(t) = a(t)x$, where x is the comoving distance.

The Hubble radius $r_H = H^{-1}$ provides a good estimate for the distance light has travelled since the Big Bang. Formally, the integral

$$\eta = \int_0^t \frac{ds}{a(s)}, \quad (2.31)$$

defines the comoving distance travelled by a free photon since $t = 0$ and until time t . This is important because no information could have travelled further than η . This defines the ‘comoving particle horizon’. In the above integral η can be taken also as the conformal time. In a matter dominated universe $\eta \propto a^{1/2}$, while in radiation domination $\eta \propto a$. In a de Sitter inflationary universe

$$\eta = \int \frac{ds}{a(s)} = \int \frac{da}{Ha^2} = -\frac{H^{-1}}{a(t)}. \quad (2.32)$$

This shows that in an inflationary phase $\eta \rightarrow -\infty$ as the universe approaches the initial singularity $a = 0$, and increases monotonically towards 0. This leads us to consider the mag-

nitude $|\eta|$ when we use the conformal time in our calculations for inflation. The maximum distance light travels from time $t = 0$ to us is simply the comoving horizon times the scale factor,

$$d_H = a(t_{\text{now}}) \int_0^{t_{\text{now}}} \frac{ds}{a(s)}. \quad (2.33)$$

This is called the particle horizon, i.e., the radius of the region which is in causal contact with us. This equation can be applied to find the horizon radius at times different from t_{now} . Considering the current dark energy domination and a cold dark matter component (with density parameter Ω_m), the horizon size does not coincide exactly with the Hubble scale. However, an approximate solution to the integral Eq. (2.33) shows that,

$$d_H(t_{\text{now}}) \approx 2H_{\text{now}}^{-1} \frac{1 + 0.084 \ln \Omega_m}{\sqrt{\Omega_m}} \simeq 3.5H_{\text{now}}^{-1}, \quad (2.34)$$

where the last expression assumes $\Omega_m = 0.25$ [Hu et al., 1998].

2.2.5 Particular gauges

Let us now focus on the expressions for the curvature perturbation on three useful choices of time slicing and threading. These are the uniform curvature gauge, the uniform density gauge and the comoving gauge.

For the first case the spatial hypersurfaces present an unperturbed 3-metric, which means $\tilde{\psi} = \tilde{E} = 0$, in other words, curvature perturbations of the three-metric are set to zero. We distinguish the quantities written in this gauge with a subscript κ indicating a constant curvature. So for a general coordinate system we require the following transformations:

$$\xi_{\kappa=\text{const}}^0 = \frac{\psi}{\mathcal{H}}, \quad \xi_{\kappa} = E. \quad (2.35)$$

In this case, the scalar perturbation becomes

$$\delta f_{\kappa} = \delta f - f'_0 \frac{\psi}{\mathcal{H}}. \quad (2.36)$$

In particular, for scalar fields, this is the gauge-invariant Sasaki-Mukhanov variable [Sasaki,

1986; Mukhanov, 1988], explicitly,

$$\delta\phi_\kappa = \delta\phi - \phi'_0 \frac{\psi}{\mathcal{H}}. \quad (2.37)$$

In the uniform density gauge, the requirement $\tilde{\delta}\rho = 0$ for constant-time hypersurfaces implies

$$\xi_{\delta\rho}^0 = \frac{\delta\rho}{\rho'}. \quad (2.38)$$

The gauge-invariant curvature perturbation on these hypersurfaces is denoted by ζ and defined as

$$\zeta \equiv \tilde{\psi}_{\delta\rho} = \psi - \mathcal{H} \frac{\delta\rho}{\rho}. \quad (2.39)$$

In this case, there is another degree of freedom and one can pick either \tilde{B} , \tilde{E} or \tilde{v} to be zero. The gauge invariance is made explicit when the curvature perturbation is written in terms of the Bardeen variables. We will return to this point once we have defined the curvature in the comoving gauge.

The comoving gauge is subject to the condition that the spatial coordinates comove with the fluid, that is, for a constant-time slice the 3-velocity of the fluid vanishes, $v_{,i} = 0$. The threading is chosen so that the constant- η hypersurfaces are orthogonal to the 4-velocity w^μ , which demands $\tilde{v} + \tilde{B} = 0$. An immediate consequence of this choice of gauge is that the total 3-momentum vanishes on constant-time hypersurfaces. For this reason several authors call this gauge the zero-momentum gauge. Using Eqs. (2.25) and (2.13), the chosen conditions imply that

$$\xi_m^0 = -(v + B), \quad \xi_m = - \int v d\eta + \tilde{\xi}(x^i), \quad (2.40)$$

with $\tilde{\xi}(x^i)$ the residual coordinate gauge freedom. This quantity is not specified at this stage because it is not required for the determination of the scalar quantities like curvature, expansion and shear. For arbitrary coordinates, the scalar perturbations in the comoving orthogonal

gauge are given by

$$\tilde{\varphi}_m = \varphi + \frac{1}{a} [(v + B)a]', \quad \tilde{\psi}_m = \psi + \mathcal{H}(v + B), \quad \tilde{E}_m = E + \int v d\eta - \tilde{\xi}. \quad (2.41)$$

The scalars $\tilde{\varphi}_m$ and $\tilde{\psi}_m$ defined in this way are gauge-invariant. The density perturbation in the comoving gauge is also given in gauge-invariant form by

$$\delta\tilde{\rho}_m = \delta\rho + \rho'(v + B). \quad (2.42)$$

Some authors use the gauge-invariant density perturbation in the comoving gauge by defining the combination $\Delta \equiv \tilde{\delta\rho}_{m,i}{}^i / \rho_0$ [Bardeen, 1980; Kodama & Sasaki, 1984].

The curvature perturbation ψ in the comoving gauge was first used by Lukash [1980] and first denoted as \mathcal{R} by Liddle & Lyth [1993]. It is mathematically defined as

$$\mathcal{R} \equiv \tilde{\psi}_m = \psi + \mathcal{H}(v + B). \quad (2.43)$$

In the next section we will find that, through the Einstein equations and gauge-invariant quantities Ψ_B and Φ_B , defined in Eqs. (2.16) and (2.15), one can establish an equivalence at large scales between the curvature perturbation to linear order in the uniform density gauge and the same perturbation defined in the comoving gauge. Taking this equivalence for granted, in the meantime, allows us to relate \mathcal{R} and $\delta\rho$ directly. Indeed, if we consider the gauge transformation (2.39) from an initial flat hypersurface, then

$$\mathcal{R} = \zeta = -\mathcal{H} \frac{\delta\rho_\kappa}{\rho}, \quad (2.44)$$

at scales beyond the cosmological horizon (as will be made explicit below).

This last transformation shows the way of avoiding the gauge anomaly. One can always change the gauge (or frame of reference) and establish the equivalence between the perturbations of any two gauges as long as a particular gauge is chosen at the start and all quantities are initially defined in this gauge.

2.3 Evolution of perturbations and conserved quantities

Just as the perturbed scalars in the metric are gauge dependent, so are the evolution equations for these quantities and they must be treated carefully in order to avoid spurious gauge modes.

The equations governing the dynamics of space-time are found by varying the action \mathcal{I} with respect to the metric and matter components. The action is defined as

$$\mathcal{I} = \int_{-\infty}^{\infty} \mathcal{L} \sqrt{-g} d^4x, \quad (2.45)$$

where \mathcal{L} is the Lagrangian density of the matter and the gravitational field. The gravitational Lagrangian of general relativity is,

$$\mathcal{L} = -R/2, \quad (2.46)$$

where R is the Ricci scalar. The Lagrangian density for a classical matter field minimally coupled to gravity is

$$\mathcal{L} = K - V - R/2, \quad (2.47)$$

with K the kinetic energy and V the potential energy. For the matter sector of the Lagrangian we can define the energy-momentum tensor as

$$T_{\mu\nu} = -2 \frac{\partial \mathcal{L}}{\partial g^{\mu\nu}} + g_{\mu\nu} \mathcal{L}. \quad (2.48)$$

In particular, the energy-momentum tensor for a perfect fluid with density ρ and isotropic pressure p and 4-velocity u^μ is given by Eq. (2.17).

Let us now look at the Lagrangian density of a single scalar field ϕ , minimally coupled to gravity. Its kinetic energy is $K = -1/2 g^{\mu\nu} \partial_\mu \phi \partial_\nu \phi$, so from Eq. (2.47) we find a canonic action

$$\mathcal{L}_M = -\frac{1}{2} [g^{\mu\nu} \partial_\mu \phi \partial_\nu \phi + 2V(\phi)]. \quad (2.49)$$

Using the definition Eq. (2.48), it is easy to show that the scalar field energy-momentum tensor is

$$T_{\mu}^{\nu} = g^{\alpha\nu} \phi_{,\mu} \phi_{,\alpha} - \delta_{\mu}^{\nu} \left(V(\phi) + \frac{1}{2} g^{\alpha\beta} \phi_{,\alpha} \phi_{,\beta} \right). \quad (2.50)$$

The comparison between the last expression with Eq. (2.17), $T_{\mu\nu}$ for a perfect fluid, shows that we can define the density, isotropic pressure and velocity as [Tabensky & Taub, 1973]

$$u_{\mu} = \frac{\phi_{,\mu}}{|g^{\mu\nu} \phi_{,\mu} \phi_{,\nu}|}, \quad \rho = -g^{\mu\nu} \phi_{,\mu} \phi_{,\nu} + V, \quad p = -g^{\mu\nu} \phi_{,\mu} \phi_{,\nu} - V. \quad (2.51)$$

This identification provides an easy way to quantify the energy density of a scalar field and its perturbations. The Lagrangian density for two real fields is

$$\mathcal{L}_M = -\frac{1}{2} (g^{\mu\nu} \phi_{,\mu} \phi_{,\nu}) - \frac{1}{2} (g^{\mu\nu} \chi_{,\mu} \chi_{,\nu}) - U(\phi, \chi), \quad (2.52)$$

which features the joint potential $U(\phi, \chi)$ of the participating fields, each minimally coupled to gravity. This case is what concerns us in the rest of the chapter and we shall focus on its dynamical equations.

2.3.1 Background equations

The Einstein equations are found by varying the action (2.47) with respect to the metric. Under regular conditions, with no variations of the fields at the boundaries, the equations are found by applying the operator

$$\left[\frac{\delta}{\delta g} - \partial_{\mu} \frac{\delta}{\delta(\partial_{\mu} g)} \right] \quad (2.53)$$

to the Lagrangian. The Einstein equations dictate the dynamics relating the local spacetime curvature to the local energy-momentum. In the adopted natural units,

$$G_{\mu\nu} = T_{\mu\nu}, \quad (2.54)$$

where the left-hand side is the Einstein tensor, defined as

$$G_{\mu\nu} = R_{\mu\nu} - \frac{1}{2}g_{\mu\nu}R. \quad (2.55)$$

The Einstein equations can be split into components that are parallel or orthogonal to the time-like field N^μ at any order in perturbation expansion. The two independent equations obtained at the background level are the Friedmann and acceleration equations:

$$\mathcal{H}^2 = \frac{1}{3}a^2\rho_0, \quad (2.56)$$

$$\mathcal{H}' = -\frac{1}{6}a^2(3p_0 + \rho_0). \quad (2.57)$$

Additionally, the Bianchi identities $G^\mu{}_{\nu;\mu} = 0$ imply the local conservation of energy and momentum,

$$T^\mu{}_{\nu;\mu} = 0, \quad (2.58)$$

where $;$ denotes a covariant derivative with respect to the metric $g_{\mu\nu}$.

For the background quantities, the energy-momentum conservation equations provide an expression for the expansion in terms of the matter fields. For the case of a single fluid in the background FRW universe, the equation $T^\nu{}_{0;\nu} = 0$ gives

$$\rho_0' = -3\mathcal{H}(p_0 + \rho_0). \quad (2.59)$$

Note that the isotropy assumption means there is no net background momentum and thus no other conservation equation at zeroth order. Moreover, Eq. (2.59) can also be obtained as a combination of the Einstein equations (2.56) and (2.57).

The homogeneous Einstein equations can be solved for the variables $a(t)$, $\rho(t)$, $p(t)$ when an equation of state for the matter components is provided. This is dictated by the micro-physics of the matter. In particular, the equation of state

$$p = w\rho, \quad (2.60)$$

describes most of the relevant cases of the post-inflationary cosmology. For the case of pure radiation $w = 1/3$, while for pressureless dust $w = 0$. For fluids with such an equation of state, the solutions to the Einstein equations are

$$\frac{\rho}{\rho_i} = \left(\frac{a}{a_i}\right)^{-3(w+1)}, \quad \frac{a}{a_i} = \left(\frac{\eta}{\eta_i}\right)^{2/(3w+5)}, \quad (2.61)$$

with initial conditions $\rho = \rho_i$ and $a = a_i$ at $\eta = \eta_i$.

When more than one fluid is present, we account for the contribution of each component $\rho^{(j)}$ to the total matter density by defining a dimensionless density parameter

$$\Omega_{(j)} = \frac{a^2 \rho^{(j)}}{3\mathcal{H}^2}, \quad (2.62)$$

where the factor $3\mathcal{H}^2/a^2$ is the critical density. In the flat universe that concerns us, the curvature contribution Ω_κ is zero and the sum of all matter contributions is unity, i.e.,

$$\sum_j \Omega_{(j)} = \Omega_0 = 1. \quad (2.63)$$

(note that the dark energy that dominates the expansion in the present stage of our universe should also be included in this sum. This component is customarily denoted by Ω_Λ .) With these definitions Eq. (2.56) can be written in the form

$$\left(\frac{\mathcal{H}}{\mathcal{H}_i}\right)^2 = a^2 \left\{ \sum_j \Omega_{(j)} \left(\frac{a}{a_i}\right)^{-3(1+w^{(j)})} \right\}. \quad (2.64)$$

For the case in which the matter is dominated by a single scalar field ϕ , energy density conservation leads to the Klein-Gordon equation,

$$\phi_{;\mu}{}^\mu = \frac{dV}{d\phi}, \quad (2.65)$$

which can also be derived from the variation of the action with respect to ϕ . The potential V is assumed to be an explicit function of the field alone. In the case where there is more than one field, a Klein-Gordon equation is obtained for every scalar field, with an interaction potential U . Note that the Klein-Gordon equation is valid at all orders in the perturbation

expansion. We will rely on this important fact to derive the contribution of nonlinear perturbations to the non-Gaussianity of the primordial fluctuations, the ultimate objective of this chapter.

The Klein-Gordon equation for a homogeneous scalar field ϕ_0 for a FRW background metric is

$$\ddot{\phi}_0 + 3H\dot{\phi}_0 + \frac{dV}{d\phi} = 0. \quad (2.66)$$

The solutions of this equation will be explored in the context of inflation in Section 2.4. The inflationary behaviour is guaranteed when the dominating scalar field meets the so called slow-roll conditions. The dynamics of inflation will be discussed in more depth in the following sections. In the meantime we note that, as mentioned in Section 1.2, the perturbations produced during a period of inflation exit the cosmological horizon due to the shrinking of the latter scale. In a super-horizon regime, under suitable conditions, the curvature inhomogeneities are time-invariant.

2.3.2 Dynamics of perturbations

At linear order, the scalar metric perturbations are related to matter perturbations via the Einstein equations. The density and momentum constraints are

$$3\mathcal{H}(\mathcal{H}\varphi - \psi') + \nabla^2[\psi - \mathcal{H}\sigma] = -\frac{1}{2}a^2\delta\rho, \quad (2.67)$$

$$[\psi' - \mathcal{H}\varphi] = \frac{1}{2}a^2(\rho_0 + p_0)[v + B], \quad (2.68)$$

and two evolution equations for the scalar metric perturbations

$$\psi'' + 2\mathcal{H}\psi' - \mathcal{H}\phi' - (2\mathcal{H}' + \mathcal{H}^2)\varphi = -\frac{1}{2}a^2\delta p, \quad (2.69)$$

$$\sigma' + 2\mathcal{H}\sigma + \psi - \phi = 0. \quad (2.70)$$

The energy-momentum conservation equations for the perturbed spacetime are related to the ones above via the Bianchi identities. Specifically, the evolution for the energy density

perturbation is

$$\delta\rho' + 3\mathcal{H}(\delta p + \delta\rho) = -(p_0 + \rho_0) [3\psi' + \nabla^2(v + E')], \quad (2.71)$$

and the momentum conservation equation is

$$[(p_0 + \rho_0)(v + B)]' + \delta p = -(p_0 + \rho_0)[\varphi + 4\mathcal{H}(v + B)]. \quad (2.72)$$

Instead of solving the equations at first order, let us show how the dynamical linear equations encode two important implications for cosmological perturbations. A convenient way to find conserved quantities is to work in Fourier space (the Fourier transformation is here denoted by \mathcal{F} .) In this case, a generic coordinate-dependent perturbation $f(t, \mathbf{x})$ is decomposed into harmonic functions of time:

$$f(t, \mathbf{x}) = \frac{1}{(2\pi)^3} \int_0^\infty \exp(-i\mathbf{k} \cdot \mathbf{x}) f_k(t), \quad \text{i.e.,} \quad \mathcal{F}[f(t, \mathbf{x})] = f_k(t). \quad (2.73)$$

Each function $f_k(t)$ is referred as a perturbation mode and labelled by its comoving wavenumber k and has an associated scale $\lambda_k = a(t)/k$. The only characteristic scale of the unperturbed universe is the Hubble scale or cosmological horizon as defined in Eq. (2.33). When perturbation modes lie well outside the cosmological horizon, the ratio

$$\varepsilon \equiv d_H/\lambda_k = k/a(t)H(t) \quad (2.74)$$

is much smaller than one. Since the spatial derivatives ∇ are transformed to \mathbf{k}/a , this shows that we can neglect gradients terms in the equations compared to the time derivative which scales as H , i.e., for a given function $f(t, x)$ with Fourier transform $f_k(t)$,

$$|\mathcal{F}[\nabla f(t, x)]| = \left| \frac{\mathbf{k}}{a} f_k(t) \right| \ll H. \quad (2.75)$$

This simplifies the equations considerably and shows under which conditions the curvature perturbations are conserved in the superhorizon regime.

Let us use this approximation to look at the equivalence of the curvature perturbation

on large scales in different gauges. From the Einstein equations we can rewrite the gauge invariant curvature perturbation \mathcal{R} in terms of the curvature perturbation variables. Making use of the momentum constraint Eq. (2.68), we note that

$$v + B = \frac{\mathcal{H}\varphi - \psi'}{\mathcal{H}' - \mathcal{H}^2}. \quad (2.76)$$

We can insert this in the definition of \mathcal{R} in Eq. (2.43) and write the latter in terms of the Bardeen gauge-invariant quantities. That is,

$$\mathcal{R} = -\Psi_B + \frac{\mathcal{H}(\mathcal{H}\Phi_B + \Psi'_B)}{\mathcal{H}' - \mathcal{H}^2}, \quad (2.77)$$

which represents an alternative form of Eq. (2.68).

We can follow a similar procedure for Eq. (2.67) and write the uniform density curvature perturbation ζ in terms of Bardeen invariants:

$$\zeta \left(\frac{\mathcal{H}' - \mathcal{H}^2}{\mathcal{H}} \right) = \Psi'_B + \mathcal{H}\Phi_B - \left(\frac{\mathcal{H}' - \mathcal{H}^2}{\mathcal{H}} \right) \Psi_B - \frac{1}{3\mathcal{H}} \nabla^2 \Psi_B. \quad (2.78)$$

Note that, because the curvature perturbations in the last two equations are written in terms of gauge-invariant quantities, \mathcal{R} and ζ are manifestly gauge-invariant themselves. Moreover, the combination of these equations leads to the gauge-invariant generalisation of the Poisson equation,

$$\nabla^2 \Psi_B = 3 (\mathcal{H}' - \mathcal{H}^2) (\mathcal{R} - \zeta) = \frac{a^2}{2} \delta\rho_m. \quad (2.79)$$

As before, if gradients are discarded, both \mathcal{R} and ζ coincide. This result is important in view of the consequent correspondence (2.44), which is used extensively throughout this thesis.

A second important feature is the evolution of ζ on superhorizon scales. The energy conservation Eq. (2.71) can be written in coordinate time as

$$\dot{\delta\rho} + 3H (\delta\rho + \delta p) = - (p_0 + \rho_0) \left[3\dot{\psi} + \nabla^2 \left(\frac{v}{a} + \dot{E} \right) \right]. \quad (2.80)$$

This leads to an evolution equation for the perturbed energy density when we include Eq. (2.59):

$$[\rho_0 + \delta\rho] \dot{+} 3 \left(H + \dot{\psi} \right) [p_0 + \delta p + \rho_0 + \delta\rho] = -\nabla \left(\frac{v}{a} + \dot{E} \right) + \mathcal{O}(\delta^2), \quad (2.81)$$

which in view of the definition of the expansion $\theta_{(t)}$, Eq. (2.30), gives to first order

$$\dot{\rho} + \theta_{(t)} [p + \rho] = \nabla^2 \left[\frac{v}{a} + \dot{E} \right] + \nabla^2 (\sigma_{(t)}) [p_0 + \rho_0] + \mathcal{O}(\delta^2). \quad (2.82)$$

We emphasise that, in our notation, the density and pressure with no subscript represent the sum of the background function and its perturbation, i.e., $\rho = \rho_0 + \delta\rho$. The $\mathcal{O}(\delta^2)$ term indicates that the above equation is valid to first order in perturbation expansion.

Since we are discarding spatial gradients in the equations of motion on super-horizon scales, Eq. (2.81) provides an evolution equation for the curvature perturbation:

$$\dot{\psi} [p_0 + \rho_0] = -\frac{\dot{\rho}}{3} - H (p + \rho), \quad (2.83)$$

or

$$\dot{\psi} = -\frac{1}{3} \frac{\dot{\delta\rho}}{p_0 + \rho_0} + \frac{\dot{\rho}_0}{3} \left(\frac{\delta p + \delta\rho}{(p_0 + \rho_0)^2} \right). \quad (2.84)$$

If we work in a gauge where the time slices are uniform-density hypersurfaces, i.e., the uniform-density gauge, we may set

$$\delta\rho \rightarrow 0, \quad \delta p \rightarrow \delta p_{\delta\rho}, \quad \psi \rightarrow \psi_{\delta\rho} \equiv \zeta.$$

All perturbations, including the pressure perturbation in this gauge are independent of the density perturbation. From thermodynamics we know that in fluids where entropy is constant the pressure is a function of the density. In this category fall the barotropic fluids, defined as those fluids in which the pressure is only a function of the density ρ and vice-versa. In general the pressure of a thermodynamic system (in our case the universe) is a function of both the density and the entropy,

$$\delta p = c_s^2 \delta\rho|_s + \delta p|_\rho, \quad (2.85)$$

where $c_s^2 = \partial p / \partial \rho|_s$ is the adiabatic sound speed in the system (see e.g. Christopherson & Malik [2009] for a careful treatment of thermodynamics of fluids in cosmology). If one defines the entropy perturbation δs from the identity $\delta p|_\rho = \dot{p} \delta s$, then one has

$$\delta s = \frac{\delta p}{\dot{p}} - \frac{\delta \rho}{\dot{\rho}}. \quad (2.86)$$

In view of this, Eq. (2.84) for the curvature perturbation reduces to

$$\dot{\zeta} = \frac{\dot{\rho}_0}{3} \left(\frac{\delta p_{\delta \rho}}{(p_0 + \rho_0)^2} \right) = -\frac{H \dot{\rho}_0}{p_0 + \rho_0} \delta s. \quad (2.87)$$

This result is important in the description of the evolution of perturbations after inflation. It indicates that for inhomogeneities with characteristic scales much larger than the size of the cosmological horizon, the curvature can only be modified if the matter content of the universe has a non-adiabatic or entropy component [Wands et al., 2000]. It is also remarkable that this argument requires the conservation of the energy-momentum tensor, and not necessarily the Einstein equations. This means that the described property is valid for any theory of gravity in which energy is conserved.

This result has been extended beyond linear order in the perturbation expansion. On superhorizon scales, the expression at second order is [Malik & Wands, 2004],

$$\dot{\zeta}_2 = \frac{\dot{\rho}_0}{3(p_0 + \rho_0)^2} \delta p_2|_\rho - \left[\frac{2}{(p_0 + \rho_0)} \delta p_1|_\rho - 2(p_0 + \rho_0) \zeta_1 \right] \dot{\zeta}_1, \quad (2.88)$$

where numerical indices indicate the order of each quantity in the perturbation expansion. This result shows that, as in the case of the linear ζ , the evolution at second order depends only on the entropy perturbation and its derivatives. This has also been proved to all orders by Lyth et al. [2005]. This result generalises the special cases of a constant equation of state, i.e., $p/\rho = \text{const.}$ and the single field inflationary case, for which the conservation of ζ had been previously been verified [Shibata & Sasaki, 1999; Salopek & Bond, 1990].

Eqs. (2.87) and (2.88) have motivated several studies searching for significant growth of ζ on superhorizon scales during and after inflation. In particular, theories of multi-field inflation have been proposed to generate the the curvature perturbation and, at the same

time, an observable signature of non-Gaussianity [Mollerach, 1990; Lyth & Wands, 2002; Enqvist & Nurmi, 2005]. We will now study the effects of considering an auxiliary field, with special attention to those models where a large non-Gaussian contribution arises. We start with a short description of inflation in the next section.

2.4 Inflation

One can define cosmological inflation as the epoch when the scale factor of the universe is accelerating¹:

$$\ddot{a} > 0. \quad (2.89)$$

This condition can be written in terms of a more physical quantity. The period of inflation can be considered as an epoch in which the comoving Hubble horizon decreases with time:

$$\frac{d}{dt} (\mathcal{H}^{-1}) < 0. \quad (2.90)$$

Within general relativity, the above conditions on the time dependence of the scale factor give conditions on the matter content through the Einstein equations. In particular, Eq. (2.57) can be used to write the condition (2.90) as

$$3p_0 + \rho_0 < 0. \quad (2.91)$$

Demanding a positive energy density $T_0^0 = \rho_0$ is a sensible physical condition. The condition $T^{00} > 0$ is known as the weak energy condition. In view of this, the above equation demands that the dominant matter must have negative pressure during a period of inflation. The simplest matter field with this property is a scalar field, which is composed of spin-0 particles. The concept of a scalar field is prevalent in particle physics where scalars such as the Higgs scalar are essential in the construction of the standard model. Although no scalar particle has so far been observed, they play a fundamental role in cosmology, as they possess

¹This does not include the late time acceleration at the current epoch which is attributed to dark energy. Whereas inflation-like scalar fields may be responsible for such behaviour (see, e.g., Martin [2008]), in this thesis we are not concerned with the dynamics of the late universe

the unusual feature of their potential energy dominating over their kinetic energy.

As indicated by Eq. (2.51), the Lagrangian definition of the energy-momentum tensor requires that the energy density and pressure for a homogeneous scalar field be

$$\rho_0 = \frac{1}{2}\dot{\phi}^2 + V(\phi), \quad p_0 = \frac{1}{2}\dot{\phi}^2 - V(\phi). \quad (2.92)$$

This shows that in order to meet condition (2.91) we require the potential $V(\phi)$ to dominate over the ‘kinetic’ term. This can be dynamically achieved with a sufficiently flat potential provided the field is displaced away from its minimum. Such physical conditions are controlled by two parameters:

$$\epsilon_{\text{SR}} \equiv \frac{M_{\text{P}}^2}{2} \left(\frac{V'}{V} \right)^2, \quad \eta_{\text{SR}} \equiv M_{\text{P}} \frac{V''}{V}. \quad (2.93)$$

These are called the slow-roll parameters and, during inflation, they are subject to the slow-roll and friction-dominated conditions

$$\epsilon_{\text{SR}} \ll 1, \quad \eta_{\text{SR}} \ll 1. \quad (2.94)$$

The first condition, the ‘slow-roll’ condition, ensures the slow rolling of the field down its potential. The second, a ‘friction-domination’ condition constrains the potential to be very flat one for the period of inflation. This condition is imposed to allow for an extended period of inflation (which should last for over 60 e-folds of expansion), required to recover a sufficiently flat and homogeneous universe in the observed scales. When both slow-roll parameters are much smaller than one, the dynamics of the single field ϕ guarantees an accelerated expansion with a shrinking comoving Hubble horizon.

The scalar field satisfying these properties is called the inflaton. The equations dictating the background dynamics of a universe dominated by the inflaton are

$$H^2 = \frac{V(\phi)}{3}, \quad (2.95)$$

$$3H\dot{\phi} = -V'(\phi). \quad (2.96)$$

The homogeneous Klein-Gordon equation (2.66), reduces to Eq. (2.96) in the slow-roll

regime. The exact solution to these equations requires the specification of the potential as a function of the homogeneous scalar field $\phi(t)$. However, the first equation already shows that, if we assume a constant V ,

$$a(t) \propto \exp(\sqrt{V/3}t). \quad (2.97)$$

This illustrates explicitly the exponential growth of the scale factor in the inflationary regime. Additionally, the field depends only linearly on time to lowest order, as expected for a slow rolling field. An expansion in powers of the slow-roll parameters shows that any deviation from this behaviour should be orders of magnitude smaller than the form expressed here [Stewart & Lyth, 1993]. In the following we focus on the study of the tiny inhomogeneities produced by quantum fluctuations of the inflationary field. This aspect is crucial in understanding the origin of the observed structure in the universe.

2.4.1 Inflationary field power spectrum

The mean amplitude of matter or curvature perturbations is inferred from their power spectrum. This is constructed through the quantization of real perturbation fields, as prescribed by quantum field theory [Birrell & Davies, 1984]. Following a perturbative expansion, we split the scalar field as

$$\phi(t, \mathbf{x}) = \phi_0(t) + \delta\phi(t, \mathbf{x}). \quad (2.98)$$

Such an expansion separates the general Klein-Gordon equation (2.65) into its homogeneous part (2.66) and the perturbation equation

$$\delta\ddot{\phi} + 3H\delta\dot{\phi} - \frac{\nabla^2\delta\phi}{a^2} + m_{\delta\phi}^2\delta\phi = 0, \quad (2.99)$$

where the effective mass of the field fluctuation is defined as

$$m_{\delta\phi}^2 = m_\phi^2 + V''_{NL}, \quad (2.100)$$

and $V_{NL} = V - m_\phi^2\phi^2/2$ represents the nonlinear part of the potential. Note that here we have

neglected the perturbations of the metric which enter the Klein-Gordon equation through the operator ∂_ν^ν . In this case, Eq. (2.99) is a valid approximation because we consider ϕ to be subject to the slow-roll conditions.

In order to compute the power spectrum of the field perturbations, we need to consider the free field $\delta\phi_I$, or the field in the so-called *interaction picture* of quantum field theory [Peskin & Schroeder, 1995]. This field is the solution to the Klein-Gordon equation (2.99) in the absence of the nonlinear term, i.e.

$$\delta\ddot{\phi}_I + 3H\delta\dot{\phi}_I - \frac{\nabla^2\delta\phi_I}{a^2} + m_\phi^2\delta\phi_I = 0. \quad (2.101)$$

In the quantum framework we Fourier decompose this field as

$$\delta\phi_I(\mathbf{x}, t) = \int \frac{dk^3}{(2\pi)^3} \left(e^{i\mathbf{k}\cdot\mathbf{x}} a_k \delta\phi_{I\mathbf{k}}(t) + e^{-i\mathbf{k}\cdot\mathbf{x}} a_k^\dagger \delta\phi_{I\mathbf{k}}^*(t) \right), \quad (2.102)$$

where $*$ denotes complex conjugation and \dagger the hermitian adjoint operator. a_k and a_k^\dagger are operators satisfying the usual canonical commutation relations,

$$[a_k, a_p^\dagger] = \delta^{(3)}(\mathbf{k} - \mathbf{p}), \quad [a_k, a_p] = [a_k^\dagger, a_p^\dagger] = 0, \quad (2.103)$$

and $\delta^{(3)}(\mathbf{k})$ is the three-dimensional Dirac delta function. Thus the field fluctuations in Fourier space are solutions of the linear equation

$$\delta\ddot{\phi}_{I\mathbf{k}} + 3H\delta\dot{\phi}_{I\mathbf{k}} + \left(\frac{k^2}{a^2} + m_\phi^2 \right) \delta\phi_{I\mathbf{k}} = 0. \quad (2.104)$$

For simplicity, we only consider de Sitter inflation, where H is constant, and the scale factor is $a = -1/(H\eta)$. As mentioned above, this is a good approximation in slow-roll inflation.

In terms of conformal time, the previous equation can be written as

$$\delta\phi_{I\mathbf{k}}'' + 3\eta^{-1}\delta\phi_{I\mathbf{k}}' + \left[k^2 + \eta^{-2} \left(\frac{m_\phi}{H} \right)^2 \right] \delta\phi_{I\mathbf{k}} = 0. \quad (2.105)$$

The solution to this equation involves the set of Bessel complex functions. After proper normalisation, i.e., taking the Bunch-Davies vacuum for the de Sitter spacetime [Bunch &

[Davies, 1988], one finds

$$\delta\phi_{I\mathbf{k}}(\eta) = \frac{\sqrt{\pi}}{2a} \sqrt{-\eta} H_\nu^{(1)}(|k\eta|), \quad (2.106)$$

where $H_\nu^{(1)}$ is the Hankel function of the first kind and of order

$$\nu = \sqrt{\frac{9}{4} - \frac{m_\phi^2}{H_*^2}}. \quad (2.107)$$

The star indicates that we are evaluating H just after Hubble horizon exit², i.e., when $k = k_* = |1/\eta_*| \lesssim aH$.

The two-point function of the field fluctuations reads

$$\langle \delta\phi_{I\mathbf{k}_1}(\eta) \delta\phi_{I\mathbf{k}_2}(\eta) \rangle = (2\pi)^3 \delta^{(3)}(\mathbf{k}_1 + \mathbf{k}_2) \frac{\pi H_*^2}{4k_1^3} (|k_1\eta|)^3 |H_\nu^{(1)}(|k_1\eta|)|^2. \quad (2.108)$$

where the angled brackets indicate the expectation value, in this case, of two modes of the perturbation field, evaluated at time η . In terms of the two-point function, the power spectrum P_ϕ is defined as

$$\langle \delta\phi_{I\mathbf{k}_1}(\eta) \delta\phi_{I\mathbf{k}_2}(\eta) \rangle = (2\pi)^3 \delta^{(3)}(\mathbf{k}_1 + \mathbf{k}_2) P_\phi(\eta, k_1), \quad (2.109)$$

and the dimensionless power spectrum in this case is

$$\mathcal{P}_\phi(\eta, k) = \frac{k^3}{2\pi^2} P_\phi(\eta, k) = \frac{H_*^2}{8\pi} (|k\eta|)^3 |H_\nu^{(1)}(|k\eta|)|^2. \quad (2.110)$$

By expanding the Hankel function in Eq. (2.108) on large scales, i.e. for $|k\eta| \ll 1$, one obtains

$$\mathcal{P}_\phi(\eta, k) = 2^{-2\omega} \frac{\Gamma(\frac{3}{2} - \omega)^2}{\pi^3} H_*^2 (|k\eta|)^{2\omega} \simeq (1 + \mathcal{O}(\omega)) \left(\frac{H_*}{2\pi}\right)^2 (|k\eta|)^{2\omega}, \quad (2.111)$$

²In the perturbed KG equation the mass term is negligible because of the slow-roll condition $V''/V \ll V$, which is equivalent to $m_\phi \ll H$. Well before horizon exit the harmonic flat spacetime equation is recovered in the solution Eq. (2.106). On the other hand, there is no need to compute the correlation at times well after horizon exit. The relation (2.44) and the fact that \mathcal{R} is conserved well outside the horizon indicate that the required field power spectrum can be evaluated a few Hubble times after horizon crossing.

where

$$\omega \equiv \frac{3}{2} - \nu \sim \frac{m_\phi^2}{3H_*^2}. \quad (2.112)$$

This is negligible in the massless case which corresponds to a de Sitter inflationary phase. Note that, in this case, the approximation of a linearised potential is guaranteed by the slow-roll approximation. Higher order terms in the Klein-Gordon equation are suppressed by powers of the slow-roll parameters. In this way, interaction between Fourier modes are absent, i.e., the vacuum fluctuations of different Fourier modes are decoupled and the field fluctuations are Gaussian.

2.4.2 Observables

In the standard picture of inflation, the perturbations of the inflaton field are stretched out of the horizon and subsequently transferred into curvature perturbations which survive after the universe has reheated. Observationally, the temperature inhomogeneities in the CMB are related to the mean amplitude of the curvature perturbations through the Sachs-Wolfe effect [Sachs & Wolfe, 1967]. Thus, the power spectrum of curvature perturbations is observed to be [Komatsu et al., 2008]

$$\mathcal{P}_{\mathcal{R}} = (2.45^{+0.092}_{-0.093}) \times 10^{-9} \quad (95\% \text{ CL}). \quad (2.113)$$

at a pivot scale $k_0 = 7.5a_0H_0 \approx 0.001 h_0 \text{ Mpc}^{-1}$. The power spectrum is also probed at other scales in the CMB with various filter functions and also with the power spectrum of galaxies and clusters. The rate of change of the observed value of \mathcal{P} with k is parametrised by the spectral index n_s . This is defined by

$$n_s - 1 \equiv \frac{d \log \mathcal{P}_{\mathcal{R}}}{d \log k}, \quad (2.114)$$

where 1 is subtracted by convention due to the fact that the matter density power spectrum has the form $P_\rho \propto k^{n_s}$. Observationally, the output from WMAP [Komatsu et al., 2008], the distance measurements from type 1a supernovae [Riess et al., 2007; Astier et al., 2006] and

the baryon acoustic oscillations [Percival et al., 2007] constrain the spectral index to be

$$-0.256 < 1 - n_s < 0.025 \quad (95\% \text{ CL}). \quad (2.115)$$

for $0.001 \text{ Mpc}^{-1} < k < 0.1 \text{ Mpc}^{-1}$.

In single-field inflation, the power spectrum of curvature perturbations can be calculated from \mathcal{P}_ϕ and Eq. (2.44), which for a single scalar field can be written as

$$\mathcal{R} = -\frac{H}{\dot{\phi}} \delta\phi. \quad (2.116)$$

This relation, used at linear order in Eqs. (2.109) and (2.110), shows that

$$\mathcal{P}_{\mathcal{R}} = \left(\frac{H}{\dot{\phi}}\right)^2 \mathcal{P}_\phi \simeq (1 + \mathcal{O}(\omega)) \left(\frac{H_*^2}{2\pi\dot{\phi}_*}\right)^2 |k\eta|^{2\omega}. \quad (2.117)$$

In terms of the slow-roll parameters, using Eqs. (2.95) and (2.96) and evaluating the previous expression at horizon crossing, we have

$$\mathcal{P}_{\mathcal{R}} = \frac{2^8 V_*^3}{3 V_*'^2} = \frac{8 V_*}{3 \epsilon_*}. \quad (2.118)$$

Note that the evaluation of the power spectrum at horizon exit is justified by the fact that \mathcal{R} is constant on super-horizon scales. In this regime we can define the root-mean-square (RMS) value of \mathcal{R} (or ζ) as

$$\mathcal{R}_{\text{RMS}} = \zeta_{\text{RMS}} = \frac{H}{\dot{\phi}} \delta\phi_{\text{RMS}} \approx \frac{H^2}{2\pi\dot{\phi}}. \quad (2.119)$$

This quantity will play an important role throughout this thesis.

We can also write the spectral index as [Stewart & Lyth, 1993]

$$n_s = 1 + 2\eta_{\text{SR}} - 6\epsilon_{\text{SR}}, \quad (2.120)$$

to lowest order in slow-roll expansion. When $n_s = 1$, the power spectrum is called scale-invariant or Harrison-Zeldovich [Harrison, 1970; Zeldovich, 1972]. When $n_s \neq 1$, the spec-

trum is described as tilted and, for $n_s > 1$, it is called ‘blue’ because the power is enhanced at small wavelengths [Mollerach et al., 1994]. With the precision reached by the latest probes of cosmological structure, it has been possible to constrain the field parameters and discard some models of inflation alternative to the simplest picture presented above [Alabidi & Lyth, 2006a; Alabidi & Lidsey, 2008]. Current observations of the CMB and large-scale structure, however, are compatible with the predictions of many other models of inflation. It is therefore crucial to study additional observables which provide further insight into the characteristics of the early universe. At the level of scalar perturbations, the most convenient observables for discriminating between these models are the tensorial perturbations mean amplitude and spectral index, the running of the spectral index and the non-Gaussianity of perturbations. In this thesis we focus on the effects of the latter.

2.4.3 The δN formalism

We now present a formalism to account for the contributions of multiple fields to the curvature perturbation at all orders. An important feature of the perturbed curvature on superhorizon scales is that we can calculate its magnitude by considering the change in the number of e-folds of expansion of the relevant patch of universe with respect to a uniform background expansion. This in turn allows us to compute the amplitude of the curvature fluctuations from the matter fluctuations. The idea behind this technique is to consider ζ as a perturbation in the local expansion [Starobinsky, 1985; Salopek & Bond, 1990; Sasaki & Stewart, 1996; Sasaki & Tanaka, 1998; Lyth et al., 2005], i.e.

$$\zeta = \delta N, \tag{2.121}$$

where δN is the perturbed expansion of the uniform-density hypersurfaces with respect to spatially flat hypersurfaces.

We now describe the elements of the above formalism. The number of e-folds of expansion between two moments in proper time τ_1 and τ_2 is given in the homogeneous background

by

$$N = \int_{\tau_1}^{\tau_2} \frac{1}{3} \theta_0 d\tau = \int_{t_1}^{t_2} \frac{1}{3} \theta_{(t)} dt = \int_{t_1}^{t_2} H dt, \quad (2.122)$$

where θ_0 refers to the homogeneous expansion, that is, θ considered to lowest order in Eq. (2.29). In the perturbed metric, the number of e-foldings along an integral curve of the 4-velocity, i.e., along a comoving worldline between τ_1 and τ_2 , is

$$\mathcal{N} = \int_{\tau_1}^{\tau_2} \frac{1}{3} \theta d\tau = \int_{t_1}^{t_2} \frac{1}{3} \theta_{(t)} (1 + \varphi)(1 - \varphi) dt = \int_{t_1}^{t_2} (H + \dot{\psi}) dt. \quad (2.123)$$

The last equality holds on superhorizon scales. It is clear that the difference $\mathcal{N} - N$ will provide the change in the curvature perturbation from an initial hypersurface at time t_1 and a final one at time t_2 , i.e.,

$$\delta N = \mathcal{N} - N = \Delta\psi. \quad (2.124)$$

In particular, we can choose to integrate the expansion starting from an initial uniform-curvature hypersurface at time t_1 , that is, $\psi(t_1) = 0$. Then we can find the amplitude of the curvature perturbation at the later time t_2 by choosing a trajectory with an endpoint t_2 fixed on a comoving or uniform-density hypersurface. Denoting the difference between the background and the perturbed expansion as $\delta\theta$, we can write

$$\delta N = \int_{t_1}^{t_2} \delta\theta_{(t)} d\eta = \psi_2. \quad (2.125)$$

In particular, when we consider the endpoint embedded in a uniform-density hypersurface, then Eq. (2.121) is recovered.

On large scales, where spatial gradients can be neglected, the local physical quantities like density and expansion rate obey the same evolution equations as in a homogeneous FRW universe [Wands et al., 2000; Sasaki & Stewart, 1996]. By using homogeneous FRW universes to describe the evolution of local patches, we can evaluate the perturbed expansion in different parts of our universe with particular initial values for the fields during inflation. This is known as the ‘separate universe’ approach and means that, when we neglect the

decaying mode for the field perturbations on superhorizon scales, we can consider the local integrated expansion as a function of the local field values on the initial hypersurface. In particular, one can expand Eq. (2.121) as

$$\zeta = \delta N(\phi_i(t_1)) = \sum_i \frac{\partial N(t_2)}{\partial \phi_i} \delta \phi_i(t_1) \quad (2.126)$$

where the initial time t_1 again corresponds to some initial spatially-flat hypersurface. We can use this formula to construct the curvature power spectrum in multi-field inflation:

$$\mathcal{P}_\zeta = \sum_i \left(\frac{\partial N(t_2)}{\partial \phi_i} \right)^2 \mathcal{P}_{\delta\phi}. \quad (2.127)$$

This formalism can be extended to establish the equivalence between nonlinear matter and metric perturbations. This is done by first assuming Eq. (2.121) as the definition of the curvature perturbation and then using Eq. (2.44) to integrate ζ . This gives [Lyth et al., 2005]

$$\zeta = \frac{1}{3(w+1)} \ln \left(\frac{\rho_\kappa}{\rho_0} \right). \quad (2.128)$$

This nonlinear curvature perturbation can be written as a function of the initial field fluctuations, evaluated again at an initial flat hypersurface labelled by the time t_1 . We use a Taylor expansion

$$\zeta = \sum_i \frac{\partial N}{\partial \phi_i} \delta \phi_i(t_1) + \frac{1}{2} \frac{\partial^2 N}{\partial \phi_j \partial \phi_i} \delta \phi_j(t_1) \delta \phi_i(t_1) + \dots \quad (2.129)$$

where the leading order term coincides with the expansion (2.126). This last expansion greatly simplifies the derivation of the higher-order curvature correlations from the scalar field bispectrum.

2.5 Non-Gaussianity from isocurvature fields

The perturbed energy conservation equations show the conditions under which the curvature perturbation ζ may vary over time in a regime in which the perturbation modes lie well out-

side the horizon. Specifically, Eq. (2.87) shows that the evolution of ζ is directly related to the presence of an entropy perturbation δs . This quantity can be the intrinsic non-adiabatic pressure of a single field, or the difference in the density perturbations of any two fields which contribute to the curvature perturbation. This effect motivates the study of models of inflation in which the observed inhomogeneities are the result of non-adiabatic field fluctuations [Mollerach, 1990; Linde & Mukhanov, 1997; Enqvist & Sloth, 2002; Lyth & Wands, 2002; Moroi & Takahashi, 2001]. Here we are interested specifically in models in which a highly nonlinear ζ can be generated from the aforementioned entropy perturbation. Out of the multiple stages in which this field may have influenced ζ , we focus on the case of an auxiliary scalar field during inflation generally referred as the isocurvature field χ [Zaldarriaga, 2004; Enqvist & Nurmi, 2005; Enqvist et al., 2005b].

A first approximation to nonlinear ζ involves the first and second order perturbations in real space:

$$\zeta(t, \mathbf{x}) = \zeta_1(t, \mathbf{x}) + \frac{1}{2}\zeta_2(t, \mathbf{x}). \quad (2.130)$$

The second order perturbation is conventionally written in terms of the first order perturbation and the parameter f_{NL} [Komatsu & Spergel, 2001]. This gives

$$\zeta(t, \mathbf{x}) = \zeta_1(t, \mathbf{x}) - \frac{3}{5}f_{\text{NL}} (\zeta_1^2(t, \mathbf{x}) - \langle \zeta_1^2(t, x) \rangle), \quad (2.131)$$

which in Fourier space is written as a convolution

$$\zeta(\mathbf{k}) = \zeta_1(\mathbf{k}) - \frac{3}{5}f_{\text{NL}} ([\zeta_1 \star \zeta_1](\mathbf{k}) - \langle \zeta_1^2(k) \rangle). \quad (2.132)$$

Note that Eq. (2.132) shows explicitly the superposition of modes that characterise non-Gaussian statistics.

Statistically, non-Gaussianity refers to the non-vanishing higher order moments of the quantity in question. In quantum mechanics this corresponds to the n -point correlation functions with $n \geq 3$. To lowest order, the bispectrum $B_\zeta(k_1, k_2, k_3)$ is defined by the expectation

value of the product of three copies of the curvature field:

$$\langle \zeta(\mathbf{k}_1)\zeta(\mathbf{k}_2)\zeta(\mathbf{k}_3) \rangle = (2\pi)^3 B_\zeta(k_1, k_2, k_3) \delta^{(3)}(\mathbf{k}_1, \mathbf{k}_2, \mathbf{k}_3). \quad (2.133)$$

The amplitude of f_{NL} is given in terms of the bispectrum by substituting Eq. (2.132) in this:

$$\frac{6}{5} f_{\text{NL}} = \frac{\prod_i k_i^3}{\sum_i k_i^3} \frac{B_\zeta}{4\pi^4 \mathcal{P}_\zeta}. \quad (2.134)$$

In this section we present a method to compute the nonlinear ζ by determining nonlinear solutions to the Klein-Gordon equation of the field fluctuation. Then with the aid of the δN formalism we will construct the three-point correlator of ζ . Special attention will be paid to the cases in which a large f_{NL} can be obtained.

2.5.1 Two-field inflation

Here we consider a spacetime inflating by the action of a potential which depends on two minimally coupled fields. In this case, in addition to the canonical inflationary field, we consider a second field χ described by the action

$$\mathcal{S}_\chi = \int dx^4 \sqrt{-g} \left[-\frac{1}{2} g^{\mu\nu} \partial_\mu \chi \partial_\nu \chi - \frac{1}{2} m_\chi^2 \chi^2 - W(\chi) \right], \quad (2.135)$$

where $W(\chi)$ plays the role of a nonlinear potential. The joint Lagrangian density of the two scalar fields in this model is given by Eq. (2.52). The model in question demands that there is no contribution of χ to the background matter content. This is guaranteed by the following condition on the potential of the two-field Lagrangian defined in Eq. (2.52):

$$U(\phi, \chi) \approx V(\phi) \quad \Rightarrow \quad W(\chi) + \frac{1}{2} m_\chi^2 \chi^2 \ll V(\phi). \quad (2.136)$$

To analyse the dynamics of this auxiliary field, let us consider a background homogeneous part and a coordinate-dependent field fluctuation,

$$\chi(t, \mathbf{x}) = \chi_0(t) + \delta\chi(t, \mathbf{x}). \quad (2.137)$$

The Klein-Gordon equation derived by varying the action (2.135) with respect to χ yields for the background field

$$\ddot{\chi}_0 + 3H\dot{\chi}_0 + m_\chi^2\chi_0 + W'(\chi_0) = 0, \quad (2.138)$$

and for the field fluctuation

$$\delta\ddot{\chi} + 3H\delta\dot{\chi} - \frac{\nabla^2\delta\chi}{a^2} + m_{\delta\chi}^2\delta\chi + \sum_{n=3} \frac{W^{(n)}}{(n-1)!}\delta\chi^{n-1} = 0. \quad (2.139)$$

Here a superscript (n) denotes the n -th derivative and $m_{\delta\chi}^2$ is the effective mass for the field fluctuation defined as

$$m_{\delta\chi}^2 = m_\chi^2 + W''. \quad (2.140)$$

Following the same steps as with the inflaton power spectrum, we recover a solution similar to Eq. (2.106). Specifically,

$$\mathcal{P}_\chi(\eta, k) = \frac{H^2}{8\pi} (|k\eta|)^3 |H_\mu^{(1)}(|k\eta|)| = 2^{-2\alpha} \frac{\Gamma(\frac{3}{2} - \alpha)^2}{\pi^3} H_*^2 (|k\eta|)^{2\alpha}, \quad (2.141)$$

with α and μ defined through the equation

$$\alpha \equiv \sqrt{\mu^2 - \frac{9}{4}} \approx \frac{m_{\delta\chi}^2}{3H^2} > 0. \quad (2.142)$$

Because of this, the spectrum of χ is blue. The power spectrum \mathcal{P}_χ vanishes on large scales for large values of α , i.e. when $m_{\delta\chi} \gtrsim H_*$, so we only consider the case

$$m_{\delta\chi} \lesssim H_*. \quad (2.143)$$

Indeed, we assume $m_\chi \ll H_*$. As shown below, the interesting values of W'' are those which are large enough to generate a large nonlinear coupling, but sufficiently small to satisfy condition (2.143), which also implies

$$W'' \lesssim H_*^2. \quad (2.144)$$

For example, for

$$W = \frac{M}{3!}\chi^3 + \frac{\lambda}{4!}\chi^4, \quad (2.145)$$

this condition turns into conditions on M and λ :

$$M \lesssim \frac{H_*^2}{\chi_0}, \quad \lambda^{1/2} \lesssim \frac{H_*}{\chi_0}. \quad (2.146)$$

Typically we have a nonzero expectation value χ_0 . Working in a perturbative expansion then requires that the quantum fluctuations $\delta\chi$ do not exceed this expectation value, i.e., we require $\chi_0 \gtrsim H_*$. This imposes additional constraints on the parameters M and λ in the specific model of Eq. (2.145), as described below.

2.5.2 Non-Gaussianity and nonlinear evolution

The expectation value of the product of three fields was first computed by Maldacena [2003] for the case of single-field inflation, including slow-roll scalar field and gravitational interactions. In our case, since the field gives a negligible contribution to the energy density of the Universe, we will neglect its coupling to gravity.

The three-point correlation function of the field perturbations $\delta\chi$ can be computed using the expression given by Maldacena:

$$\langle \delta\chi(t, \mathbf{x}_1)\delta\chi(t, \mathbf{x}_2)\delta\chi(t, \mathbf{x}_3) \rangle = i \int_{-\infty}^t dt' \langle [H_I(t'), \delta\chi_I(t, \mathbf{x}_1)\delta\chi_I(t, \mathbf{x}_2)\delta\chi_I(t, \mathbf{x}_3)] \rangle, \quad (2.147)$$

where H_I is the interaction Hamiltonian written in terms of the field perturbation in the interaction picture, i.e. in our case

$$H_I(t') = - \int dx^3 \sqrt{-g} \mathcal{L}_I = \sum_{n=3} \int dx^3 a(t')^3 \frac{W^{(n)}}{n!} \delta\chi_I^n. \quad (2.148)$$

Note that on the left-hand side of Eq. (2.147) the expectation value is taken with respect to the vacuum of the interacting theory, while on the right-hand side it is taken with respect to

the vacuum of the free theory. A generalisation of this expression to higher order correlators, including loop corrections, has been provided by Weinberg [2005].

Recently, Musso [2006] showed that the general expression for the correlators of m field fluctuations can also be derived by solving perturbatively the field equation of motion and using the expression for the two-point function of the free field fluctuation. Here we make use of this formalism to show that Eq. (2.147) can be derived by solving Eq. (2.139) perturbatively.

As mentioned before, the evolution equation for $\delta\chi_I$ is given in identical form to the inflaton case, providing $\phi \rightarrow \chi$ in Eq. (2.105). On the other hand, the evolution equation for the full nonlinear $\delta\chi$ can be given perturbatively providing $|(\delta\chi - \delta\chi_I)/\delta\chi| \ll 1$. Rewriting Eq. (2.139) and re-expressing the nonlinear term in terms of $\delta\chi_I$, we obtain

$$\delta\ddot{\chi} + 3H\delta\dot{\chi} - \frac{\nabla^2\delta\chi}{a^2} + m_{\delta\chi}^2\delta\chi = -\sum_{n=3} \frac{W^{(n)}}{(n-1)!} \delta\chi_I^{n-1}. \quad (2.149)$$

This equation can be then solved by Green's method and its solution is

$$\delta\chi(t, \mathbf{x}) = \delta\chi_I(t, \mathbf{x}) - \sum_{n=3}^{\infty} \frac{1}{(n-1)!} \int d^3y \int dt' a(t')^3 G_R(t, \mathbf{x}; t', \mathbf{y}) W^{(n)} \delta\chi_I^{n-1}(t', \mathbf{y}), \quad (2.150)$$

where $G_R(t, \mathbf{x}; t', \mathbf{y}')$ is the retarded Green's function

$$G_R(t, \mathbf{x}; t', \mathbf{y}') = i\Theta(t - t') [\delta\chi_I(t, \mathbf{x}), \delta\chi_I(t', \mathbf{y}')]. \quad (2.151)$$

where

$$\Theta(x) = \int_{-\infty}^x \delta(z) dz \quad (2.152)$$

is the Heaviside step function. By using the fact that the free-field perturbation is Gaussian, i.e.

$$\langle \delta\chi_I(\mathbf{x}_1, t) \delta\chi_I(\mathbf{x}_2, t) \delta\chi_I(\mathbf{x}_3, t) \rangle = 0, \quad (2.153)$$

one can rewrite the three-point correlation function of $\delta\chi$ making use of Eq. (2.150):

$$\begin{aligned} \langle \delta\chi(t, \mathbf{x}_1)\delta\chi(t, \mathbf{x}_2)\delta\chi(t, \mathbf{x}_3) \rangle &= - \sum_{n=3}^{\infty} \frac{i}{(n-1)!} \int dy^3 \int dt' a(t')^3 W^{(n)} \times \\ &[\delta\chi_I(t, \mathbf{x}_1), \delta\chi_I(t', \mathbf{y})] \langle \delta\chi_I^{n-1}(t', \mathbf{y})\delta\chi_I(t, \mathbf{x}_2)\delta\chi_I(t, \mathbf{x}_3) \rangle + \{\text{Perms.}\} \end{aligned} \quad (2.154)$$

Using this equation and the result [Musso, 2006],

$$\begin{aligned} n [\delta\chi_I(t, \mathbf{x}_1), \delta\chi_I(t', \mathbf{y})] \langle \delta\chi_I^{n-1}(t', \mathbf{y})\delta\chi_I(t, \mathbf{x}_2)\delta\chi_I(t, \mathbf{x}_3) \rangle + \{\text{perms}\} = \\ - \langle [\delta\chi_I^n(t', \mathbf{y}), \delta\chi_I(t, \mathbf{x}_1)\delta\chi_I(t, \mathbf{x}_2)\delta\chi_I(t, \mathbf{x}_3)] \rangle, \end{aligned} \quad (2.155)$$

one can derive Maldacena's formula (2.147) for the χ -Hamiltonian (2.148) after some manipulation. This shows that one can obtain Maldacena's formula either from considering perturbations in the action or from the perturbative expansion of the equations of motion. In the case of slow-roll inflation, this equivalence was shown by Seery et al. [2008]. Equation (2.147) can be generalised to higher correlation functions:

$$\begin{aligned} \langle \delta\chi(t, \mathbf{x}_1)\delta\chi(t, \mathbf{x}_2) \dots \delta\chi(t, \mathbf{x}_m) \rangle = \\ i \int_{-\infty}^t dt' \langle [H_I(t'), \delta\chi_I(t, \mathbf{x}_1)\delta\chi_I(t, \mathbf{x}_2) \dots \delta\chi_I(t, \mathbf{x}_m)] \rangle. \end{aligned} \quad (2.156)$$

2.5.3 Field bispectrum

Here we are interested in the three-point function of the scalar field, also called the field bispectrum $F(k_1, k_2, k_3)$, defined as

$$\langle \delta\chi_{\mathbf{k}_1}(\eta)\delta\chi_{\mathbf{k}_2}(\eta)\delta\chi_{\mathbf{k}_3}(\eta) \rangle = (2\pi)^3 \delta^{(3)}\left(\sum_i \mathbf{k}_i\right) F(\eta; k_1, k_2, k_3). \quad (2.157)$$

For simplicity, we assume that the nonlinear potential of the scalar field is dominated by the cubic interaction W''' and that this is approximately constant. This reduces the expansion in Eq. (2.148) to the first term only. Substituting this in Eq. (2.147) and using Eqs. (2.150) and

(2.155), the field bispectrum becomes

$$F(\eta; k_1, k_2, k_3) = \tag{2.158}$$

$$W''' \eta^{9/2} \frac{H_*^2}{4} \text{Re} \left\{ -i \frac{\pi^3}{2^3} \prod_i H_\mu^{(1)}(|k_i \eta|) \int_{-\infty}^{\eta} d\eta' \sqrt{|\eta'|} \prod_j H_\mu^{(2)}(|k_j \eta'|) \right\}.$$

During de Sitter inflation, the ratio k/aH can be written as the product $|k\eta|$ and we will use this to parametrise the various stages of evolution of the bispectrum.

It is instructive to first evaluate the bispectrum (2.158) during inflation ($\eta \leq \eta_{\text{reh}}$) for the case of a massless field fluctuation (i.e., $m_{\delta\chi} = \alpha = 0$, $\mu = 3/2$). In this case, the integral in Eq. (2.158) can be evaluated analytically [Bernardeau & Uzan, 2003; Zaldarriaga, 2004] using the expressions for the Hankel functions,

$$H_{3/2}^{(1)}(z) = -i \sqrt{\frac{2}{\pi}} (1 - iz) \frac{e^{iz}}{z^{3/2}}, \quad H_{3/2}^{(2)}(z) = i \sqrt{\frac{2}{\pi}} (1 + iz) \frac{e^{-iz}}{z^{3/2}}. \tag{2.159}$$

One finds³

$$F(\eta; k_1, k_2, k_3) = \frac{W''' H_*^2}{4 \prod_i k_i^3} \left[-\frac{4}{9} k_t^3 + k_t \sum_{i < j} k_i k_j + \frac{1}{3} \left(\frac{1}{3} + \gamma + \ln(|k_t \eta|) \right) \sum_i k_i^3 \right], \tag{2.160}$$

where $k_t = \sum_i k_i$. The integral in Eq. (2.158) has been evaluated for three different stages: when the modes are well inside the Hubble radius, around the Hubble radius and outside the Hubble radius. The first stage does not give any contribution to the integral because the Hankel functions oscillate rapidly for $|k_i \eta| \gg 1$ and the fields can be taken as free in the asymptotic past. At late time, the integral is dominated by the modes that are around the Hubble scale or larger, $|k\eta| \lesssim 1$. In particular, we will show below that the time-dependent term in Eq. (2.160), with the typical local momentum dependence, essentially comes from the nonlinear and classical super-Hubble evolution of the field perturbation. The finite part, with the non-trivial momentum dependence, comes from integrating over times corresponding to Hubble-crossing.

³Our result coincides with the one found in Zaldarriaga [2004], modulo the overall sign and the factor 1/3 inside the parentheses.

Let us now consider the case with $m_{\delta\chi} \neq 0$, and $1/2 < \mu < 3/2$. The integral inside Eq. (2.158) cannot be integrated analytically in this case. One can only evaluate it over the period when all modes are well outside the Hubble radius because, for small arguments, Hankel functions can be written in terms of Bessel functions (which for real arguments are real). Decomposing Eq. (2.158) in this fashion, using the Bessel function expansion for small arguments and retaining the dominant real part, then yields

$$F(\eta, k_1, k_2, k_3) = F(\eta_*, k_1, k_2, k_3) + \frac{W''' H_*^2 2^{3-4\alpha} \Gamma(\mu)^4}{12 \mu \pi^2 \alpha} \times \quad (2.161)$$

$$\left\{ \frac{2\mu}{3(\mu - \frac{1}{2})} \left[1 - \frac{\alpha (\eta/\eta_*)^{3-3\alpha}}{2\mu} \right] - (\eta/\eta_*)^{-\alpha} \right\} \frac{(-\eta)^{4\alpha} \sum_i (k_i)^{2\mu}}{\prod_i (k_i)^{2\mu}}.$$

The first term on the right-hand side is the non-Gaussianity at Hubble exit and it can only be computed numerically. The second term represents the non-Gaussianity generated at late times during inflation, when the large-scale local term dominates over the finite Hubble-crossing term.

Now we will show that the large-scale local contribution to the non-Gaussianity of Eqs. (2.160) and (2.161) can be derived by solving the equation of motion of the field perturbation on large scales. The nonlinear evolution of the field fluctuation is derived by taking the large-scale limit $|k\eta| \rightarrow 0$ in Eq. (2.105) for the free-field $\delta\chi_I$ and Eq. (2.149) for the nonlinear $\delta\chi$. This leads to the equations

$$\ddot{\delta\chi}_{I\mathbf{k}} + 3H\dot{\delta\chi}_{I\mathbf{k}} + m_{\delta\chi}^2 \delta\chi_{I\mathbf{k}} = 0, \quad (2.162)$$

$$\ddot{\delta\chi}_{\mathbf{k}} + 3H\dot{\delta\chi}_{\mathbf{k}} + m_{\delta\chi}^2 \delta\chi_{\mathbf{k}} = \mathcal{S}_{\mathbf{k}}, \quad (2.163)$$

where the source on the left-hand side is given in terms of the linear solution,

$$\mathcal{S}_{\mathbf{k}} = -\frac{W'''}{2} (\delta\chi_I \star \delta\chi_I)_{\mathbf{k}}, \quad (2.164)$$

and where \star denotes the convolution operation. The growing solution of the homogeneous Eq. (2.162) is

$$\delta\chi_{I\mathbf{k}}(\eta) = \delta\chi_{I\mathbf{k}}(\eta_*) (|k\eta|)^{\frac{3}{2}-\mu}. \quad (2.165)$$

Only in the massless limit is this constant. One can find the solution of the inhomogeneous equation by using the method of variation of parameters, which yields

$$\delta\chi_{\mathbf{k}}(\eta) = \delta\chi_{\mathbf{k}}(\eta_*) (|k\eta|)^{\frac{3}{2}-\mu} + \frac{1}{2\mu H_*} \left[(|k\eta|)^{-\frac{3}{2}+\mu} \int_{\eta_*}^{\eta} d\eta' a(\eta') (|k\eta|)^{-\frac{3}{2}-\mu} \mathcal{S}_{\mathbf{k}}(\eta') - (|k\eta|)^{-\frac{3}{2}-\mu} \int_{\eta_*}^{\eta} d\eta' a(\eta') (|k\eta|)^{-\frac{3}{2}+\mu} \mathcal{S}_{\mathbf{k}}(\eta') \right]. \quad (2.166)$$

Using the source (2.164) with Eq. (2.165) and integrating over conformal time, one obtains

$$\delta\chi_{\mathbf{k}}(\eta) = \delta\chi_{\mathbf{k}}(\eta_*) (|k\eta|)^{\alpha} + \frac{W'''}{6H_*^2} f(\eta/\eta_*) [\delta\chi_I(\eta) \star \delta\chi_I(\eta)]_{\mathbf{k}}, \quad (2.167)$$

where

$$f(x) = \begin{cases} \frac{1}{3}(1-x^3) + \ln(x) & \text{for } \mu = 3/2, \\ \frac{1}{\alpha(\mu-1/2)} \left(1 - \frac{\alpha}{2\mu} x^{3-3\alpha}\right) - \frac{3}{2\mu\alpha} x^{-\alpha} & \text{for } 1/2 < \mu < 3/2. \end{cases} \quad (2.168)$$

We can now use Eq. (2.167) to compute the bispectrum from its definition (2.157). In terms of the power spectrum of the field perturbation, this is

$$F(\eta; k_1, k_2, k_3) = F(\eta_*; k_1, k_2, k_3) + \frac{W'''}{3H_*^2} f(\eta/\eta_*) \sum_{i<j} P(\eta, k_i) P(\eta, k_j), \quad (2.169)$$

which correctly reproduces the large-scale contribution to the non-Gaussianity in Eqs. (2.160) and (2.161). Note that, in the limit $\mu \rightarrow 3/2$ and $\alpha \rightarrow 0$, the large-scale expression for a massive field converges to the massless case, as can be checked by taking this limit in the lower expression on the right-hand side of Eq. (2.168) and using

$$\frac{2\mu}{3(\mu - \frac{1}{2})} \rightarrow 1 + \frac{\alpha}{3} + \mathcal{O}(\alpha^2), \quad (2.170)$$

$$x^{-\alpha} = \exp[-\alpha \ln(x)] \rightarrow 1 - \alpha \ln(x) + \mathcal{O}(\alpha^2). \quad (2.171)$$

In summary, at late times the non-Gaussianity of the field is dominated by the nonlinear evolution on large scales and thus the bispectrum of the field perturbation is of the local form, i.e. proportional to the product of two power spectra (See Sec. 1.3 for the definition

of triangulation of the bispectrum). In the massless case, in which $\mu = 3/2$, the power spectrum of the field fluctuation is constant while the bispectrum grows as $\ln(a)$. In the massive case, however, the power spectrum decays as $a^{-2\alpha}$ and the bispectrum decays as $a^{-3\alpha}$, thus ‘growing’ as a^α with respect to the product of two power spectra. This relative growth is important for the non-Gaussianity in the curvaton mechanism, as can be seen from Eq. (2.134). The curvaton case will be discussed below in more detail.

Before making contact with curvature perturbations, let us extend the solution (2.167) and consider the evolution of the non-adiabatic perturbations in a radiation-dominated era. This applies once inflation has ceased and the inflaton field has been thermalised, but before the isocurvature perturbation is converted into an adiabatic one.

During the radiation dominated era, $H = (2t)^{-1}$ and the field perturbation evolves on large scales according to

$$\delta\ddot{\chi}_{I\mathbf{k}} + \frac{3}{2t}\delta\dot{\chi}_{I\mathbf{k}} + m_{\delta\chi}^2\delta\chi_{I\mathbf{k}} = 0, \quad (2.172)$$

$$\delta\ddot{\chi}_{\mathbf{k}} + \frac{3}{2t}\delta\dot{\chi}_{\mathbf{k}} + m_{\delta\chi}^2\delta\chi_{\mathbf{k}} = \mathcal{S}_{\mathbf{k}}. \quad (2.173)$$

The growing mode of the homogeneous equation is a Bessel function of the first kind J [Langlois & Vernizzi, 2004],

$$\delta\chi_{I\mathbf{k}}(t) = \delta\chi_{I\mathbf{k}}(t_{\text{reh}}) \frac{\pi}{2^{5/4}\Gamma(3/4)} \frac{J_{1/4}(m_{\delta\chi}t)}{(m_{\delta\chi}t)^{1/4}}. \quad (2.174)$$

For $m_{\delta\chi}t \ll 1$, well before decay, the growing mode is constant. Indeed, by solving Eq. (2.173) at lowest order in $m_{\delta\chi}t$, we find⁴

$$\delta\chi_{\mathbf{k}}(t) = \delta\chi_{\mathbf{k}}(t_{\text{reh}}) \frac{\pi}{2^{5/4}\Gamma(3/4)} \frac{J_{1/4}(m_{\delta\chi}t)}{(m_{\delta\chi}t)^{1/4}} - \frac{W^{(3)}}{10m_{\delta\chi}^2} (m_{\delta\chi}t)^2 [\delta\chi_I(t) \star \delta\chi_I(t)]_{\mathbf{k}}. \quad (2.175)$$

This result shows that the isocurvature fluctuation continues its nonlinear evolution throughout the radiation era. We will use this result in the context of a curvaton field to account for the consequences of considering a nonlinear source in the bispectrum of the field and then compute the corresponding non-Gaussian parameter f_{NL} .

⁴This result is in agreement with Enqvist & Nurmi [2005] where the computation considered a general nonlinear potential up to order $\mathcal{O}((m_{\delta\chi}t/2)^8)$.

2.5.4 The curvaton

The curvaton is an alternative inflationary mechanism to generate the matter density fluctuations [Mollerach, 1990; Linde & Mukhanov, 1997; Enqvist & Sloth, 2002; Lyth & Wands, 2002; Moroi & Takahashi, 2001]. This is achieved without appealing to the perturbations in the original inflaton field. Instead, an auxiliary 'curvaton' field, subdominant during inflation, generates isocurvature fluctuations which transform into adiabatic ones after the inflationary phase, during the decaying oscillations of the curvaton field. During inflation, the isocurvature field presents a negligible contribution to the energy density. After inflation the field still plays no significant role in the background evolution as long as its mass m_χ is negligible compared to the Hubble parameter. However, once $m_\chi^2 \approx H^2$, the curvaton field starts oscillating at the bottom of its potential. At this stage the potential can be approximated as quadratic. The energy density of the field decays during the oscillations like a non-relativistic component ($\rho_\chi \propto 1/a^3$). The curvaton then contributes significantly to the energy density of the universe and the curvaton fluctuations are transformed into adiabatic matter fluctuations (for the simplest version of this mechanism see Bartolo & Liddle [2002]).

We can write the number of e-folds of expansion in terms of the value of the field χ :

$$N(t_{\text{dec}}, t_{\text{in}}) = \frac{1}{3} \ln \left(\frac{\rho_{\chi_{\text{in}}}}{\rho_{\chi_{\text{dec}}}} \right), \quad (2.176)$$

where

$$\rho_{\chi_{\text{in}}} = \frac{1}{2} m_\chi^2 \chi_{\text{in}}^2, \quad \rho_{\chi_{\text{dec}}} = \frac{1}{2} m_\chi^2 \chi_{\text{dec}}^2, \quad (2.177)$$

are the energy densities of the curvaton at the onset of the oscillations (on a flat slicing) and at the moment of decay (on a uniform density slicing), respectively.

The non-Gaussianities generated by the curvaton mechanism have been studied in several papers. In the following we consider and combine all the possible effects, including the intrinsic non-Gaussianity of the curvaton field fluctuation and the nonlinear relation between the curvature perturbation ζ and the curvaton fluctuation. The intrinsic non-Gaussianity of the curvaton can be generated inside and outside the Hubble radius due to its nonlinear potential. In particular, as discussed later in this section, we take into account the nonlinear

evolution during both inflation [Bernardeau & Uzan, 2003; Zaldarriaga, 2004] and the radiation epoch [Enqvist & Nurmi, 2005; Lyth, 2004].

In order to compute ζ and its n-point functions, one can follow two equivalent procedures:

1. Expand the perturbed number of e-folds δN on an initial flat slice at the onset of the oscillations ($t = t_{\text{in}}$), in terms of the field fluctuations $\delta\chi(t_{\text{in}})$, and then use Eqs. (2.169) and (2.175) to introduce the three-point correlators of the field fluctuations.
2. Expand the perturbed number of e-folds δN on an initial flat slice at Hubble crossing ($t = t_*$) in terms of the field fluctuations $\delta\chi(t_{\text{in}})$ and then take into account the nonlinear relation between the field fluctuation at $t = t_{\text{in}}$ and the one at $t = t_*$ using Eqs. (2.167) and (2.175).

We will follow the latter procedure, which has been used in the rest of the literature on the curvaton. We write, as in Eq. (2.129)

$$\zeta = N_{,\chi_*} \delta\chi(t_*) + \frac{1}{2} N_{,\chi_*\chi_*} \delta\chi^2(t_*), \quad (2.178)$$

where N is given by Eq. (2.176).

In general, as we have seen in the previous section, χ_{in} is a nonlinear function of the field value at Hubble exit, and we parameterise this dependence by the function $g(\chi(t_*))$ and its derivatives:

$$g = \chi_0(t_{\text{in}}), \quad (2.179)$$

$$\delta\chi(t_{\text{in}}) = \sum_{n=1} \frac{g^{(n)}}{n!} \delta\chi^n(t_*). \quad (2.180)$$

Using $\frac{\partial}{\partial\chi_*} = g' \frac{\partial}{\partial g}$ and Eq. (2.177), one can differentiate N in Eq. (2.176) to obtain

$$N_{,\chi_*} = \frac{2}{3} \frac{g'}{g} \mathcal{C}, \quad (2.181)$$

where the prime denotes here a derivative with respect to χ_* and

$$\mathcal{C} = 1 - \frac{\partial \ln \bar{\rho}_{\chi_{\text{dec}}}}{\partial \ln \bar{\rho}_{\chi_{\text{in}}}} \approx \left. \frac{3\bar{\rho}_{\chi}}{4\bar{\rho} - \bar{\rho}_{\chi}} \right|_{\text{dec}}, \quad (2.182)$$

where $\bar{\rho}$ is the unperturbed total energy density. Here we have taken a uniform $\bar{\rho}_{\text{dec}}$ assuming that the radiation is unperturbed. Also, to arrive at the last equality we used $(\bar{\rho}_{\chi_{\text{dec}}}/\bar{\rho}_{\chi_{\text{in}}})^{1/3} = [(\bar{\rho}_{\text{dec}} - \bar{\rho}_{\chi_{\text{dec}}})/(\bar{\rho}_{\text{in}} - \bar{\rho}_{\chi_{\text{in}}})]^{1/4}$.

To compute the power spectrum we neglect the evolution during the radiation dominated era, and from Eq. (2.167) we obtain $g'/g = (|k\eta|)^\alpha$, which yields

$$\mathcal{P}_\zeta(t, k) = \frac{4}{9} \mathcal{C}^2 \mathcal{P}_\chi(t, k). \quad (2.183)$$

The spectral index is given by Lyth & Wands [2002] as

$$n_s - 1 = 2 \frac{\dot{H}}{H^2} = 2\alpha, \quad (2.184)$$

where Eq. (2.142) implies

$$\alpha \sim \frac{m_{\delta\chi}^2}{3H_*^2} \ll 1. \quad (2.185)$$

If α is not too small, the spectrum can be extremely blue and this is ruled out by observations [Komatsu et al., 2008]. Differentiating N in Eq. (2.176) once more yields

$$N_{,\chi^*\chi^*} = N_{,\chi^*}^2 \left[\frac{3}{2\mathcal{C}} \left(1 + \frac{gg''}{g'^2} \right) - 2 - \mathcal{C} \right]. \quad (2.186)$$

If we neglect the non-Gaussianity of the field fluctuations at Hubble crossing, which are subdominant with respect to the ones accumulated during the super-Hubble evolution, and the definition (2.134) gives

$$f_{\text{NL}} = \frac{5}{4\mathcal{C}} \left(1 + \frac{gg''}{g'^2} \right) - \frac{5}{3} - \frac{5\mathcal{C}}{6}. \quad (2.187)$$

We have arrived to a well known result obtained without assuming a dominant contribution of W''' in the perturbation equations [Bartolo et al., 2004; Lyth & Rodriguez, 2005b; Sasaki et al., 2006].

By comparing the above equation with the nonlinear evolution given by Eqs. (2.167) and

(2.175), and stopping the nonlinear evolution of perturbations when the field starts oscillating at $t \simeq 1/m_{\delta\chi}$, the non-Gaussianity in the curvature perturbation becomes

$$f_{\text{NL}} = \frac{5}{4\mathcal{C}} \left[1 + \frac{\chi_{0 \text{ in}} W^{(3)}}{m_{\delta\chi}^2} \left(\frac{m_{\delta\chi}^2}{3H_*^2} f(\eta_{\text{reh}}/\eta_*) - \frac{1}{5} \right) \right] - \frac{5}{3} - \frac{5\mathcal{C}}{6}, \quad (2.188)$$

where the function f has been defined in Eq. (2.168). At late times, f can be approximated by

$$f(\eta_{\text{reh}}/\eta_*) \simeq \begin{cases} -\Delta N & \text{for } \alpha\Delta N \lesssim 1, \\ -\frac{1}{\alpha} e^{\alpha\Delta N} & \text{for } \alpha\Delta N \gtrsim 1, \end{cases} \quad (2.189)$$

where we have used Eq. (2.185) and $\Delta N = N_{\text{reh}} - N_* \simeq 60$ is the number of e-folds between Hubble crossing and the end of inflation.

Note that our result, Eq. (2.188), can also be obtained by computing the field bispectrum from the isocurvature field evolution during radiation domination Eq. (2.175). In this context, the field bispectrum is given by

$$F(t; k_1, k_2, k_3) = F(t_{\text{reh}}; k_1, k_2, k_3) - \frac{W^{(3)}}{5m_{\delta\chi}^2} \sum_{i < j} P(\eta, k_i) P(\eta, k_j), \quad (2.190)$$

which clearly evolves with time before the decay of the curvaton. This non-Gaussianity is transferred to the curvature correlation by expanding the perturbed number of e-folds δN on an initial flat slice taken at the onset of the oscillations ($t = t_{\text{in}}$). Then we can write $\zeta = \delta N$ in terms of the field fluctuations $\delta\chi(t_{\text{in}})$ as in Eq. (2.129). With the aid of Eqs. (2.169) and (2.190), we then replace the three-point correlators of the field fluctuations in the curvature perturbation bispectrum. Our result in Eq. (2.188) is thus recovered.

2.6 Model discrimination through observations

In its simplest version, the curvaton model proposes an isocurvature field whose quantum fluctuations reproduce the spectrum of curvature fluctuations we observe in the CMB. Fixing the required perturbation amplitude and spectral index imposes important restrictions on the possible values of χ . Additionally, the non-Gaussianity of the curvaton could constrain the

parameter space further.

As an example, let us consider a curvaton with bare mass $m_\chi \ll H_*$ and nonlinear potential $W = \frac{M}{3!}\chi^3$, such that $m_{\delta\chi}^2 \simeq W'' = \chi_{0*} M$ and $W''' = M$. Note that the negligible mass in this case allows for a scale-invariant power spectrum in the field fluctuations and consequently the curvature perturbations. For simplicity we take $\chi_{0\text{ osc}} \simeq \chi_{0*}$, which is consistent with neglecting the nonlinear potential in Eq. (2.138)), since this would only contribute a term of order $\mathcal{O}(\alpha^2)$. When the nonlinear coupling is very small, Eq. (2.188) reduces to

$$f_{\text{NL}} = \frac{1}{\mathcal{C}} \left(1 - \frac{5}{4}\alpha\Delta N \right) - \frac{5}{3} - \frac{5\mathcal{C}}{6}, \quad \alpha \lesssim \Delta N^{-1}, \quad (2.191)$$

and the intrinsic non-Gaussianity of the curvaton field gives a negligible contribution to the total non-Gaussianity in the curvature perturbation. However, when the nonlinear coupling is important, the nonlinear parameter is

$$f_{\text{NL}} = \frac{1}{\mathcal{C}} \left(1 - \frac{5}{4} \exp(\alpha\Delta N) \right) - \frac{5}{3} - \frac{5\mathcal{C}}{6}, \quad \Delta N^{-1} \lesssim \alpha. \quad (2.192)$$

In this case the intrinsic non-Gaussianity of the curvaton can be the main source of non-Gaussianity in the curvature perturbation. For example, with $\frac{\chi_{0*} M}{3H^2} \simeq 0.07$ and $\mathcal{C} = 1$, one finds $f_{\text{NL}} \simeq -100$, which is within reach of current and future experiments. However, in this case, if the curvaton is the only field responsible for the curvature perturbations, the spectral index of scalar fluctuations will be largely blue. This is in disagreement with current observations and is therefore excluded.

Let us finally consider the special case in which the curvaton is not responsible for the linear fluctuations observed by CMB and large-scale structure probes. Using the same potential as in the example above, this case constrains the fraction r in Eq. (2.182) to be small, as the contribution to the curvature power spectrum is controlled by this parameter (see Eq. (2.183)). On the other hand, α can take large values without violating constraints on the power spectrum, which is dominated by the inflaton perturbations. As for second order perturbations, f_{NL} is still given by the formula (2.192) and can be large due to the freedom in the mass and the small value of \mathcal{C} . This happens at all scales and the non-Gaussianity is induced through the evolution of fluctuations on superhorizon scales.

It is important to note that, in this case, the blue spectrum of the curvaton perturbations may dominate \mathcal{P}_ζ at small scales. If this happens, and if the perturbations have enough power on small scales, a significant amount of PBHs would be produced. In this special case, as in many other versions of inflation, an important constraint on the model comes from the probability of PBH formation as we will study in the following chapters.

Chapter 3

Statistics of non-Gaussian fluctuations

3.1 Introduction

In the inflationary paradigm, the prediction that the spectrum of fluctuations should exhibit Gaussian statistics has recently been challenged. This prediction follows from the fact that the curvature perturbation, which commonly refers to the comoving curvature perturbation defined in Eq. (2.43), is treated as a free field during inflation,

$$\mathcal{R}(t, \mathbf{x}) = \int \frac{d^3k}{(2\pi)^3} \mathcal{R}(t, \mathbf{k}) e^{i\mathbf{k}\cdot\mathbf{x}}, \quad (3.1)$$

where there is no coupling between the $\mathcal{R}(t, \mathbf{k})$ for different \mathbf{k} . With this understanding, Eq. (3.1) means that \mathcal{R} does not interact with either itself or any other particle species in the universe. The real-space field $\mathcal{R}(t, \mathbf{x})$ is obtained by summing an infinite number of independent, identically distributed, uncorrelated oscillators. Under these circumstances the Gaussianity of $\mathcal{R}(t, \mathbf{x})$ follows from the central limit theorem [Bardeen et al., 1986], given reasonable assumptions about the individual distributions of the $\mathcal{R}(t, \mathbf{k})$. The exact form of the distributions of the $\mathcal{R}(t, \mathbf{k})$ is mostly irrelevant for the inflationary density perturbations.

In conventional quantum field theory, all details of \mathcal{R} and its interactions are encoded in the n -point correlation functions of \mathcal{R} , written as $\langle \text{out} | \mathcal{R}(t_1, \mathbf{x}_1) \cdots \mathcal{R}(t_n, \mathbf{x}_n) | \text{in} \rangle$. Working in the Heisenberg picture, where the operators carry time dependence but the states $\{ | \text{in} \rangle, | \text{out} \rangle \}$ do not, these functions express the amplitude for the early-time vacuum $| \text{in} \rangle$ to evolve into the late-time vacuum $| \text{out} \rangle$ in the presence of the fields $\mathcal{R}(t_i, \mathbf{x}_i)$. Given

the n -point functions for all n at arbitrary \mathbf{x} and t , one can determine $\mathcal{R}(t, \mathbf{x})$ [Streater & Wightman, 2000], at least in scattering theory. In the context of the inflationary density perturbations, these vacuum evolution amplitudes are not directly relevant. Instead, one is interested in the equal time expectation values $\langle \text{in} | \mathcal{R}(t, \mathbf{x}_1) \cdots \mathcal{R}(t, \mathbf{x}_n) | \text{in} \rangle$, which can be used to measure gravitational particle creation out of the time-independent early vacuum $|\text{in}\rangle$ during inflation. These expectation values are calculated using the so-called ‘closed-time-path formalism’, which was introduced by Schwinger [1961]; see also Calzetta & Hu [1987]; Jordan [1986]; DeWitt [2003] and Hajicek [1979]. In this formalism there is a doubling of degrees of freedom, which is also manifest in finite temperature calculations [Le Bellac, 2000; Rivers, 1988]. This method has recently been used [Weinberg, 2005, 2006; Sloth, 2006; Seery, 2008] to extend the computation of the correlation functions of \mathcal{R} to beyond tree-level.

Knowledge of the expectation values of \mathcal{R} in the state $|\text{in}\rangle$ is sufficient to predict a large number of cosmological observables, including the power spectrum of the density perturbations generated during inflation [Guth & Pi, 1982; Hawking, 1982], and the two- and three-point functions of the CMB temperature anisotropies [Hu & Sugiyama, 1995; Hu, 2001; Komatsu & Spergel, 2001; Kogo & Komatsu, 2006; Okamoto & Hu, 2002; Babich et al., 2004; Babich & Zaldarriaga, 2004; Babich, 2005; Liguori et al., 2006; Cabella et al., 2006; Creminelli et al., 2006]. Because they are defined as expectation values in the quantum vacuum, these observables all have the interpretation of ensemble averages, as will be discussed in more detail below.

On the other hand, one sometimes needs to know the probability that fluctuations of some given magnitude occur in the curvature perturbation \mathcal{R} [Press & Schechter, 1974; Bardeen et al., 1986; Peacock & Heavens, 1990]. This is not a question about ensemble averages, but about the probability measure on the ensemble itself. As a result, such information cannot easily be obtained from inspection or simple manipulation of the n -point functions.

For example, if we know by some a priori means that \mathcal{R} is free, then the argument given above, based on the central limit theorem, implies that at any position \mathbf{x} , the probability

density of fluctuations in \mathcal{R} of amplitude ϱ must be

$$\mathbb{P}(\varrho) \simeq \frac{1}{\sqrt{2\pi\sigma}} \exp\left(-\frac{\varrho^2}{2\sigma^2}\right), \quad (3.2)$$

where the variance in \mathcal{R} is

$$\sigma^2 = \langle \mathcal{R}(t, \mathbf{x})^2 \rangle = \int d \ln k \mathcal{P}_{\mathcal{R}}(k). \quad (3.3)$$

The quantity $\mathcal{P}_{\mathcal{R}}(k)$ is the dimensionless power spectrum, which is defined in terms of the two-point function of \mathcal{R} , calculated from the quantum field theory in-vacuum:

$$\langle \text{in} | \mathcal{R}(t, \mathbf{k}_1) \mathcal{R}(t, \mathbf{k}_2) | \text{in} \rangle = (2\pi)^3 \delta(\mathbf{k}_1 + \mathbf{k}_2) \frac{2\pi^2}{k_1^3} \mathcal{P}_{\mathcal{R}}(k_1). \quad (3.4)$$

This is the only relevant observable, because it is a standard property of free fields that all other non-vanishing correlation functions can be expressed in terms of the two-point function (3.4), and hence the power spectrum. Those expressions can be achieved through a generalisation of Wick's theorem using an equal-time normal-ordering [Luo & Schramm, 1993]. In practice, in order to give a precise meaning to (3.2), it would be necessary to specify what it means for \mathcal{R} to develop fluctuations of amplitude ϱ , and whether it is the fluctuations in the microphysical field \mathcal{R} or some smoothed field $\bar{\mathcal{R}}$ which are measured. These details affect the exact expression (3.3) for the variance of ϱ .

The average in Eq. (3.4), denoted by $\langle \text{in} | \dots | \text{in} \rangle$, is the expectation value in the quantum in-vacuum. To relate this abstract expectation value to real-world measurement probabilities, one introduces a notional ensemble of possible universes, of which the present universe and the density fluctuations that we observe are only one possible realisation (e.g., Lyth [2006]). However, for ergodic processes, we may freely trade ensemble averages for volume averages. The ergodicity of a system refers to that property of processes by which the average value of a process characteristic measured over time is the same as the average value measured over the ensemble.

If we make the common supposition that the inflationary density perturbation is indeed ergodic, then we expect the volume average of the density fluctuation to behave like the

ensemble average: the universe may contain regions where the fluctuation is atypical, but with high probability most regions contain fluctuations with root-mean-square amplitude close to σ . Therefore the probability distribution on the ensemble, which is encoded in Eq. (3.4), translates to a probability distribution on smoothed regions of a determined size within our own universe.

In order to apply the above analysis, it is necessary to know in advance that \mathcal{R} is a free field. This knowledge allows us to use the central limit theorem to connect the correlation functions of \mathcal{R} with the probability distribution (3.2). The situation in the real universe is not so simple. In particular, the assumption that during inflation \mathcal{R} behaves as a free field, and therefore that the oscillators $\mathcal{R}(\mathbf{k})$ are uncorrelated and independently distributed, is only approximately correct. In fact, \mathcal{R} is subject to self-interactions and interactions with the other constituents of the universe, which mix \mathbf{k} -modes. Consequently, the oscillators $\mathcal{R}(\mathbf{k})$ acquire some phase correlation and are no longer independently distributed. In this situation the central limit theorem gives only approximate information concerning the probability distribution of $\mathcal{R}(\mathbf{x})$, and it is necessary to use a different method to connect the correlation functions of \mathcal{R} with its probability distribution function (PDF).

In this chapter we give a new derivation of the PDF of the amplitude of fluctuations in \mathcal{R} which directly connects $\mathbb{P}(\varrho)$ and the correlation functions $\langle \mathcal{R}(\mathbf{k}_1) \cdots \mathcal{R}(\mathbf{k}_n) \rangle$, without intermediate steps which invoke the central limit theorem or other statistical results. When the inflaton is treated as a free field, our method reproduces the familiar prediction (3.2) of Gaussian statistics. When the inflaton is ‘not’ treated as a free field, the very significant advantage of our technique is that it is possible to directly calculate the corrections to $\mathbb{P}(\varrho)$. Specifically, the interactions of \mathcal{R} can be measured by the departure of the correlation functions from the form they would take if \mathcal{R} were free. Therefore, the first corrections to the free-field approximation are contained in the three-point function, which is exactly zero when there are no interactions.

The three-point function for single-field, slow-roll inflation has been calculated by Maldacena [2003], whose result can be expressed in the form [Seery & Lidsey, 2005a]

$$\langle \mathcal{R}(\mathbf{k}_1) \mathcal{R}(\mathbf{k}_2) \mathcal{R}(\mathbf{k}_3) \rangle = 4\pi^4 (2\pi)^3 \delta\left(\sum_i \mathbf{k}_i\right) \frac{\bar{\mathcal{P}}_{\mathcal{R}}^2}{\prod_j k_j^3} \mathcal{A}(k_1, k_2, k_3), \quad (3.5)$$

where \mathcal{A} is Maldacena's \mathcal{A} -function divided by two [Maldacena, 2003]⁵. $\mathcal{P}_{\mathcal{R}}^{-2}$ measures the amplitude of the spectrum when the k_i crossed the horizon. (For earlier work on the derivation of the three-point-function, see Falk et al. [1993]; Gangui et al. [1994]; Pyne & Carroll [1996]; Acquaviva et al. [2003].) This result has since been extended to cover the non-Gaussianity produced during slow-roll inflation with an arbitrary number of fields [Maldacena, 2003; Seery & Lidsey, 2005a; Creminelli, 2003; Lyth & Rodriguez, 2005a,b; Lyth & Zaballa, 2005; Zaballa et al., 2006; Vernizzi & Wands, 2006], preheating [Enqvist et al., 2005b,a; Jokinen & Mazumdar, 2006], models where the dominant non-Gaussianity is produced by a light scalar which is a spectator during inflation [Boubekeur & Lyth, 2006; Alabidi & Lyth, 2006b; Lyth, 2006], and alternative models involving a small speed of sound for the inflaton perturbation [Seery & Lidsey, 2005b; Alishahiha et al., 2004; Calcagni, 2005; Arkani-Hamed et al., 2004; Creminelli, 2003].

For single-field, slow-roll inflation, the self-interactions of \mathcal{R} are suppressed by powers of the slow-roll parameters. This means that the correction to Gaussian statistics is not large. In terms of the \mathcal{A} -parametrised three-point function (3.5), this is most commonly expressed by writing, in an equivalent form to ζ in Eq. (2.131)

$$\mathcal{R}(t, \mathbf{x}) = \mathcal{R}_1(t, \mathbf{x}) - \frac{3}{5} f_{\text{NL}} (\mathcal{R}_1^2(t, \mathbf{x}) - \langle \mathcal{R}_1^2(t, x) \rangle), \quad (3.6)$$

with

$$f_{\text{NL}} = -\frac{5}{6} \frac{\mathcal{A}}{\sum_i k_i^3} = \mathcal{O}(\epsilon_{\text{SR}}, \eta_{\text{SR}}) \quad (3.7)$$

giving the relative contribution of the non-Gaussian piece in \mathcal{R} and \mathcal{R}_1 being a Gaussian random field [Komatsu & Spergel, 2001; Verde et al., 2000]. (Note that there are differing sign conventions for f_{NL} [Malik & Lyth, 2006], here we stick to that used by the WMAP team.) In models with more degrees of freedom, much larger non-Gaussianities are expected, perhaps with $f_{\text{NL}} \sim 10$ [Rigopoulos & Shellard, 2005; Rigopoulos et al., 2006b,a, 2007; Boubekeur & Lyth, 2006; Lyth & Rodriguez, 2005b; Vernizzi & Wands, 2006]. If the inflationary per-

⁵In Maldacena's normalisation, the numerical prefactor in Eq. (3.5) is not consistent with the square of the two-point function, Eq. (3.4). We choose \mathcal{A} so that the prefactor becomes $4\pi^2(2\pi)^3$. This normalisation of Eq. (3.5) was also employed by Seery & Lidsey [2005b,a], although the distinction from Maldacena's \mathcal{A} was not pointed out explicitly.

turbation has a speed of sound different from unity, then large non-Gaussianities may also appear (e.g. Seery & Lidsey [2005b]; LoVerde et al. [2008]), although in this case it is difficult to simultaneously achieve scale invariance. The current observational constraint, as we mentioned in Chapter 2, is of order $|f_{\text{NL}}| \lesssim 100$. In the absence of a detection, the forthcoming PLANCK mission may tighten this constraint to $|f_{\text{NL}}| \lesssim 3$ [Komatsu & Spergel, 2001; Liguori et al., 2006].

Non-Gaussian PDFs have been studied previously by several authors. The closest analysis to the method developed in this chapter comes from Matarrese et al. [2000], who worked with a path integral expression for the density fluctuation smoothed on a scale R (which they denoted by ‘ δ_R ’). Also, the analysis of Bernardeau & Uzan [2002, 2003] has some features in common with our own, being based on the cumulant generating function. Moreover, the expression for the probability density in those papers is expressed as a Laplace transform. Our final expression, Eq. (3.70), can be interpreted as a Fourier integral, viz (3.15), which (loosely speaking) can be related to a Laplace integral via a Wick transformation. Despite these similarities, the correspondence between the two analyses is complicated because Bernardeau & Uzan [2002, 2003] work in a multiple-field picture and calculate a probability density only for the isocurvature field ‘ δs ’, which acquires its non-Gaussianity via a mixing of isocurvature and adiabatic modes long after horizon exit, of which particular cases were presented in the Chapter 2. This contrasts with the situation in the present chapter, where we restrict ourselves to a single-field scenario and compute the PDF for the adiabatic mode \mathcal{R} . This would be orthogonal to δs in field space and its non-Gaussianity is generated exactly at horizon exit.

In the older literature it is more common to deal with the density fluctuation δ_ρ measured on comoving slices, rather than the curvature perturbation \mathcal{R} . For slowly varying fields, on scales larger than the horizon, \mathcal{R} and δ_ρ can be related in the comoving gauge via Eq. (25) of [Lyth, 1985]:

$$\left(\frac{aH}{k}\right)^2 \delta_\rho = - \left(\frac{3}{2} + \frac{1}{1+w}\right)^{-1} \mathcal{R}, \quad (3.8)$$

to first order in cosmological perturbation theory for a barotropic fluid. (One may use the δN formalism to go beyond leading order as in Chapter 2, but to obtain results valid on

sub-horizon scales one must use the full Einstein equations; see, e.g., Langlois & Vernizzi [2005b,a].) For fluctuations on the Hubble scale ($k \simeq aH$), this means $|\mathcal{R}| \simeq \delta_\rho$, so \mathcal{R} provides a useful measure of the density fluctuation on such scales. By virtue of this relationship with the density fluctuation, the probability distribution $\mathbb{P}(\varrho)$ is an important theoretical tool, especially in studies of structure formation. For example, it is the principal object in the Press–Schechter formalism [Press & Schechter, 1974]. As a result, there are important reasons why knowledge of the detailed form of the PDF of ϱ , and not merely the approximate answer provided by the central limit theorem, is important.

Firstly, large amplitude collapsed objects, such as primordial black holes (PBHs) naturally form in the high- ϱ tail of the distribution [Carr, 1975; Carr & Hawking, 1974]. Such large fluctuations are extremely rare. This means that a small change in the probability density for $|\varrho| \gg 0$ can make a large difference in the mass fraction of the universe which collapses into PBHs [Bullock & Primack, 1997; Ivanov, 1998]. Thus one may hope to probe the form of the PDF for ϱ using well-known and extremely stringent constraints on PBH formation in the early universe [Carr, 2003; Carr & Lidsey, 1993; Green & Liddle, 1997; Zamballa et al., 2007; Josan et al., 2009]. The corrections calculated in this chapter are therefore not merely of theoretical interest, but relate directly to observations, and have the potential to sharply discriminate between models of inflation.

Secondly, as described above, although the non-Gaussianities produced by single-field, slow-roll inflation are small, this is not mandatory. In models where non-Gaussianities are large, it will be very important to account for the effect of non-Gaussian fluctuations on structure formation [Verde et al., 2000; Matarrese et al., 2000; Verde et al., 2001; Verde & Heavens, 2001]. The formalism presented in this chapter provides a systematic way to obtain such predictions, extending the analysis given by Matarrese et al. [2000].

The outline of this chapter is as follows. In Section 3.2 we obtain the probability measure on the ensemble of possible fluctuations. This step depends on the correlation functions of \mathcal{R} . In Section 3.3, we discuss the decomposition of \mathcal{R} into harmonics. This is a technical step, which is necessary in order to write down a path integral for $\mathbb{P}(\varrho)$. First, we Fourier decompose \mathcal{R} . Then we write the path integral measure, and finally we give a precise specification of ϱ , which measures the size of fluctuations. We distinguish two interesting cases:

a ‘total fluctuation’ ϱ , which corresponds to \mathcal{R} (or approximately δ_ρ) smoothed over regions the size of the Hubble volume; and the ‘spectrum’ $\mathcal{P}_\varrho(k)$, which describes the contributions to ϱ from regions of the primordial power spectrum around the scale described by wavenumber k . In Section 3.4 we evaluate $\mathbb{P}(\varrho)$. We give the calculation for the Gaussian case first, in order to clearly explain our method with a minimum of technical detail. This is followed by the same calculation but including non-Gaussian corrections which follow from a non-zero three-point function. In Section 3.5 we calculate $\mathbb{P}[\mathcal{P}_\varrho(k)]$. Finally, we summarise our results in Section 3.6.

3.2 The probability measure on the ensemble of \mathcal{R}

Our method is to compute the probability measure $\mathbb{P}_t[\mathbf{R}]$ on the ensemble of realisations of the curvature perturbation $\mathbf{R}(\mathbf{x})$, which we define to be the value of $\mathcal{R}(t, \mathbf{x})$ at some fixed time t . This probability measure is a natural object in the Schrödinger approach to quantum field theory, where the elementary quantity is the wavefunctional $\Psi_t[\mathbf{R}]$, which is related to $\mathbb{P}_t[\mathbf{R}]$ by the usual rule of quantum mechanics, that $\mathbb{P}_t[\mathbf{R}] \propto |\Psi_t[\mathbf{R}]|^2$. Once the measure $\mathbb{P}_t[\mathbf{R}]$ is known, we can directly calculate (for example) $\mathbb{P}_t(\varrho)$ by integrating over all \mathbf{R} that produce fluctuations of amplitude ϱ . Although the concept of a probability measure on \mathbf{R} may seem rather formal, the Schrödinger representation of quantum field theory is entirely equivalent to the more familiar formulation in terms of a Fock space. This representation is briefly discussed, for example, by Polchinski [1998] and Visser [1996]. A brief introduction to infinite-dimensional probability measures is given by Albeverio et al. [1997]. Indeed, a similar procedure has been discussed by Ivanov [1998], who calculated the probability measure on a stochastic metric variable $a_{\text{ls}}(\mathbf{x})$ which can be related to our $\mathcal{R}(\mathbf{x})$. Although the approaches are conceptually similar, our method is substantially different in detail. In particular, the present calculation is exact in the sense that we make no reference to the stochastic approach to inflation, and therefore are not obliged to introduce a coarse-graining approximation. Moreover, Ivanov’s analysis appeared before the complete non-Gaussianity arising from \mathcal{R} -field interactions around the time of horizon crossing had been calculated [Maldacena, 2003], and therefore did not include this effect.

3.2.1 The generating functional of correlation functions

The expectation values $\langle \mathcal{R}(\mathbf{x}_1) \cdots \mathcal{R}(\mathbf{x}_2) \rangle$ in the vacuum $|\text{in}\rangle$ at some fixed time t can be expressed in terms of a Schwinger–Keldysh path integral,⁶

$$\begin{aligned} & \langle \mathcal{R}(t, \mathbf{x}_1) \cdots \mathcal{R}(t, \mathbf{x}_n) \rangle = \\ & \int [d\mathcal{R}_- d\mathcal{R}_+]_{|\text{in}\rangle}^{\mathcal{R}_+(t, \mathbf{x}) = \mathcal{R}_-(t, \mathbf{x})} \mathcal{R}(t, \mathbf{x}_1) \cdots \mathcal{R}(t, \mathbf{x}_n) \exp \left(i \hat{\mathcal{I}}^{(n)}[\mathcal{R}_+] - i \hat{\mathcal{I}}^{(n)}[\mathcal{R}_-] \right). \end{aligned} \quad (3.9)$$

Here $[d\mathcal{R}_+]$ is the integrand of the path integral over \mathcal{R} . In cosmology we are generally interested in \mathcal{R} evaluated at different spatial positions on the same t -slice, so we have set all the t equal in (3.9). The path integral is taken over all fields \mathcal{R} which begin in a configuration corresponding to the vacuum $|\text{in}\rangle$ at past infinity. The correlator is equal to the expectation value of three copies of \mathcal{R} at time t so we require two path integrals: the first integral $[d\mathcal{R}_+]$ evolves the vacuum state $|\text{in}\rangle$ from past infinity to the state $\mathcal{R}_+(t, \mathbf{x})$ at time t where the n copies of the field \mathcal{R} are averaged, and a second path integral $[d\mathcal{R}_-]$ which will project back the average to the vacuum state through a second functional integral. $\hat{\mathcal{I}}^{(n)}[\mathcal{R}]$ is the action for the fluctuation \mathcal{R} , which is computed perturbatively to order n in \mathcal{R} when we want to compute correlations of the same order. For example, $\hat{\mathcal{I}}^{(3)}[\mathcal{R}]$ is given to third order in \mathcal{R} by Maldacena [2003] in the context of slow-roll inflation and by Seery & Lidsey [2005a,b] in the inflationary models where the kinetic energy is not negligible. The action $\hat{\mathcal{I}}^{(n)}[\mathcal{R}]$ is time ordered for the argument \mathcal{R}_- and anti-time ordered for \mathcal{R}_+ . (For details of the Schwinger–Keldysh or ‘closed time path’ formalism, see Calzetta & Hu [1987]; Jordan [1986]; Weinberg [2005]; Le Bellac [2000]; Hajicek [1979]; Rivers [1988].)

An expression equivalent to Eq. (3.9) can be given in terms of the ‘equal time’ generating functional

$$\begin{aligned} Z_t[q] = & \int [d\mathcal{R}] \int [d\mathcal{R}_- d\mathcal{R}_+]_{|\text{in}\rangle}^{\mathcal{R}_\pm(t, \mathbf{x}) = \mathcal{R}(\mathbf{x})} \\ & \exp \left(i \hat{\mathcal{I}}^{(n)}[\mathcal{R}_+] - i \hat{\mathcal{I}}^{(n)}[\mathcal{R}_-] + i \int_{\Sigma_t} d^3x \mathcal{R}(\mathbf{x}) q(\mathbf{x}) \right), \end{aligned} \quad (3.10)$$

⁶Henceforth, we use the notation $\langle \cdots \rangle$ to mean expectation values in the in-vacuum, and no longer write $|\text{in}\rangle$ explicitly where this is unambiguous.

where q is some arbitrary source field, also known in the theory of special functions as the formal argument of the generating function. Σ_t is a spatial slice at coordinate time t . The equal-time correlation functions $\langle \mathcal{R}(t, \mathbf{x}_1) \cdots \mathcal{R}(t, \mathbf{x}_n) \rangle$ are recovered from $Z_t[q]$ by functional differentiation,

$$\langle \mathcal{R}(t, \mathbf{x}_1) \cdots \mathcal{R}(t, \mathbf{x}_n) \rangle = \frac{1}{i^n} \frac{\delta}{\delta q(\mathbf{x}_1)} \cdots \frac{\delta}{\delta q(\mathbf{x}_n)} \ln Z_t[q] \Big|_{q=0}. \quad (3.11)$$

Up to normalisation, this is merely the rule for functional Taylor coefficients, so it is straightforward to invert Eq. (3.11) for $Z_t[q]$. We obtain

$$Z_t[q] = \exp \left\{ \sum_{n=0}^{\infty} \frac{i^n}{n!} \int \cdots \int d^3x_1 \cdots d^3x_n q(\mathbf{x}_1) \cdots q(\mathbf{x}_n) \langle \mathcal{R}(t, \mathbf{x}_1) \cdots \mathcal{R}(t, \mathbf{x}_n) \rangle \right\}. \quad (3.12)$$

Eq. (3.10) for the generating functional can be rewritten in a suggestive way. We define the wavefunctional at time t as

$$\Psi_t[\mathbf{R}] = \int [d\mathcal{R}]_{\text{in}}^{\mathcal{R}(t, \mathbf{x}) = \mathbf{R}(\mathbf{x})} \exp \left(i \hat{\mathcal{I}}^{(n)}[\mathcal{R}] \right). \quad (3.13)$$

This definition is simply the functional generalisation of the familiar quantum-mechanical wavefunction. It expresses the amplitude for the field $\mathcal{R}(t, \mathbf{x})$ to have the spatial configuration $\mathbf{R}(\mathbf{x})$ at time t , given the boundary condition that \mathcal{R} started in the vacuum state in the far past. In terms of $\Psi_t[\mathbf{R}]$, the generating functional can be rewritten as

$$Z_t[q] = \int [d\mathbf{R}] \Psi_t[\mathbf{R}]^\dagger \Psi_t[\mathbf{R}] \exp \left(i \int d^3x \mathbf{R}(\mathbf{x}) q(\mathbf{x}) \right) = |\widetilde{\Psi}_t[\mathbf{R}]|^2 \propto \widetilde{\mathbb{P}}[\mathbf{R}], \quad (3.14)$$

where a tilde denotes a (functional) Fourier transform, and \dagger denotes Hermitian conjugation. Eq. (3.14) implies that $Z_t[q]$ is the complementary function for the probability distribution $\mathbb{P}_t[\mathbf{R}]$ [Albeverio et al., 1997], which can formally be obtained by inversion of $Z_t[q]$. Hence, up to an overall normalisation,

$$\mathbb{P}_t[\mathbf{R}] \propto \int [dq] \exp \left(-i \int d^3x \mathbf{R}(\mathbf{x}) q(\mathbf{x}) \right) Z_t[q]. \quad (3.15)$$

The normalisation is not determined by this procedure. We will fix the R-independent prefactor, which correctly normalises the PDF, by requiring $\int d\rho \mathbb{P}(\rho) = 1$ at the end of the calculation. For this reason, we systematically drop all field-independent prefactors in the calculation that follows.

3.2.2 The probability density on the ensemble

So far, all our considerations have been exact, and apply for any quantum field $\mathcal{R}(t, \mathbf{x})$. For any such field, Eq. (3.15) gives the probability density for a spatial configuration R at time t , and implies that to obtain $\mathbb{P}_t[R]$ we need to know all such functions for all n -point correlations and at all spatial positions \mathbf{x} . In practice, some simplifications occur when \mathcal{R} is identified as the inflationary curvature perturbation.

The most important simplification is the possibility of a perturbative evaluation. The dominant mode of the CMB fluctuation is constrained to be Gaussian to high accuracy, so the non-Gaussian corrections to the leading order cannot be large. Moreover, the amplitude of its spectrum is constrained by CMB observations. Specifically, as mentioned in Section 1.2, in the range of wavenumbers probed by the CMB, the spectrum has amplitude $\mathcal{P}_{\mathcal{R}}^{1/2} \sim 10^{-5}$. Each higher-order correlation function is suppressed by an increasing number of copies of the spectrum, $\mathcal{P}_{\mathcal{R}}(k)$, as we have shown in Chapter 2.

Provided the amplitude of $\mathcal{P}_{\mathcal{R}}$ is small, it might seem reasonable to truncate the exponential in Eq. (3.15) for a given n and to work with a perturbation series in \mathcal{P} . However, this simple approach is too naïve, because the integrals over q eventually make any given term in the series large, and this invalidates simple perturbative arguments based on power-counting in $\mathcal{P}_{\mathcal{R}}$. The perturbation series can only be justified *a posteriori*, a point to which we will return in Section 3.4.2.

We work to first-order in the three-point correlation, that is, we consider non-vanishing two and three-point correlators in Eq. (3.12),

$$Z_t[q] = \exp \left\{ -\frac{1}{2} \int \int d^3x_1 d^3x_2 q(\mathbf{x}_1) q(\mathbf{x}_2) \langle \mathcal{R}(t, \mathbf{x}_1) \mathcal{R}(t, \mathbf{x}_2) \right. \quad (3.16)$$

$$\left. -\frac{i}{6} \int \int \int d^3x_1 d^3x_2 d^3x_3 q(\mathbf{x}_1) q(\mathbf{x}_2) q(\mathbf{x}_3) \langle \mathcal{R}(t, \mathbf{x}_1) \mathcal{R}(t, \mathbf{x}_2) \mathcal{R}(t, \mathbf{x}_3) \rangle \right\}.$$

This generating functional is introduced in the expression derived for the probability, Eq. (3.15), for which we expand the exponential third order term in $q(\mathbf{x})$ in power series to lowest order.

We finally arrive to the product

$$\mathbb{P}_t[\mathbf{R}] \propto \int [dq] \Upsilon_t[q] \omega_t[q; \mathbf{R}], \quad (3.17)$$

where $\Upsilon[q]$ and $\omega[q; \mathbf{R}]$ are defined by

$$\Upsilon_t[q] = \left(1 - \frac{i}{6} \int \frac{d^3 k_1 d^3 k_2 d^3 k_3}{(2\pi)^9} q(\mathbf{k}_1) q(\mathbf{k}_2) q(\mathbf{k}_3) \langle \mathcal{R}(t, \mathbf{k}_1) \mathcal{R}(t, \mathbf{k}_2) \mathcal{R}(t, \mathbf{k}_3) \rangle \right), \quad (3.18)$$

and

$$\omega_t[q; \mathbf{R}] = \exp \left(- \int \frac{d^3 k_1 d^3 k_2}{(2\pi)^6} \frac{q(\mathbf{k}_1) q(\mathbf{k}_2)}{2} \langle \mathcal{R}(t, \mathbf{k}_1) \mathcal{R}(t, \mathbf{k}_2) \rangle - i \int \frac{d^3 k}{(2\pi)^3} q(\mathbf{k}) \mathbf{R}(\mathbf{k}) \right). \quad (3.19)$$

The expression for ω_t gives rise to the Gaussian part of the PDF. Υ is of the form 1 plus a correction which is small when the perturbative analysis is valid. Higher-order perturbative corrections in $\mathcal{P}_{\mathcal{R}}$ can be accommodated if desired by retaining higher-order terms in the power series expansion of the exponential in (3.15). Therefore our method is not restricted to corrections arising from non-Gaussianities described by three-point correlations, but can account for non-Gaussianities which enter at any order in the correlations of \mathcal{R} , limited only by the computational complexity. However, in this chapter, we work only with the three-point non-Gaussianity.

We now complete the square for $\omega_t[q; \mathbf{R}]$ in (3.19) and make the finite field redefinition

$$q(\mathbf{k}) \mapsto \hat{q}(\mathbf{k}) = q(\mathbf{k}) + (2\pi)^3 i \frac{\mathbf{R}(\mathbf{k})}{\langle \mathcal{R}(t, \mathbf{k}) \mathcal{R}(t, -\mathbf{k}) \rangle'}, \quad (3.20)$$

where the prime in $\langle \mathcal{R}(t, \mathbf{k}) \mathcal{R}(t, -\mathbf{k}) \rangle'$ indicates that the momentum-conservation δ -function is omitted. The measure $[dq]$ is formally invariant under this shift, giving $\int [dq] = \int [d\hat{q}]$, whereas $\omega_t[q; \mathbf{R}]$ can be split into an \mathbf{R} -dependent piece, which we call $\Gamma_t[\mathbf{R}]$, and a piece that

depends only on \hat{q} but not \mathbf{R} ,

$$\omega_t[q; \mathbf{R}] \mapsto \Gamma_t[\mathbf{R}] \exp \left(-\frac{1}{2} \int \frac{d^3 k_1 d^3 k_2}{(2\pi)^6} \hat{q}(\mathbf{k}_1) \hat{q}(\mathbf{k}_2) \langle \mathcal{R}(t, \mathbf{k}_1) \mathcal{R}(t, \mathbf{k}_2) \rangle \right), \quad (3.21)$$

where $\Gamma_t[\mathbf{R}]$ is a Gaussian in \mathbf{R} ,

$$\Gamma_t[\mathbf{R}] = \exp \left(-\frac{1}{2} \int d^3 k_1 d^3 k_2 \langle \mathcal{R}(t, \mathbf{k}_1) \mathcal{R}(t, \mathbf{k}_2) \rangle \frac{\mathbf{R}(\mathbf{k}_1) \mathbf{R}(\mathbf{k}_2)}{\prod_i \langle \mathcal{R}(t, \mathbf{k}_i) \mathcal{R}(t, -\mathbf{k}_i) \rangle'} \right). \quad (3.22)$$

Eq. (3.17) for the probability density becomes

$$\mathbb{P}_t[\mathbf{R}] \propto \Gamma_t[\mathbf{R}] \int [d\hat{q}] \Upsilon_t[\hat{q}] \exp \left(-\frac{1}{2} \int \frac{d^3 k_1 d^3 k_2}{(2\pi)^6} \hat{q}(\mathbf{k}_1) \hat{q}(\mathbf{k}_2) \langle \mathcal{R}(t, \mathbf{k}_1) \mathcal{R}(t, \mathbf{k}_2) \rangle \right), \quad (3.23)$$

One can easily verify that this is the correct expression, since if we ignore the three-point contribution (thus setting $\Upsilon_t = 1$), one recovers (after applying a correct normalisation)

$$\int [d\mathbf{R}] \mathbf{R}(\mathbf{k}_1) \mathbf{R}(\mathbf{k}_2) \Gamma_t[\mathbf{R}] = \langle \mathcal{R}(t, \mathbf{k}_1) \mathcal{R}(t, \mathbf{k}_2) \rangle. \quad (3.24)$$

The remaining task is to carry out the \hat{q} integrations in Υ_t . The only terms which contribute are those containing an even power of \hat{q} , since any odd function integrated against $e^{-\hat{q}^2}$ vanishes identically. In the expansion of $\prod_i q(\mathbf{k}_i)$ in terms of \hat{q} , there are two such terms: one which is quadratic in \hat{q} , and one which is independent of \hat{q} . These are accompanied by linear and cubic terms which do not contribute to $\mathbb{P}_t[\mathbf{R}]$. For any symmetric kernel \mathbf{K} and vectors $\mathbf{p}, \mathbf{q} \in \mathbb{R}^m$, one has the general results [Rivers, 1988]

$$\int [df] \exp \left(-\frac{1}{2} \int d^m x d^m y f(\mathbf{x}) f(\mathbf{y}) \mathbf{K}(\mathbf{x}, \mathbf{y}) \right) = (\det \mathbf{K})^{-1/2}, \quad (3.25)$$

$$\int [df] f(\mathbf{p}) f(\mathbf{q}) \exp \left(-\frac{1}{2} \int d^m x d^m y f(\mathbf{x}) f(\mathbf{y}) \mathbf{K}(\mathbf{x}, \mathbf{y}) \right) = \mathbf{K}^{-1}(\mathbf{p}, \mathbf{q}) (\det \mathbf{K})^{-1/2}. \quad (3.26)$$

These rules allow us to evaluate the \hat{q} integrals in Eq. (3.23), giving

$$\mathbb{P}_t[\mathbf{R}] \propto \Gamma_t[\mathbf{R}] \left(1 + \Upsilon_t^{(0)}[\mathbf{R}] + \Upsilon_t^{(2)}[\mathbf{R}] \right), \quad (3.27)$$

where

$$\Upsilon_t^{(0)}[\mathbf{R}] = -\frac{1}{6} \int d^3k_1 d^3k_2 d^3k_3 \langle \mathcal{R}(t, \mathbf{k}_1) \mathcal{R}(t, \mathbf{k}_2) \mathcal{R}(t, \mathbf{k}_3) \rangle \frac{R(\mathbf{k}_1)R(\mathbf{k}_2)R(\mathbf{k}_3)}{\prod_i \langle \mathcal{R}(t, \mathbf{k}_i) \mathcal{R}(t, -\mathbf{k}_i) \rangle'}, \quad (3.28)$$

$$\begin{aligned} \Upsilon_t^{(2)}[\mathbf{R}] = & \frac{1}{6} \int d^3k_1 d^3k_2 d^3k_3 \langle \mathcal{R}(t, \mathbf{k}_1) \mathcal{R}(t, \mathbf{k}_2) \mathcal{R}(t, \mathbf{k}_3) \rangle \times \\ & \times \frac{R(\mathbf{k}_1) \delta(\mathbf{k}_2 + \mathbf{k}_3)}{\prod_{i \neq 3} \langle \mathcal{R}(t, \mathbf{k}_i) \mathcal{R}(t, -\mathbf{k}_i) \rangle'} + \{\text{perms}\}. \end{aligned} \quad (3.29)$$

In the last expression we include the possible permutations of the labels $\{1, 2, 3\}$ since these give rise to distinct integrands.

In fact, $\Upsilon_t^{(2)}$ is negligible. This happens because the three-point function contains a momentum-conservation δ -function, $\delta(\mathbf{k}_1 + \mathbf{k}_2 + \mathbf{k}_3)$, which requires that the vectors \mathbf{k}_i sum to zero in momentum space. [For this reason, it is often known as the ‘‘triangle condition’’, and we will usually abbreviate it schematically as $\delta(\Delta)$.] In combination with the δ -function, $\delta(\mathbf{k}_2 + \mathbf{k}_3)$, the effect is to constrain two of the momenta (in this example \mathbf{k}_2 and \mathbf{k}_3) to be equal and opposite, and the other momentum (in this example, \mathbf{k}_1) to be zero. This corresponds to the extreme local or ‘squeezed’ limit [Maldacena, 2003; Creminelli & Zaldarriaga, 2004; Allen et al., 2006], in which the bispectrum reduces to the power spectrum evaluated on a perturbed background, which is sourced by the zero-momentum mode. Written explicitly, $\Upsilon_t^{(2)}$ behaves like

$$\Upsilon_t^{(2)}[\mathbf{R}] \simeq \frac{1}{6} \int \frac{d^3k_1 d^3k_2}{(2\pi)^3} \alpha R(\mathbf{k}_1) \delta(\mathbf{k}_1) + \{\text{perms}\}, \quad (3.30)$$

where we have written $\lim_{k_1 \rightarrow 0} \mathcal{A} = \alpha k_2^3$, for some known constant α . In particular, Eq. (3.30) vanishes, provided $R(\mathbf{k})$ approaches zero as $k \rightarrow 0$. This condition is typically satisfied, since by construction $R(\mathbf{k})$ should not contain a zero mode. Indeed, any zero mode, if present, would constitute part of the zero-momentum background, and not a part of the perturbation R . Accordingly, Eqs. (3.27)–(3.28) with $\Upsilon_t^{(2)} = 0$ give $\mathbb{P}_t[\mathbf{R}]$ explicitly in terms of the two- and three-point correlation functions.

3.2.3 The smoothed curvature perturbation

The probability density $\mathbb{P}_t[\mathcal{R}] \propto (1 + \Upsilon_t^{(0)}[\mathcal{R}])\Gamma_t[\mathcal{R}]$ expressed in Eq. (3.23) relates to the microphysical field $\mathcal{R}(t, \mathbf{x})$ which appeared in the quantum field theory Lagrangian. A given \mathbf{k} -mode of this field begins in the vacuum state at $t \rightarrow -\infty$. At early times, the mode is far inside the horizon ($k \gg aH$). In this (‘subhorizon’) regime, the \mathbf{k} -mode cannot explore the curvature of spacetime and is immune to the fact that it is living in a de Sitter universe. It behaves like a Minkowski space oscillator. At late times, the mode is far outside the horizon ($k \ll aH$). In this (‘superhorizon’) regime, the \mathbf{k} -mode asymptotes to a constant amplitude, provided that only one field is dynamically relevant during inflation [Lyth et al., 2005; Wands et al., 2000].⁷ If we restrict attention to tree-level diagrams, then under reasonable conditions the integrals which define the expectation values of \mathcal{R} are typically dominated by the intermediate (‘horizon crossing’) regime, where $\mathcal{R}(\mathbf{k})$ is exiting the horizon ($k \sim aH$) [Weinberg, 2005, 2006]. As a result, the correlation functions generally depend only on the Hubble and slow-roll parameters around the time of horizon exit.

The simple superhorizon behaviour of \mathcal{R} means that we can treat the power spectrum as constant outside the horizon. As has been described, its value depends only on the Hubble parameter and the slow-roll parameters around the time that the mode corresponding to k exited the horizon. For this reason, the time t at which we evaluate the wavefunctional $\Psi_t[\mathcal{R}]$, the generating functional $Z_t[q]$ and the PDF $\mathbb{P}_t[\mathcal{R}]$ is irrelevant, provided it is taken to be late enough that the curvature perturbation on interesting cosmological scales has already been generated and settled down to its final value. Indeed, we have implicitly been assuming that t is the time evaluated in comoving slices, so that observers on slices of constant t see no net momentum flux. Because \mathcal{R} is gauge-invariant and constant outside the horizon, our formalism is independent of how we choose to label the spatial slices. The evolution of \mathcal{R} outside the horizon is the principal obstacle involved in extending our analysis to the multiple-field scenario.

When calculating the statistics of density fluctuations on some given length scale $2\pi/k_H$, one should smooth the perturbation field over wavenumbers larger than k_H . To take ac-

⁷Where multiple fields are present, there will typically be an isocurvature perturbation between them: hypersurfaces of constant pressure and density will not coincide. Under these circumstances \mathcal{R} will evolve [Wands et al., 2000]. We do not consider the evolving case in this chapter, but rather restrict our attention to the single-field case where the superhorizon behaviour of \mathcal{R} is simple.

count of this, we introduce a smoothed field \bar{R} which is related to R via the rule $\bar{R}(\mathbf{k}) = \mathcal{W}(k, k_H)R(\mathbf{k})$, where \mathcal{W} is some window function. The probabilities we wish to calculate and compare to the real universe relate to \bar{R} rather than R . The exact choice of filter \mathcal{W} is mostly arbitrary. For the purpose of analytical calculations, it is simplest to pick a sharp cutoff in \mathbf{k} -space, which removes all modes with $k < k_H$. Such window function is given by

$$\mathcal{W}(k, k_H) = \Theta(k - k_H), \quad (3.31)$$

where, $\Theta(x)$ is the Heaviside step function defined in Eq. (2.152). This choice of window function has the disadvantage that it is non-local and oscillatory in real space, which makes physical interpretations difficult. The most common alternative choices, which do not suffer from such drawbacks, are (i) a Gaussian or (ii) the so-called ‘top hat’, which has a sharp cutoff in real space. We allow for a completely general choice of C^0 function \mathcal{W} , subject to the restriction that $\mathcal{W} \neq 0$ except at $k = \infty$ and possibly at an isolated set of points elsewhere (we will work with more specific forms of the window function in the following Chapters 4 and 5). This restriction is made so that there is a one-to-one relationship between \bar{R} and R . If this were not the case, it would be necessary to coarse-grain over classes of microphysical fields R which would give rise to the same smoothed field \bar{R} .

In addition to this smoothing procedure, the path integral must be regulated before carrying out the calculation in the next Section. This is achieved by artificially compactifying momentum space, so that the range of available wavenumbers is restricted to $k < \Lambda$, where Λ is an auxiliary hard cutoff or ‘regulator’. At the end of the calculation we take $\Lambda \rightarrow \infty$. Some care is necessary in carrying out this compactification. We set $\bar{R} = 0$ for $k > \Lambda$. In order to maintain continuity at $k = \Lambda$, we introduce a 1-parameter family of functions \mathcal{W}_Λ . These functions are supposed to satisfy the matching condition $\lim_{\Lambda \rightarrow \infty} \mathcal{W}_\Lambda(k) = \mathcal{W}(k)$, and are subject to the restriction $\mathcal{W}_\Lambda(\Lambda) = 0$. (These conditions could perhaps be relaxed.) The relationship between R and \bar{R} becomes

$$\bar{R}(\mathbf{k}) = \Theta(\Lambda - k)\mathcal{W}_\Lambda(k; k_H)R(\mathbf{k}) \quad (3.32)$$

To minimise unnecessary clutter in equations, we frequently suppress the Λ and k_H depen-

dences in \mathcal{W} , writing only $\mathcal{W}(k)$ with the smoothing scale k_H and hard cutoff Λ left implicit. Both the Gaussian and the ‘top-hat’ window functions approach zero as $k \rightarrow \infty$, and are compatible with (3.32) in the $\Lambda \rightarrow \infty$ limit. In this limit, the final result is independent of the exact choice of $\mathcal{W}_\Lambda(k, k_H)$.

We are interested in the probability of observing a given filtered field \bar{R} . One can express this via the rule [Matarrese et al., 2000; Taylor & Watts, 2000]

$$\mathbb{P}_t[\bar{R}] = \int [dR] \mathbb{P}_t[R] \delta[\bar{R} = \theta(\Lambda - k)\mathcal{W}R]. \quad (3.33)$$

3.3 Harmonic decomposition of the curvature perturbation

In the previous Section, we obtained the probability density for a given smoothed spatial configuration of the curvature perturbations. Given this probability density, the probability \mathbb{P} that the configuration exhibits some characteristic of \mathcal{R} , such as fluctuations of amplitude ϱ or a ‘fluctuation spectrum’ of the form $\mathcal{P}_\varrho(k)$, is formally obtained by integrating over all configurations of \bar{R} which exhibit the criteria which define ϱ [Matarrese et al., 2000]. In this section, we give a precise specification of these criteria. Before doing so, however, we exploit the compactification of momentum space introduced in (3.32) to define a complete set of partial waves. The smoothed field \bar{R} can be written as a superposition of these partial waves with arbitrary coefficients. Moreover, the path integral measure can formally be written as a product of conventional integrals over these coefficients [Hawking, 1977].

In the following we assemble the necessary formulae for the partial-wave decomposition. In particular, we will obtain expressions for the decomposition of \bar{R} , for the characteristics ϱ and $\mathcal{P}_\varrho(k)$, and a precise specification of the path integral measure.

3.3.1 Harmonic expansion of \bar{R}

We expand $\bar{R}(\mathbf{k})$ in harmonics on the unit sphere and along the radial $k = |\mathbf{k}|$ coordinate:

$$\bar{R}(\mathbf{k}) = \sum_{\ell=0}^{\infty} \sum_{m=-\ell}^{\ell} \sum_{n=1}^{\infty} \bar{R}_{\ell n}^m Y_{\ell m}(\theta, \phi) \psi_n(k). \quad (3.34)$$

The $Y_{\ell m}(\theta, \phi)$ are the standard spherical harmonics on the unit 2-sphere, while the $\psi_n(k)$ are any complete, orthogonal set of functions on the finite interval $[0, \Lambda]$. These harmonics should satisfy the following conditions⁸:

1. $\psi_n(k) \rightarrow 0$ smoothly as $k \rightarrow 0$, so that power is cut off on very large scales, and the universe remains asymptotically FRW with the zero-mode $a(t)$, which was used when computing the expectation values $\langle \mathcal{R} \cdots \mathcal{R} \rangle$;
2. $\psi_n(k) \rightarrow 0$ smoothly as $k \rightarrow \Lambda$, so that the resulting \bar{R} is compatible with Eq. (3.32);
3. $\psi_n(k)$ should have dimension $[M^{-3}]$, in order that Eq. (3.34) is dimensionally correct;
4. the $\psi_n(k)$ should be orthogonal in the measure $\int_0^\Lambda dk k^5 \mathcal{P}_{\mathcal{R}}^{-1}(k) \mathcal{W}^{-2}(k)$.

In addition, there is a constraint on the coefficients $\bar{R}_{\ell|n}^m$, because $\bar{R}(\mathbf{k})$ should be real in configuration space and therefore must obey the Fourier reality condition $\bar{R}(\mathbf{k})^* = \bar{R}(-\mathbf{k})$, where an asterisk denotes complex conjugation. The $\bar{R}_{\ell|n}^m$ are generically complex, so it is useful to separate the real and imaginary parts by writing $\bar{R}_{\ell|n}^m = a_{\ell|n}^m + ib_{\ell|n}^m$. The condition that \bar{R} is real in configuration space implies

$$a_{\ell|n}^{-m} = (-1)^{\ell+m} a_{\ell|n}^m, \quad (3.35)$$

$$b_{\ell|n}^{-m} = (-1)^{\ell+m+1} b_{\ell|n}^m. \quad (3.36)$$

These conditions halve the number of independent coefficients, since the a and b coefficients with strictly negative m are related to those with strictly positive m , whereas for the $m = 0$ modes, the b coefficients vanish if ℓ is even and the a coefficients vanish if ℓ is odd.

Condition 1 is made because, in the absence of this constraint, \bar{R} could develop unbounded fluctuations on extremely large scales, which would renormalise $a(t)$. Therefore, condition 1 can be interpreted as a consistency requirement, since the inflationary two- and three-point functions are calculated using perturbation theory on a FRW background with

⁸When expanding functions on \mathbb{R}^3 in terms of polar coordinates, a more familiar expansion involves spherical waves $Z_{\ell m|k} \propto J_\ell(kr) Y_{\ell m}(\theta, \phi)$, where J_ℓ is a spherical Bessel function. These waves are eigenfunctions of the Laplacian in polar coordinates, viz, $\nabla^2 Z_{\ell m|k} = -k^2 Z_{\ell m|k}$. An arbitrary function on \mathbb{R}^3 can be written in terms of spherical waves, which is equivalent to a Fourier expansion. We do not choose spherical waves as an appropriate complete, orthogonal set of basis functions here because we do not wish to expand 'arbitrary' functions, but rather functions obeying particular boundary conditions at $k = 0$. The spherical waves for low ℓ behave improperly at small k for this purpose. Moreover, it is not possible to easily impose the boundary condition $\bar{R}(k) \rightarrow 0$ as $k \rightarrow \Lambda$.

some given $a(t)$, which must be recovered asymptotically as $|\mathbf{x}| \rightarrow \infty$. It will later be necessary to sharpen this condition to include constraints on the behaviour of $\mathcal{P}_{\mathcal{R}}(k)$ near $k = 0$ beyond the weak requirement that $\sigma^2 = \int \mathcal{P}_{\mathcal{R}}(k) d \ln k$ is finite. Condition 4 is a technical requirement made for future convenience. Any other choice of normalisation would work just as well, but this choice is natural, given the k -dependence in the Gaussian kernel $\mathbb{G}[\bar{\mathbb{R}}]$. Indeed, with this condition, the Gaussian prefactor in $\mathbb{P}(\varrho)$ will reduce to the exponential of the sum of the squares of the $a_{\ell|n}^m$ and $b_{\ell|n}^m$. Condition 3 ensures that the inner product of two $\psi_n(k)$ in the measure $\int_0^\Lambda dk k^5 \mathcal{P}_{\mathcal{R}}^{-1}(k) \mathcal{W}^{-2}(k)$ is dimensionless. Condition 2 has less fundamental significance. It follows from the condition $\mathcal{W}_\Lambda(\Lambda) = 0$ and the artificial compactification of momentum space. However, as in the usual Sturm–Liouville theory [Morse & Feshbach, 1953], the precise choice of boundary condition is immaterial when $\Lambda \rightarrow \infty$, so this does not affect the final answer.

To demonstrate the existence of a suitable set of $\psi_n(k)$, we can adopt the definition

$$\psi_n(k) = \frac{\sqrt{2}}{J_{\nu+1}(\alpha_\nu^n)} \frac{\mathcal{P}_{\mathcal{R}}(k) \mathcal{W}(k)}{\Lambda k^2} J_\nu \left(\alpha_\nu^n \frac{k}{\Lambda} \right), \quad (3.37)$$

where $J_\nu(z)$ is the Bessel function of the first kind and of order ν , which is regular at the origin, and α_ν^n is its n -th zero. The order ν is arbitrary, except that in order to obey condition 1 above, we must have $k^{\nu-2} \mathcal{P}_{\mathcal{R}}(k) \rightarrow 0$ as $k \rightarrow 0$. This assumes that $\mathcal{W}(k) \rightarrow 1$ as $k \rightarrow 0$, as is usual for a volume-normalised window function. The $\psi_n(k)$ obey the orthonormality condition

$$\int_0^\Lambda dk \frac{k^5}{\mathcal{P}_{\mathcal{R}}(k) \mathcal{W}^2(k)} \psi_n(k) \psi_m(k) = \delta_{mn}, \quad (3.38)$$

where δ_{mn} is the Kronecker delta. The completeness relation can be written

$$\delta(k - k_0)|_{k \in [0, \Lambda]} = \frac{k_0^5}{\mathcal{P}_{\mathcal{R}}(k_0) \mathcal{W}^2(k_0)} \sum_n \psi_n(k) \psi_n(k_0), \quad (3.39)$$

where the range of k is restricted to the compact interval $[0, \Lambda]$.

Although we have given an explicit form for the ψ_n in order to demonstrate existence, the argument does not depend in detail on Eq. (3.37). The only important properties are

Eqs. (3.38)–(3.39), which follow from condition 4.

3.3.2 The path integral measure

Since any real C^0 function \bar{R} obeying the boundary conditions $\bar{R}(\mathbf{k}) \rightarrow 0$ as $k \rightarrow 0$ and $\bar{R}(\mathbf{k}) \rightarrow 0$ as $k \rightarrow \Lambda$ can be expanded in the form (3.34), one can formally integrate over all such \bar{R} by integrating over the coefficients $\bar{R}_{\ell|n}^m$. This prescription has been widely used for obtaining explicit results from path integral calculations. (For a textbook treatment, see Kleinert [2004].) In the present case, one should include in the integral only those $\bar{R}(\mathbf{x})$ which are real and so correspond to a physical curvature perturbation in the universe. Since the $Y_{\ell m}$ are complex, this means that instead of integrating unrestrictedly over the $\bar{R}_{\ell|n}^m$, the reality conditions (3.35) must be respected. A simple way to achieve this is to integrate only over those $a_{\ell|n}^m$ or $b_{\ell|n}^m$ with $m \geq 0$. The $m = 0$ modes must be treated separately since the a and b coefficients vanish for odd and even ℓ , respectively.

The integral over real \bar{R} can now be written as

$$\int_{\mathbb{R}} [d\bar{R}] = \left[\prod_{\ell=0}^{\infty} \prod_{m=1}^{\infty} \prod_{n=1}^{\ell} \mu \int_{-\infty}^{\infty} da_{\ell|n}^m \int_{-\infty}^{\infty} db_{\ell|n}^m \right] \left[\prod_{\substack{r=0 \\ r \text{ even}}}^{\infty} \prod_{s=1}^{\infty} \tilde{\mu} \int_{-\infty}^{\infty} da_{r|s}^0 \int_{-\infty}^{\infty} db_{r+1|s}^0 \right], \quad (3.40)$$

where the subscript \mathbb{R} on the integral indicates schematically that only real $\bar{R}(\mathbf{x})$ are included. The constants μ and $\tilde{\mu}$ account for the Jacobian determinant which arises in writing $\int [d\bar{R}]$ in terms of the harmonic coefficients $\bar{R}_{\ell|n}^m$. Their precise form is of no importance in the present calculation as they will be absorbed by the final normalisation factor.

As noted above, the detailed form of the measure (3.40) is not absolutely necessary for our argument. The important point is that each a or b integral can be carried out independently for $m \geq 0$. For this purpose, it is sufficient that the spectrum of partial waves be discrete, which follows from the (artificial) compactness of momentum space. However, although it is necessary to adopt some ‘regulator’ Λ in order to write the path integral measure in a concrete form such as (3.40), we expect the answer to be independent of the specific regulator which is chosen. In the present context, this means that our final expressions should not depend on Λ , so that the passage to the $\Lambda \rightarrow \infty$ limit becomes trivial.

3.3.3 The total fluctuation ϱ and the spectrum $\mathcal{P}_\varrho(k)$

There are at least two useful ways in which one might attempt to measure the amplitude of fluctuations in \bar{R} . The first is the ‘total smoothed fluctuation’ at a given point $\mathbf{x} = \mathbf{x}_0$. By a suitable choice of coordinates, we can always arrange that \mathbf{x}_0 is the origin, so the parameter becomes $\varrho \equiv \bar{R}(\mathbf{0})$. When \bar{R} is smoothed on scales of order the horizon size this gives a measure of the fluctuation in each Hubble volume, since distances of less than a horizon size no longer have any meaning. For example, Shibata & Sasaki [1999] have proposed that ϱ defined in this way represents a useful criterion for the formation of PBHs, with formation occurring whenever ϱ exceeds a threshold value ϱ_{th} of order unity [Green et al., 2004]. This measure of the fluctuation is non-local in momentum space. Making use of the relation $\int d\Omega(\theta, \phi) Y_{\ell m}(\theta, \phi) = \sqrt{4\pi} \delta_{\ell,0} \delta_{m,0}$ for the homogeneous mode of the spherical harmonics, one can characterise the amplitude as

$$\varrho \equiv \bar{R}(\mathbf{0}) = \int \frac{d^3k}{(2\pi)^3} \bar{R}(\mathbf{k}) e^{i\mathbf{k}\cdot\mathbf{x}}|_{\mathbf{x}=\mathbf{0}} = \frac{\sqrt{4\pi}}{(2\pi)^3} \int dk k^2 \sum_{n=1}^{\infty} a_{0|n}^0 \psi_n(k). \quad (3.41)$$

On the other hand, one might be interested in contributions to the total smoothed fluctuation in each Hubble volume which arise from features in the spectrum near some characteristic scale of wavenumber k . For this reason, we consider a second measure of the fluctuation, which we call the ‘fluctuation spectrum’, defined by

$$\mathcal{P}_\varrho(k) = \frac{d\bar{R}(\mathbf{0})}{d \ln k}. \quad (3.42)$$

(Thus the total smoothed fluctuation can be obtained by integrating its spectrum according to the usual rule, viz, $\varrho = \int \mathcal{P}_\varrho(k) d \ln k$.) This condition is local in \mathbf{k} -space. Differentiating (3.41), one can characterise $\mathcal{P}_\varrho(k)$ by the functional constraint

$$\mathcal{P}_\varrho(k) = \frac{\sqrt{4\pi}}{(2\pi)^3} \sum_{n=1}^{\infty} a_{0|n}^0 k^3 \psi_n(k). \quad (3.43)$$

We will calculate the statistics of both the total fluctuation ϱ and the spectrum $\mathcal{P}_\varrho(k)$. In each case, the calculation is easily adapted to other observables which are non-local or local in

momentum space⁹. Indeed, both the non-local ϱ and the local $\mathcal{P}_\varrho(k)$ are members of a large class of observables, which we can collectively denote by ϑ , and which all share nearly-Gaussian statistics. Specifically, Eqs. (3.41) and (3.43) can be written in a unified manner in the form

$$\sum_{n=1}^{\infty} a_{0|n}^0 \Sigma_n(k) = \frac{(2\pi)^3}{\sqrt{4\pi}} \vartheta(k), \quad (3.44)$$

where

$$\Sigma_n = \begin{cases} \int_0^\Lambda dk k^2 \psi_n(k) & (\vartheta = \varrho); \\ k^3 \psi_n(k) & (\vartheta = \mathcal{P}_\varrho(k)). \end{cases} \quad (3.45)$$

Note that, in the first case, the Σ_n are independent of k . Any characteristic which can be put in this form, coupling only to the real zero-modes $a_{0|n}^0$ of $\bar{\mathbb{R}}$, will necessarily develop nearly-Gaussian (i.e., weakly non-Gaussian) statistics. More general choices of characteristic are possible, which cannot be cast in the form (3.44). For example, one can consider characteristics which depend non-linearly on the $a_{0|n}^0$. Such characteristics will generally lead to strongly non-Gaussian probabilities. The Gaussianity of the final PDF depends on the geometry of the constraint surface in an analogous way to the decoupling of the Fadeev-Popov ghost fields in gauge field theory [Weinberg, 2005]. These non-Gaussian choices of characteristic can also be handled by generalising our technique, but we do not consider them here.

3.4 The probability density function for ϱ

We first calculate the probability density for the non-local constraint ϱ , given by Eq. (3.41).

The expression is

$$\mathbb{P}(\varrho) \propto \int_{\mathbb{R}} [d\bar{\mathbb{R}}] \mathbb{P}[\bar{\mathbb{R}}] \delta \left[\sum_{n=1}^{\infty} a_{0|n}^0 \Sigma_n - \frac{(2\pi)^3}{\sqrt{4\pi}} \varrho \right]. \quad (3.46)$$

⁹The local and non-local variables defined here should not be confused with the local and equilateral triangulations which are specifically defined for the bispectrum in Chapter 2.

To obtain this density, one treats ϱ as a collective coordinate parameterising part of $\bar{\mathbb{R}}$. The remaining degrees of freedom, which are orthogonal to ϱ , are denoted by $\bar{\mathbb{R}}^\perp$. Therefore the functional measure $[d\bar{\mathbb{R}}]$ can be broken into $[d\bar{\mathbb{R}}^\perp]$ and $d\varrho$. After integrating the functional density $\mathbb{P}[\bar{\mathbb{R}}] [d\bar{\mathbb{R}}]$ over $\bar{\mathbb{R}}^\perp$, the quantity which is left is the probability density $\mathbb{P}(\varrho) d\varrho$. In this case, the integration over the orthogonal degrees of freedom $\bar{\mathbb{R}}^\perp$ is accomplished via the δ -function, which filters out only those members of the ensemble which satisfy Eq. (3.41). We emphasise that this is a conventional δ -function, not a δ -functional. There is no need to take account of a Fadeev–Popov type factor because the Jacobian associated with the constraint (3.44) is field-independent, in virtue of the linearity of Eq. (3.41) in $a_{0|n}^0$.

3.4.1 The Gaussian case

We first give the calculation in the approximation that only the two-point function is retained. In this approximation, the PDF of ϱ will turn out to be purely Gaussian, which allows us to develop our method without the extra technical difficulties introduced by including non-Gaussian effects.

If all correlation functions of order three and higher are set to zero, then we are in a Gaussian regime and hence $\mathbb{P}[\bar{\mathbb{R}}] \propto \mathbb{G}[\bar{\mathbb{R}}]$. Using (3.4), one can write

$$\begin{aligned} \mathbb{G}[\bar{\mathbb{R}}] &= \exp\left(-\frac{1}{2} \int d\Omega \int k^2 dk \frac{k^3}{(2\pi)^3 2\pi^2} \frac{1}{\mathcal{P}_{\mathcal{R}}(k) \mathcal{W}^2(k)}\right) \\ &\times \sum_{\ell_1, m_1, n_1} \sum_{\ell_2, m_2, n_2} \bar{\mathbb{R}}_{\ell_1|n_1}^{m_1} \bar{\mathbb{R}}_{\ell_2|n_2}^{m_2\dagger} Y_{\ell_1 m_1}(\theta, \phi) Y_{\ell_2, m_2}^\dagger(\theta, \phi) \psi_{n_1}(k) \psi_{n_2}(k). \end{aligned} \quad (3.47)$$

The harmonics $Y_{\ell m}$ and ψ_n integrate out of this expression entirely, using the orthonormality relation (3.38) and the spherical harmonic completeness relation

$$\int d\Omega Y_{\ell_1 m_1} Y_{\ell_2 m_2}^\dagger = \delta_{\ell_1 \ell_2} \delta_{m_1 m_2}. \quad (3.48)$$

Moreover, after rewriting the a and b coefficients with $m < 0$ in terms of the $m > 0$ coeffi-

cients, we obtain

$$\mathbb{G}[\bar{\mathbf{R}}] = \exp \left(- \frac{1}{2\pi^2(2\pi)^3} \sum_{\ell=0}^{\infty} \sum_{m=1}^{\ell} \sum_{n=1}^{\infty} [|a_{\ell|n}^m|^2 + |b_{\ell|n}^m|^2] - \frac{1}{4\pi^2(2\pi)^3} \sum_{\substack{\ell=0 \\ \ell \text{ even}}}^{\infty} \sum_{n=1}^{\infty} [|a_{\ell|n}^0|^2 + |b_{\ell+1|n}^0|^2] \right). \quad (3.49)$$

The δ -function in (3.46) constrains one of the $a_{0|n}^0$ (e.g. $a_{0|0}^0$) in terms of ϱ and the other coefficients. It would then be possible to evaluate $\mathbb{P}(\varrho)$ by integrating out the δ -function immediately. However, this does not turn out to be a convenient procedure. Instead, we introduce the Fourier representation of the δ -function and rewrite (3.46) as

$$\mathbb{P}(\varrho) \propto \int_{\mathbb{R}} [d\bar{\mathbf{R}}] \int_{-\infty}^{\infty} dz \mathbb{G}[\bar{\mathbf{R}}] \exp \left(iz \left[\sum_{n=1}^{\infty} a_{0|n}^0 \Sigma_n - \frac{(2\pi)^3}{\sqrt{4\pi}} \varrho \right] \right), \quad (3.50)$$

where the functional measure is understood to be Eq. (3.40). The final answer is obtained by integrating out z together with all of the a and b coefficients. In order to achieve this, it is necessary to separate $a_{0|n}^0$, z and ϱ from each other by successively completing the square in $a_{0|0}^0$ and z . Working with $a_{0|0}^0$ first, we find

$$\begin{aligned} & \exp \left(- \frac{1}{4\pi^2} \frac{1}{(2\pi)^3} \sum_{n=1}^{\infty} |a_{0|n}^0|^2 + iz \sum_{n=1}^{\infty} a_{0|n}^0 \Sigma_n \right) \\ &= \exp \left(- \frac{1}{4\pi^2} \frac{1}{(2\pi)^3} \sum_{n=1}^{\infty} (a_{0|n}^0 - 2\pi^2(2\pi)^3 iz \Sigma_n)^2 - (2\pi)^3 \pi^2 z^2 \Sigma^2 \right), \end{aligned} \quad (3.51)$$

where we have introduced a function $\Sigma^2 \equiv \sum_{n=1}^{\infty} \Sigma_n^2$. In the final PDF, Σ^2 will turn out to be the variance of ϱ . From Eq. (3.51), it is clear that making the transformation $a_{0|n}^0 \mapsto a_{0|n}^0 + 2\pi^2(2\pi)^3 iz \Sigma_n$ suffices to separate $a_{0|n}^0$ from z . The measure, Eq. (3.40), is formally invariant under this transformation. Exactly the same procedure can now be applied to z and ϱ , giving

$$\exp \left(- (2\pi)^3 \pi^2 z^2 \Sigma^2 - \frac{(2\pi)^3}{\sqrt{4\pi}} i \varrho z \right) = \exp \left[- (2\pi)^3 \pi^2 \Sigma^2 \left(z + \frac{i \varrho}{2\pi^2 \sqrt{4\pi} \Sigma^2} \right)^2 - \frac{\varrho^2}{2\Sigma^2} \right]. \quad (3.52)$$

As before, the finite shift $z \mapsto z - i\varrho/2\pi^2\sqrt{4\pi}\Sigma^2$ leaves the measure intact and decouples z

and ϱ . The a , b and z integrals can be done independently, but since they do not involve ϱ , they contribute only an irrelevant normalisation to $\mathbb{P}(\varrho)$. Thus, we obtain Gaussian statistics for ϱ :

$$\mathbb{P}(\varrho) \propto \exp\left(-\frac{\varrho^2}{2\Sigma^2}\right). \quad (3.53)$$

It remains to evaluate the variance Σ^2 . In the present case, we have $\Sigma_n = \int_0^\Lambda dk k^2 \psi_n(k)$. From the completeness relation Eq. (3.39), it follows that

$$\sum_n k_0^2 \psi_n(k_0) k^2 \psi_n(k) = \frac{k^2 \mathcal{P}_{\mathcal{R}}(k_0) \mathcal{W}^2(k_0)}{k_0^3} \delta(k - k_0). \quad (3.54)$$

Σ^2 is now obtained by integrating term-by-term under the summation. The result coincides with the ‘smoothed’ conventional variance (cf. Eq. (3.3)),

$$\Sigma_\Lambda^2(k_H) = \int_0^\Lambda d \ln k \mathcal{W}^2(k; k_H) \mathcal{P}_{\mathcal{R}}(k). \quad (3.55)$$

Thus, as expected, Eq. (3.53) reproduces the Gaussian distribution (3.2) which was derived on the basis of the central limit theorem, with the proviso that parameters (such as Σ^2) describing the distribution of ϱ are associated with the smoothed field $\bar{\mathcal{R}}$ rather than the microphysical field \mathcal{R} . Σ^2 is therefore implicitly a function of scale, with the scale-dependence entering through the window function. Note that it was only necessary to use the completeness relation to obtain this result, which follows from condition 4 in Section 3.3.1.

3.4.2 The non-Gaussian case

The non-Gaussian case is a reasonably straightforward extension of the calculation described in the preceding section, with the term $\Upsilon^{(0)}$ in Eq. (3.27) now being included. However, some parts of the calculation become algebraically long, and there are subtleties connected with the appearance of the bispectrum.

The inclusion of $\Upsilon^{(0)}$ corrects the pure Gaussian statistics by a quantity proportional to the three-point function, $\langle \mathcal{R} \mathcal{R} \mathcal{R} \rangle$, which is given in Eq. (3.5). This correction is written in terms of the representative spectrum $\bar{\mathcal{P}}_{\mathcal{R}}^2$, which prescribes when the slow-roll prefactor,

given by the amplitude of the spectrum, should be evaluated [Maldacena, 2003]. For modes which cross the horizon almost simultaneously, with size $k_1 \sim k_2 \sim k_3$, this prefactor should be $\bar{\mathcal{P}}_{\mathcal{R}}^2 = \mathcal{P}_{\mathcal{R}}(k)^2$, where k is the common magnitude of the k_i . In the alternative case, where one \mathbf{k} -mode crosses appreciably before the other two, $\bar{\mathcal{P}}_{\mathcal{R}}^2$ should be roughly given by

$$\bar{\mathcal{P}}_{\mathcal{R}}^2 = \mathcal{P}_{\mathcal{R}}(\max k_i) \mathcal{P}_{\mathcal{R}}(\min k_i). \quad (3.56)$$

Since the difference between this expression and the expression when all the k are of the same magnitude is very small, it is reasonable to adopt Eq. (3.56) as our definition of $\bar{\mathcal{P}}_{\mathcal{R}}^2$. We stress that this prescription relies on the conservation of \mathcal{R} outside the horizon [Allen et al., 2006], and it would therefore become more complicated if extended to a multiple-field scenario.

With this parametrization, the probability measure on the ensemble is obtained by combining (3.4), (3.27), (3.28) and (3.5):

$$\mathbb{P}[\bar{\mathbf{R}}] \propto \mathbb{G}[\bar{\mathbf{R}}] \left(1 - \frac{1}{6} \int \frac{d^3 k_1 d^3 k_2 d^3 k_3}{(2\pi)^6 2\pi^2} \delta(\Delta) \frac{\bar{\mathcal{P}}_{\mathcal{R}}^2 \mathcal{A}}{\prod_i \mathcal{P}_{\mathcal{R}}(k_i)} \frac{\bar{\mathbf{R}}(\mathbf{k}_1) \bar{\mathbf{R}}(\mathbf{k}_2) \bar{\mathbf{R}}(\mathbf{k}_3)}{\mathcal{W}(k_1) \mathcal{W}(k_2) \mathcal{W}(k_3)} \right). \quad (3.57)$$

This expression should be integrated with the constraint (3.41) and measure (3.40) to obtain the probability $\mathbb{P}(\varrho)$. At first this appears to lead to an undesirable consequence, since the integral of any odd function of $\bar{\mathbf{R}}$ multiplied by $\mathbb{G}[\bar{\mathbf{R}}]$ must be zero. It may therefore seem that the non-Gaussian corrections we are trying to obtain will cancel out. This would certainly be correct if the integral were unconstrained. However, the presence of the δ -function constraint means that the shifts of $a_{0|n}^0$ and z which are necessary to decouple the integration variables give rise to a non-vanishing correction.

The finite shift necessary to decouple $a_{0|n}^0$ and z is not changed by the presence of non-Gaussian corrections, since it only depends on the argument of the exponential term. This is the same in the Gaussian and non-Gaussian cases. After making this shift, which again leaves the measure invariant, the integration becomes

$$\mathbb{P}(\varrho) \propto \int_{\mathbb{R}} [d\bar{\mathbf{R}}] \int_{-\infty}^{\infty} dz \mathbb{G}[\bar{\mathbf{R}}] \exp \left(-(2\pi)^3 \pi^2 \Sigma^2 z^2 - \frac{(2\pi)^3}{\sqrt{4\pi}} i z \varrho \right) (1 - \mathcal{J}_0 - \mathcal{J}_2), \quad (3.58)$$

where

$$\mathcal{J}_0 = \int d^3k_1 d^3k_2 d^3k_3 \frac{2\pi^4(2\pi)^3}{3(4\pi)^{3/2}} \delta(\Delta) \frac{\bar{\mathcal{P}}_{\mathcal{R}}^2 \mathcal{A}}{\prod_i \mathcal{P}_{\mathcal{R}}(k_i)} \quad (3.59)$$

$$\sum_{n_1, n_2, n_3} i^3 z^3 \sum_{\Sigma_{n_1}} \sum_{\Sigma_{n_2}} \sum_{\Sigma_{n_3}} \frac{\psi_{n_1}(k_1) \psi_{n_2}(k_2) \psi_{n_3}(k_3)}{\mathcal{W}(k_1) \mathcal{W}(k_2) \mathcal{W}(k_3)},$$

and

$$\mathcal{J}_2 = \left[\int \frac{d^3k_1 d^3k_2 d^3k_3}{6(2\pi)^3 \sqrt{4\pi}} \delta(\Delta) \frac{\bar{\mathcal{P}}_{\mathcal{R}}^2 \mathcal{A}}{\prod_i \mathcal{P}_{\mathcal{R}}(k_i)} \sum_{n_1} \sum_{\ell_2, m_2, n_2} \sum_{\ell_3, m_3, n_3} \quad (3.60)$$

$$\times i z \sum_{\Sigma_{n_1}} \frac{\psi_{n_1}(k_1)}{\mathcal{W}(k_1)} \bar{R}_{\ell_2|n_2}^{m_2} \bar{R}_{\ell_3|n_3}^{m_3} Y_{\ell_2 m_2}(\theta_2, \phi_2) Y_{\ell_3 m_3}(\theta_3, \phi_3) \frac{\psi_{n_2}(k_2) \psi_{n_3}(k_3)}{\mathcal{W}(k_2) \mathcal{W}(k_3)} \right]$$

$$+ [\mathbf{1} \Leftrightarrow \mathbf{2}] + [\mathbf{1} \Leftrightarrow \mathbf{3}].$$

The symbol $[\mathbf{1} \Leftrightarrow \mathbf{2}]$ represents the expression in square brackets with the labels 1 and 2 exchanged, and similarly for $[\mathbf{1} \Leftrightarrow \mathbf{3}]$. The range of the m_2 and m_3 summations is from $-\ell_2$ to ℓ_2 and $-\ell_3$ to ℓ_3 , respectively. In addition, the shift of $a_{0|n}^0$ generates other terms linear and cubic in the $\bar{R}_{\ell|n}^m$, but these terms do not contribute to $\mathbb{P}(\varrho)$ and we have omitted them from (3.58).

After shifting z to decouple z and ϱ , the integrals J_0 and J_2 develop terms proportional to z^0 , z , z^2 and z^3 . Of these, only the z^0 and z^2 survive the final z integration. Consequently, we suppress terms linear and cubic in z from the following expressions. The integral \mathcal{J}_0 becomes

$$\mathcal{J}_0 = \int d^3k_1 d^3k_2 d^3k_3 \frac{\pi^2(2\pi)^3}{3(4\pi)^2} \left(\frac{1}{16\pi^5} \frac{\varrho^3}{\Sigma^6} - 3 \frac{z^2 \varrho}{\Sigma^2} \right) \delta(\Delta) \frac{\bar{\mathcal{P}}_{\mathcal{R}}^2 \mathcal{A}}{\prod_i \mathcal{P}_{\mathcal{R}}(k_i)} \quad (3.61)$$

$$\times \sum_{n_1, n_2, n_3} \sum_{\Sigma_{n_1}} \sum_{\Sigma_{n_2}} \sum_{\Sigma_{n_3}} \frac{\psi_{n_1}(k_1) \psi_{n_2}(k_2) \psi_{n_3}(k_3)}{\mathcal{W}(k_1) \mathcal{W}(k_2) \mathcal{W}(k_3)},$$

while \mathcal{J}_2 simplifies to

$$\mathcal{J}_2 = \left[\int \frac{d^3k_1 d^3k_2 d^3k_3}{48\pi^3(2\pi)^3} \frac{\varrho}{\Sigma^2} \sum_{n_1} \sum_{\ell_2, m_2, n_2} \sum_{\ell_3, m_3, n_3} \quad (3.62)$$

$$\times \sum_{\Sigma_{n_1}} \frac{\psi_{n_1}(k_1)}{\mathcal{W}(k_1)} R_{\ell_2|n_2}^{m_2} R_{\ell_3|n_3}^{m_3} Y_{\ell_2 m_2}(\theta_2, \phi_2) Y_{\ell_3 m_3}(\theta_3, \phi_3) \frac{\psi_{n_2}(k_2) \psi_{n_3}(k_3)}{\mathcal{W}(k_2) \mathcal{W}(k_3)} \right]$$

$$+ [\mathbf{1} \Leftrightarrow \mathbf{2}] + [\mathbf{1} \Leftrightarrow \mathbf{3}],$$

the m summations being over the same range as before. Thus \mathcal{J}_0 contains corrections proportional to ϱ and ϱ^3 , whereas \mathcal{J}_2 only contains corrections proportional to ϱ .

The a , b and z integrations can now be performed, with the integrand written entirely in terms of the $a_{\ell|n}^m$ and $b_{\ell|n}^m$ with $m \geq 0$. There are no a or b integrations in J_0 . There are no z integrations in \mathcal{J}_2 but the a and b integrations involved in the product $\bar{R}_{\ell_2|n_2}^{m_2} \bar{R}_{\ell_3|n_3}^{m_3}$ fix $\ell_2 = \ell_3$, $m_2 = m_3$ and $n_2 = n_3$. One then uses the spherical harmonic completeness relation,

$$\sum_{\ell=0}^{\infty} \sum_{m=-\ell}^{\ell} Y_{\ell m}(\theta_1, \phi_1) Y_{\ell m}^{\dagger}(\theta_2, \phi_2) = \delta(\phi_1 - \phi_2) \delta(\cos \theta_1 - \cos \theta_2) \quad (3.63)$$

and the equivalent relationship for the ψ -harmonics, Eq. (3.39), to obtain

$${}^0\mathcal{J}_2 = \left[\int \frac{d^3 k_1 d^3 k_2 d^3 k_3}{24\pi} \frac{\varrho}{\Sigma^2} \delta(\Delta) \frac{\bar{\mathcal{P}}_{\mathcal{R}}^2 \mathcal{A}}{\prod_i \mathcal{P}_{\mathcal{R}}(k_i) \mathcal{W}(k_i)} \frac{\mathcal{P}_{\mathcal{R}}(k_2) \mathcal{W}^2(k_2)}{k_2^3} \right. \\ \left. \sum_n \Sigma_n \psi_n(k_1) \delta(\mathbf{k}_2 + \mathbf{k}_3) \right] + [\mathbf{1} \Leftrightarrow \mathbf{2}] + [\mathbf{1} \Leftrightarrow \mathbf{3}]. \quad (3.64)$$

The terms with 1 exchanged with 2 and 3 generate the same integral as the first term and can be absorbed into an overall factor of 3.

\mathcal{J}_0 involves only z integrations. It can be written as

$$\mathcal{J}_0 = \int \frac{d^3 k_1 d^3 k_2 d^3 k_3}{96\pi^2} \left(\frac{\varrho^3}{\Sigma^6} - 3 \frac{\varrho}{\Sigma^4} \right) \delta(\Delta) \frac{\bar{\mathcal{P}}_{\mathcal{R}}^2 \mathcal{A}}{\prod_i \mathcal{P}_{\mathcal{R}}(k_i) \mathcal{W}(k_i)} \\ \times \sum_{n_1, n_2, n_3} \Sigma_{n_1} \Sigma_{n_2} \Sigma_{n_3} \psi_{n_1}(k_1) \psi_{n_2}(k_2) \psi_{n_3}(k_3). \quad (3.65)$$

To simplify these expressions further, it is necessary to obtain the value of the sum $\sum_{n=1}^{\infty} \Sigma_n \psi_n(k)$.

Reasoning as before from the completeness relation Eq. (3.39), it follows that

$$\sum_{n=1}^{\infty} \Sigma_n \psi_n(k) = \frac{\mathcal{P}_{\mathcal{R}}(k) \mathcal{W}^2(k)}{k^3}. \quad (3.66)$$

From this, it is straightforward to show that

$$\mathcal{J}_0 = \int \frac{d^3 k_1 d^3 k_2 d^3 k_3}{96\pi^2 \prod_i k_i^3 \mathcal{W}^{-1}(k_i)} \delta(\Delta) \bar{\mathcal{P}}_{\mathcal{R}}^2 \mathcal{A} \left(\frac{\varrho^3}{\Sigma^6} - 3 \frac{\varrho}{\Sigma^4} \right), \quad (3.67)$$

where Σ^2 is the smoothed variance, Eq. (3.55). On the other hand J_2 becomes

$$\mathcal{J}_2 = \int \frac{d^3k_1 d^3k_2 d^3k_3}{24\pi/3} \frac{\varrho}{\Sigma^2} \delta(\Delta) \frac{\bar{\mathcal{P}}_{\mathcal{R}}^2}{\mathcal{P}_{\mathcal{R}}(k_2)} \mathcal{W}(k_1) \mathcal{A} \frac{\delta(\mathbf{k}_2 + \mathbf{k}_3)}{k_1^3 k_2^3}. \quad (3.68)$$

After integrating out \mathbf{k}_3 and the angular part of \mathbf{k}_1 and \mathbf{k}_2 , this gives

$$\mathcal{J}_2 = 2\pi \int dk_2 k_2^2 \int dk_1 \delta(k_1) \frac{\varrho}{\Sigma^2} \mathcal{W}(k_1) \frac{1}{k_2^3 \mathcal{P}_{\mathcal{R}}(k_2)} \lim_{k_1 \rightarrow 0} \mathcal{A} \frac{\mathcal{P}_{\mathcal{R}}(k_1)}{k_1^3}, \quad (3.69)$$

where we have used the fact that k_1 is constrained to zero by the δ -function to evaluate the bispectrum \mathcal{A} in the ‘squeezed’ limit where one of the momenta goes to zero [Maldacena, 2003; Allen et al., 2006; Creminelli & Zaldarriaga, 2004]. In this limit, $\min(k_i) = k_1$ and $\max(k_i) = k_2 = k_3$, so it is possible to expand $\bar{\mathcal{P}}_{\mathcal{R}}^2$ unambiguously. Moreover, $\lim_{k_1 \rightarrow 0} \mathcal{A} = \alpha k_2^3$, so $\mathcal{J}_2 = 0$ if $\mathcal{P}_{\mathcal{R}}(k)/k^3 \rightarrow 0$ as $k \rightarrow 0$. This more stringent condition on how strongly large-scale power is suppressed was anticipated in Section 3.3.1. It requires that $\mathcal{P}_{\mathcal{R}}(k)$ falls at small k faster than k^3 . If this does not occur, then the integral diverges. (There is a marginal case when $\mathcal{P}_{\mathcal{R}}(k)/k^3$ tends to a finite limit as k approaches zero. We assume that this is not physically relevant.)

The \mathcal{J}_2 integral contains a δ -function $\delta(\mathbf{k}_2 + \mathbf{k}_3)$. It can therefore be interpreted as counting contributions to the bispectrum which come from a correlation between the modes \mathbf{k}_2 and \mathbf{k}_3 , in a background created by \mathbf{k}_1 , which exited the horizon in the asymptotic past. As we have already argued, modes of this sort are included in the FRW background around which we perturb to obtain the correlation functions of \mathcal{R} , so we can anticipate that its contribution should be zero, as the above analysis shows explicitly. In this interpretation, the condition $\mathcal{P}_{\mathcal{R}}(k)/k^3 \rightarrow 0$ as $k \rightarrow 0$ ensures that the perturbation does not destroy the FRW background. Indeed, fluctuations on very large scales in effect describe transitions from one FRW world to another via a shift in the zero-momentum modes of the background metric. In this case, there is only one such mode, which is the scale factor $a(t)$. These transitions are rather like changing the vacuum state in a quantum field theory. As a result, fluctuations of a large volume of the universe between one FRW state and another are strongly suppressed.

For fluctuations on the Hubble scale, therefore, the PDF should be

$$\mathbb{P}(\varrho) = \frac{1}{\sqrt{2\pi}\Sigma} \left[1 - \left(\frac{\varrho^3}{\Sigma^6} - 3\frac{\varrho}{\Sigma^4} \right) \mathcal{J} \right] \exp\left(-\frac{\varrho^2}{2\Sigma^2}\right), \quad (3.70)$$

where we have used the fact that the corrections are odd in ϱ and therefore do not contribute to the overall normalisation of $\mathbb{P}(\varrho)$. The (dimensionless) coefficient \mathcal{J} is

$$\mathcal{J} = \int \frac{d^3k_1 d^3k_2 d^3k_3}{96\pi^2 \prod_i k_i^3 \mathcal{W}^{-1}(k_i)} \delta(\Delta) \bar{\mathcal{P}}_{\mathcal{R}}^2 \mathcal{A}. \quad (3.71)$$

This explicit expression is remarkably simple. Although it is preferable for calculation, it can be recast directly as the integrated bispectrum with respect to \mathcal{W} :

$$\mathcal{J} = \frac{1}{48(2\pi)^3(2\pi^2)^3} \int d^3k_1 d^3k_2 d^3k_3 \langle \mathcal{R}(\mathbf{k}_1) \mathcal{R}(\mathbf{k}_2) \mathcal{R}(\mathbf{k}_3) \rangle \mathcal{W}(k_1) \mathcal{W}(k_2) \mathcal{W}(k_3). \quad (3.72)$$

As a consistency check, we note that the expectation of ϱ , defined as $E(\varrho) = \int \varrho \mathbb{P}(\varrho) d\varrho$, is zero. This is certainly necessary, since the universe must contain as many underdense regions as overdense ones, but it is a non-trivial restriction, since both the ϱ and ϱ^3 corrections to $\mathbb{P}(\varrho)$ do not separately average to zero. The particular combination of coefficients in (3.70) is the unique correction [up to $\mathcal{O}(\varrho^3)$], containing only odd powers of ϱ which maintains $E(\varrho) = 0$.

Finally, we note that Eqs. (3.70)–(3.71) do not explicitly involve the cut-off Λ , except as a limit of integration in quantities such as Σ_Λ^2 and \mathcal{W}_Λ which possess a well-defined, finite limit at large Λ . As a result, there is no obstruction to taking the $\Lambda \rightarrow \infty$ limit to remove the regulator entirely.

3.4.3 When is perturbation theory valid?

It is known from explicit calculation that the bispectrum is of order $\mathcal{P}_{\mathcal{R}}^2$ multiplied by the quantity, f_{NL} , which is predicted to be small when slow-roll is valid. It is therefore reasonable to suppose that whenever the window functions \mathcal{W} are peaked around some probe wavenumber k_* , one has the order of magnitude relations $\Sigma^2 \sim \mathcal{P}_*$ and $\mathcal{J} \sim \mathcal{P}_*^2$, where \mathcal{P}_*

represents the spectrum evaluated at $k = k_*$. Since the ϱ^3 correction dominates for $\varrho > \sqrt{3}\Sigma$, this means that for ϱ not too large, $\varrho \ll \mathcal{P}_*^{-3/2}$, the perturbative correction we have calculated will be small. As ϱ increases, so that $\varrho \gg \mathcal{P}_*^{-3/2}$, perturbation theory breaks down and the power series in ϱ needs resummation. In any case, at such large values of ϱ , the calculation described above ought to be supplemented by new physics which can be expected to become important at high energy densities. The details of these corrections presumably do not matter too much, because at any finite order, the fast-decaying exponential piece suppresses any contributions from large values of ϱ .

At some value of ϱ , corrections coming from the trispectrum can be expected to become comparable to those coming from the bispectrum that we have computed. We do not know precisely which are the dominant contributions of the correction from the trispectrum. Such corrections to the non-Gaussian PDF are to be explored in the future.

3.5 The probability density function for $\mathcal{P}_\varrho(k)$

The probability density function for $\mathcal{P}_\varrho(k)$ can be obtained by a reasonably straightforward modification of the above argument, taking account of the fact that the constraint, Eq. (3.43) is now a functional constraint. This means that, when splitting the functional measure $[d\bar{\mathbf{R}}]$ into a product of $[d\mathcal{P}_\varrho(k)]$ and the orthogonal degrees of freedom $[d\bar{\mathbf{R}}^\perp]$, the result after integrating out the $\bar{\mathbf{R}}^\perp$ coordinates gives a functional probability density in $[d\mathcal{P}_\varrho(k)]$. In particular, with the definition (3.45), the δ -function in Eq. (3.50) is now represented as

$$\int [dz] \exp \left[i \int_0^\infty dk z(k) \left(\sum_{n=1}^\infty a_{0|n}^0 k^3 \psi_n(k) - \frac{(2\pi)^3}{\sqrt{4\pi}} \mathcal{P}_\varrho(k) \right) \right]. \quad (3.73)$$

In order to carry out this calculation, we write $z(k)$ formally as

$$z(k) = \sum_{n=1}^\infty \frac{k^2}{\mathcal{P}_\mathcal{R}(k)\mathcal{W}^2(k)} z_n \psi_n(k). \quad (3.74)$$

The integration measure $\int [dz]$ becomes $\prod_n \check{\mu} \int_{-\infty}^\infty dz_n$, where, as before, $\check{\mu}$ is a field-independent Jacobian representing the change of variables from $z(k) \mapsto z_n$. Its value is not relevant to

the present calculation. In addition, we introduce a set of coefficients $\tilde{\mathcal{P}}_{\varrho_n}$ to describe $\mathcal{P}_\varrho(k)$,

$$\frac{\mathcal{P}_\varrho(k)}{k^3} = \sum_{n=1}^{\infty} \tilde{\mathcal{P}}_{\varrho_n} \psi_n(k). \quad (3.75)$$

The $\tilde{\mathcal{P}}_{\varrho_n}$ can be calculated using the rule $\tilde{\mathcal{P}}_{\varrho_n} = \int_0^\Lambda dk k^2 \mathcal{P}_{\mathcal{R}}^{-1}(k) \mathcal{W}^{-2}(k) \mathcal{P}_\varrho(k) \psi_n(k)$. Note that, in order to do so, we have made the implicit assumption that $\mathcal{P}_\varrho(k)/k^3 \rightarrow 0$ as $k \rightarrow 0$, to ensure that (3.75) is compatible with the boundary conditions for the $\psi_n(k)$. In other words, we make the ansatz of a suppression of power in modes with low k .

With these choices, the δ -function constraint becomes

$$\prod_n \check{\mu} \int_{-\infty}^{\infty} dz_n \exp \left[i \sum_{m=1}^{\infty} \left(a_{0|n}^0 z_n - \frac{(2\pi)^3}{\sqrt{4\pi}} z_n \tilde{\mathcal{P}}_{\varrho_n} \right) \right]. \quad (3.76)$$

In contrast to the nonlocal case of ϱ , where a single extra integration over z coupled to ϱ , we now have a situation where a countably infinite tower of integrations over z_n couple to the coefficients $\tilde{\mathcal{P}}_{\varrho_n}$. In all other respects, however, the calculation is much the same as the nonlocal one, and can be carried out in the same way. The shift of variables necessary to decouple $a_{0|n}^0$ and z_n is

$$a_{0|n}^0 \mapsto a_{0|n}^0 + i2\pi^2(2\pi)^3 z_n; \quad (3.77)$$

and the shift necessary to decouple the z_n and $\tilde{\mathcal{P}}_{\varrho_n}$ is

$$z_n \mapsto z_n - \frac{i\tilde{\mathcal{P}}_{\varrho_n}}{2\pi^2\sqrt{4\pi}}. \quad (3.78)$$

When only the two-point function is included, we obtain a Gaussian in the $\tilde{\mathcal{P}}_{\varrho_n}$,

$$\mathbb{P}[\mathcal{P}_\varrho(k)] \propto \exp \left(-\frac{1}{2} \sum_n \tilde{\mathcal{P}}_{\varrho_n}^2 \right). \quad (3.79)$$

The sum over the $\tilde{\mathcal{P}}_{\varrho_n}$ can be carried out using Eq. (3.75) and the completeness and orthog-

onality relations for the $\psi_n(k)$:

$$\sum_n \tilde{\mathcal{P}}_{\varrho n}^2 = \int d \ln k \frac{\mathcal{P}_\varrho^2(k)}{\mathcal{P}_\mathcal{R}(k)\mathcal{W}^2(k)}. \quad (3.80)$$

Using this expression, and integrating over all $\mathcal{P}_\varrho(k)$ which give rise to a fluctuation of amplitude ϱ , one recovers the Gaussian probability profile Eq. (3.53) with variance given by Eq. (3.55). This serves as a consistency check for Eqs. (3.79) and (3.53).

When the non-Gaussian correction $\Upsilon^{(0)}$ is included, one again generates a probability density of the form

$$\mathbb{P}[\mathcal{P}_\varrho(k)] \propto (1 - K_0 - K_2) \exp\left(-\frac{1}{2} \sum_n \tilde{\mathcal{P}}_{\varrho n}^2\right), \quad (3.81)$$

where K_2 has the same form as \mathcal{J}_2 , and therefore vanishes for the same reasons, and

$$K_0 = \int \frac{d^3 k_1 d^3 k_2 d^3 k_3}{96\pi^2 \prod_i \mathcal{P}_\mathcal{R}(k_i)\mathcal{W}(k_i)} \delta(\Delta) \bar{\mathcal{P}}_\mathcal{R}^2 \times \left(3 \frac{\mathcal{P}_\varrho(k_1)}{k_1^3} \frac{\mathcal{P}_\mathcal{R}(k_2)\mathcal{W}^2(k_2)}{k_2^5} \delta(\mathbf{k}_2 + \mathbf{k}_3) - \prod_i \frac{\mathcal{P}_\varrho(k_i)}{k_i^3} \right). \quad (3.82)$$

The first term contains a δ -function which squeezes k_1 into the asymptotic past. It formally vanishes by virtue of our assumption about the behaviour of $\mathcal{P}_\varrho(k)$ near $k = 0$, which is implicit in Eq. (3.75). As a result, the total probability density for the fluctuation spectrum can be written as

$$\mathbb{P}[\mathcal{P}_\varrho(k)] \propto (1 - K) \exp\left(-\frac{1}{2} \int d \ln k \frac{\mathcal{P}_\varrho(k)^2}{\mathcal{P}_\mathcal{R}(k)\mathcal{W}^2(k)}\right), \quad (3.83)$$

where

$$K = - \int \frac{d^3 k_1 d^3 k_2 d^3 k_3}{96\pi^2 \prod_i \mathcal{P}_\mathcal{R}(k_i)\mathcal{W}(k_i)} \delta(\Delta) \bar{\mathcal{P}}_\mathcal{R}^2 \prod_i \frac{\mathcal{P}_\varrho(k_i)}{k_i^3}. \quad (3.84)$$

As before, one can show that this expression is consistent with Eqs. (3.70)–(3.71) by integrating over all $\mathcal{P}_\varrho(k)$ which reproduce a total fluctuation of amplitude ϱ , after dropping another term which is squeezed into the asymptotic past owing to the presence of a δ -function. This

is a non-trivial consistency check of Eqs. (3.83)–(3.84).

As in the local case, Eqs. (3.83)–(3.84) are entirely independent of Λ (except as a limit of integration), so the regulator can be freely removed by setting $\Lambda = \infty$.

3.6 Summary of results

In this chapter we have obtained the connection between the n -point correlation functions of the primordial curvature perturbation, evaluated at some time t , $\langle \mathcal{R}(\mathbf{k}_1) \cdots \mathcal{R}(\mathbf{k}_n) \rangle$, and the PDF of fluctuations in the spatial configuration of \mathcal{R} . We have obtained an explicit expression for the PDF of a fluctuation of amplitude ϱ when \mathcal{R} is smoothed over regions of order the horizon size. This is a probability density in the conventional sense. In addition, we have obtained an expression for the probability that ϱ has a spectrum $\mathcal{P}_\varrho(k)$. This is given by $\int d \ln k \mathcal{P}_\varrho(k) = \varrho$, although mapping $\mathcal{P}_\varrho(k) \mapsto \varrho$ is many-to-one. This is a functional probability density, and can potentially be used to identify features in the fluctuation spectrum near some specific wavenumber $k \simeq k_*$. Our result is independent of statistical reasoning based on the central limit theorem and provides a direct route to incorporate non-Gaussian information from the correlators of the effective quantum field theory of the inflaton into theories of structure formation.

Both these probabilities are Gaussian in the limit where \mathcal{R} only possesses a two-point connected correlation function. If there are higher-order connected correlation functions, then \mathcal{R} exhibits deviations from Gaussian statistics, which we have explicitly calculated using determinations of the inflationary three-point function during an epoch of slow-roll inflation. Our method can be extended to incorporate corrections from higher connected n -point functions to any finite order in n . We have not computed these higher corrections, since we anticipate that their contribution is subdominant to the three-point correction (which is already small).

Our argument is based on a formal decomposition of the spatial configuration of the curvature perturbation in \mathbf{k} -space into spherical harmonics, together with harmonics along the radial k direction. However, we have emphasised that our results do not depend on the details of this construction, but require only a minimal set of assumptions or conditions. The first assumption is that the power spectrum $\mathcal{P}_\mathcal{R}(k)$ goes to zero sufficiently fast on large

scales, specifically $\mathcal{P}_{\mathcal{R}}(k)/k^3 \rightarrow 0$ as $k \rightarrow 0$. (In addition, in the case of the fluctuation spectrum, we require $\mathcal{P}_{\varrho}(k)/k^3 \rightarrow 0$ as $k \rightarrow 0$.) Such a condition is certainly consistent with our understanding of large-scale structure in the universe and, within the perturbative approach we are using, we have argued that in fact it describes a self-consistency condition which prevents perturbative fluctuations from destroying the background FRW spacetime. Our second assumption is that the spatial configuration \mathcal{R} can be smoothed to $\bar{\mathcal{R}}$ via a window function \mathcal{W} to obtain a configuration for which $\bar{\mathcal{R}} \rightarrow 0$ as $k \rightarrow \infty$. In this case, it is fair to compare $\bar{\mathcal{R}}$ to the primordial power spectrum.

In addition to these fundamental assumptions, which relate to the behaviour of real physical quantities, a large part of the calculation has relied on an auxiliary technical construction. This construction is based on an artificial compactification of momentum space, implemented by a hard cutoff Λ . There is an associated boundary condition on $\bar{\mathcal{R}}$ at $k = \Lambda$ which discretises the harmonics (partial waves) in k . However, in both the non-local (total fluctuation ϱ) and local (fluctuation spectrum $\mathcal{P}_{\varrho}(k)$) cases, the final probability density is independent of both the details of the partial wave construction and Λ (except as a limit of integration). It is also independent of the choice of the family of window functions $\mathcal{W}_{\Lambda}(k; k_H)$, and depends only on the limit $\lim_{\Lambda \rightarrow \infty} \mathcal{W}_{\Lambda}(k; k_H) = \mathcal{W}(k; k_H)$. Therefore the regulator can be removed by taking the limit $\Lambda \rightarrow \infty$. Moreover, the boundary condition at $k = \Lambda$ becomes irrelevant in this limit, which is a familiar result from the theory of Sturm–Liouville operators. As a consistency check, one can integrate $\mathbb{P}[\mathcal{P}_{\varrho}(k)]$ with the condition $\int d \ln k \mathcal{P}_{\varrho}(k) = \varrho$ in order to obtain $\mathbb{P}(\varrho)$.

In Chapters 4 and 5 we present applications of this method, and the PDF obtained, to improve the estimation of the probability of PBH formation.

Chapter 4

Probability of primordial black hole formation

4.1 Introduction

Primordial Black Holes (PBHs) are a unique tool to probe inhomogeneities in the early universe. The probability of PBH formation is extensively studied because it is useful in constraining the amplitude of primordial inhomogeneities generated by inflation (e.g., Carr et al. [1994]; Liddle & Green [1998]; Sendouda et al. [2006]; Zaballa et al. [2007]; Bugaev & Klimai [2006]). What makes PBHs a unique tool in cosmology is the range of scales that can be probed by their formation. The anisotropies probed by the CMB data cover the range of wavenumbers $7 \times 10^{-4} \leq k/\text{Mpc}^{-1} \leq 0.021$. Equivalently these modes enter the horizon when the cosmological horizon or Hubble mass is between $10^{19} \lesssim M/M_{\odot} \lesssim 10^{23}$ while the overdensities forming galactic haloes have associated masses $10^8 \lesssim M/M_{\odot} \lesssim 10^{12}$. The inhomogeneities forming PBHs are much smaller and they can span the range of wavenumbers $10^3 \lesssim k/\text{Mpc}^{-1} \lesssim 10^{16}$ which correspond to $10^{-24} \lesssim M/M_{\odot} \lesssim 10^6$, a set of values that can change with the model of inflation and its reheating scale. In any case, this is the largest range of scales probed by any single observable in the universe.

Another advantage of studying PBH statistics is that, in a radiation background, the gravitational collapse of fluctuations takes place shortly after horizon crossing. Consequently, PBH statistics do not suffer the bias problem or the late-time nonlinear evolution that signif-

icantly modifies the mass and statistics of other bound objects.

The absence of direct detections of PBHs has prompted studies of processes that could be influenced by the gravitational effects of PBHs or their evaporations. Some of the processes and observations that limit the abundance of PBHs are the following:

1. If the number of PBHs is large enough, they could constitute a significant fraction of the dark matter. The current density of PBHs therefore cannot exceed the observed density of dark matter, i.e., $\Omega_{\text{PBH}}(M \geq 10^{15} \text{g}) \leq \Omega_{\text{DM}} = 0.28$ [Komatsu et al., 2008].
2. The Hawking radiation from PBHs [Hawking, 1974] can be the source of the background radiation at various wavelengths in our universe [Carr, 1976; Page & Hawking, 1976; Bugaev & Konishchev, 2001] and cosmic rays [Bugaev & Konishchev, 2001]. As mentioned in Chapter 1, PBHs of mass $M_{\text{evap}} = 5 \times 10^{14} \text{g}$ should be evaporating today and observations of the gamma-ray background imply $\Omega_{\text{PBH}}(M_{\text{evap}}) \lesssim 5 \times 10^{-8}$ [Page & Hawking, 1976; Carr, 1976; MacGibbon & Carr, 1991; Kim et al., 1999]. This is the tightest constraint on the density of PBHs although future observations of the 21 cm radiation might impose a tighter limit [Mack & Wesley, 2008].
3. Black holes with mass $M < M_{\text{evap}}$ have already evaporated and the decay products should not spoil the well understood chemical history of the universe. Indeed, limits on $\beta_{\text{PBH}}(M)$ can be obtained in the mass range $10^9 < M/\text{g} < 10^{12}$ by looking at the effects of hadrons and neutrinos emitted by PBHs on the Big Bang nucleosynthesis of helium and deuterium [Miyama & Sato, 1978; Novikov et al., 1979].

A complete list of numerical bounds can be found in Table I, as compiled by Green & Liddle [1997]. All these bounds have been used to probe early universe fluctuations [Carr et al., 1994; Liddle & Green, 1998; Sendouda et al., 2006; Zaballa et al., 2007; Bugaev & Klimai, 2006]. They can be translated into limits on the root-mean-square amplitude of density or curvature perturbations \mathcal{R}_{RMS} on scales inaccessible to the CMB.

Here we explore how the bounds to \mathcal{R}_{RMS} can be modified in view of the consideration of a non-Gaussian probability distribution. We use the PDF derived in Chapter 3 and calculate the mass fraction of PBHs with the aid of the Press-Schechter formalism. The effects of non-Gaussian perturbations on PBHs have already been studied for specific models [Bullock

& Primack, 1997; Ivanov, 1998; Pina Avelino, 2005] but a precise quantification of the non-Gaussian effects is still required. Indeed, it is only now, with a much better understanding of the effects of higher order perturbations, that we are able to describe the general effects on PBHs. This discussion is crucial in the light of recent claims that only exotic extensions of the canonical slow-roll inflationary potentials can produce an appreciable number of PBHs [Chongchitnan & Efstathiou, 2007; Bugaev & Klimai, 2008] (see however [Peiris & Easter, 2008] where it's argued that a large number of PBHs can be formed even within the slow-roll regime). Here we explore whether the consideration of non-Gaussian perturbations in inflationary models could increase the mass fraction of PBHs significantly.

Table I Constraints on the mass fraction $\beta_{\text{PBH}}(M)$ of the universe going into PBHs

CONSTRAINT	MASS RANGE (g)	NATURE
$1.25 \times 10^{-8} \left(\frac{M}{10^{11}\text{g}}\right)^{-1}$	$< 10^{11}$	entropy of the universe
$4.1 \times 10^{-3} \left(\frac{M}{10^9\text{g}}\right)^{1/2}$	$10^9 - 10^{11}$	pair-production at nucleosynthesis
$4.9 \times 10^{-7} \left(\frac{M}{10^{10}\text{g}}\right)^{3/2}$	$10^{10} - 10^{11}$	Deuterium destruction
$6.5 \times 10^{-5} \left(\frac{M}{10^{11}\text{g}}\right)^{7/2}$	$10^{11} - 10^{13}$	Helium-4 spallation
$10^{-18} \left(\frac{M}{10^{11}\text{g}}\right)^{-1}$	$10^{11} - 10^{13}$	CMB distortion
3.1×10^{-27}	$3.6 \times 10^{14} - 10^{15}$	γ -rays from evaporating PBHs
$10^{-19} \left(\frac{M}{10^{15}\text{g}}\right)^{1/2}$	$> 10^{15}$	$\Omega_{\text{PBH}}(t_0) \leq 0.47$

4.2 The non-Gaussian PDF

Let us introduce the elements of the non-Gaussian distribution of probabilities for the curvature perturbation field \mathcal{R} . We first describe how the Gaussian PDF is constructed in the context of the linear theory. The amplitude of the curvature perturbations \mathcal{R} is derived by solving the perturbed Einstein equations to linear order. Statistically, the mean amplitude is

written in terms of the two-point correlation function as

$$\langle \mathcal{R}_G(\mathbf{k}_1) \mathcal{R}_G(\mathbf{k}_2) \rangle = (2\pi)^3 \delta(\mathbf{k}_1 + \mathbf{k}_2) |\mathcal{R}_{\text{RMS}}(k)|^2, \quad (4.1)$$

where, as before, $\mathcal{R}_G(\mathbf{k})$ are Gaussian perturbations in Fourier space.

The two-point correlator defines the dimensionless power spectrum $\mathcal{P}(k)$ through the relation

$$\langle \mathcal{R}_G(\mathbf{k}_1) \mathcal{R}_G(\mathbf{k}_2) \rangle = (2\pi)^3 \delta(\mathbf{k}_1 + \mathbf{k}_2) \frac{2\pi^2}{k_1^3} \mathcal{P}(k_1). \quad (4.2)$$

As discussed in Chapter 3, the perturbations are smoothed over a given mass scale k_M . Here we choose a truncated Gaussian window function

$$\mathcal{W}_M(k) = \Theta(k_{\text{max}} - k) \exp\left(-\frac{k^2}{2k_M^2}\right), \quad (4.3)$$

where Θ represents the Heaviside function and the fiducial scale k_{max} is introduced to avoid ultraviolet divergences. The smoothing scale k_M is defined by

$$k_M = 2\pi H_M = M/2, \quad (4.4)$$

where M is the Hubble mass at the time the scale k_M enters the horizon.

The variance of the smoothed field is related to the power spectrum by

$$\Sigma_{\mathcal{R}}^2(M) = \int \frac{dk}{k} \mathcal{W}_M^2(k) \mathcal{P}(k). \quad (4.5)$$

The power spectrum encodes important information about the underlying cosmological model. For example, in the case of perturbations deriving from the quantum fluctuations of a single inflationary field ϕ with a potential V dominating the cosmological dynamics, the explicit expression is [Stewart & Lyth, 1993]

$$\mathcal{P}(k) = \frac{H_*^4}{(2\pi)^2 \dot{\phi}_*^2 m_{\text{P}}^2} \approx \frac{V_*^3}{(dV/d\phi)_*^2 m_{\text{P}}^2}, \quad (4.6)$$

Here an asterisk denotes values at the time when the relevant perturbation mode exits the

cosmological horizon, $k = a_* H_* = a(t_*) H(t_*)$.

The tilt of the power spectrum is parametrised with a second observable, the spectral index, which is defined as

$$n_s - 1 = \frac{d}{d \ln k} \ln \mathcal{P}(k). \quad (4.7)$$

If $n_s < 1$, the root-mean-square amplitude \mathcal{R}_{RMS} increases on larger scales, corresponding to a red spectrum. Conversely, $n_s > 1$ indicates larger power on smaller scales and corresponds to a blue spectrum.

The power spectrum and the tilt are derived directly from linear perturbations as reviewed in Section 2.4 of Chapter 2. In observations of the CMB, it is possible to determine with great accuracy the numerical values of the power spectrum and its tilt on scales larger than the horizon at the time of last scattering, that is ($k \leq k_{\text{ls}} = 1.7 \times 10^{-3} \text{Mpc}^{-1}$). On such scales, the five-year results of WMAP, combined with the galaxy counts, give $\mathcal{P}(k_{\text{ls}}) = 2.4 \times 10^{-9}$ and $n_s = 0.95 \pm 0.1$ [Komatsu et al., 2008].

In linear perturbation theory one makes use of the central limit theorem to construct the PDF. To first order, the perturbation modes are independent of each other. If we assume the field of linear perturbations $\bar{\mathcal{R}}$ has zero spatial average, then the central limit theorem indicates that the PDF of $\bar{\mathcal{R}}$ is a normal distribution which depends only on the variance $\Sigma_{\mathcal{R}}^2$,

$$\mathbb{P}_{\text{G}}(\bar{\mathcal{R}}) = \frac{1}{\sqrt{2\pi}\Sigma_{\mathcal{R}}} \exp\left(-\frac{\bar{\mathcal{R}}^2}{2\Sigma_{\mathcal{R}}^2(M)}\right). \quad (4.8)$$

A successful linear theory of structure formation will predict this probability distribution and match the numerical values at the relevant observational scales. Higher order correlations of the perturbation field \mathcal{R} offer an exciting way to distinguish between cosmological models with common properties at linear order. As discussed in Chapter 1 and Chapter 2, the deviations from Gaussianity are described to lowest order by the nonlinear parameter f_{NL} . This parameter appears in the expansion (e.g. Lyth & Rodriguez [2005a])

$$\mathcal{R}(k) = \mathcal{R}_{\text{G}}(k) - \frac{3}{5} f_{\text{NL}} (\mathcal{R}_{\text{G}} \star \mathcal{R}_{\text{G}}(k) - \langle \mathcal{R}_{\text{G}}^2 \rangle), \quad (4.9)$$

where a star denotes the convolution of two copies of the field. The interaction of Fourier modes does not admit the use of the central limit theorem and the non-Gaussian probability distribution must be constructed by other means.

In Chapter 3 we have provided a method to calculate the correction to the Gaussian PDF, and to derive a new PDF which includes the linear order contribution from the 3-point function. Such a correlator can be derived through a second order expansion of the perturbations in the Einstein equations [Bartolo et al., 2004; Rigopoulos & Shellard, 2005; Seery et al., 2008]. Alternatively, an explicit expression for the three-point correlator can be obtained from the third-order quantum perturbations to the Einstein-Hilbert action. Pioneering works using this method come from Maldacena [2003] and Seery & Lidsey [2005b,a]. Here we use the expression derived by Lyth & Rodriguez [2005a] for the correlator in Fourier space. At tree-level this reduces to

$$\langle \mathcal{R}(k_1)\mathcal{R}(k_2)\mathcal{R}(k_3) \rangle = - (2\pi)^3 \delta \left(\sum_i \mathbf{k}_i \right) 4\pi^4 \frac{6}{5} f_{\text{NL}} \left[\frac{\mathcal{P}(k_1)\mathcal{P}(k_2)}{k_1^3 k_2^3} + \{\text{perms}\} \right]. \quad (4.10)$$

Current observations provide numerical bounds for f_{NL} through the three-point correlation of the temperature fluctuation modes. The WMAP satellite gives the constraints $-151 < f_{\text{NL}}^{\text{equil.}} < 253$ [Komatsu et al., 2008] for an equilateral triangulation of the bispectrum and $-4 < f_{\text{NL}}^{\text{local}} < 80$ [Smith et al., 2009] for a local triangulation (the local and equilateral triangulations have been defined in Sec. 1.3). Both of these values are determined at the 95% confidence level and consider an invariant value at all scales probed by the CMB.

In the following, the basic components of the non-Gaussian PDF derived in Chapter 3 are presented. The amplitude of the perturbation is characterised by its value at the centre of the configuration

$$\vartheta_0 \equiv \bar{\mathcal{R}}(\mathbf{x} = 0). \quad (4.11)$$

This specification is necessary to construct an explicit expression of the PDF. The parameter ϑ_0 is particularly useful to discriminate the relevant inhomogeneities forming PBHs [Shibata & Sasaki, 1999; Green et al., 2004]. The non-Gaussian probability distribution function for

a perturbation with central amplitude ϑ_0 , derived in Eq. (3.70), is

$$\mathbb{P}_{\text{NG}}(\vartheta_0) = \frac{1}{\sqrt{2\pi}\Sigma_{\mathcal{R}}} \left[1 + \left(\frac{\vartheta_0^3}{\Sigma_{\mathcal{R}}^3} - \frac{3\vartheta_0}{\Sigma_{\mathcal{R}}} \right) \frac{\mathcal{J}}{\Sigma_{\mathcal{R}}^3} \right] \exp\left(-\frac{\vartheta_0^2}{2\Sigma_{\mathcal{R}}^2}\right), \quad (4.12)$$

where the factor \mathcal{J} encodes the non-Gaussian contribution to the PDF:

$$\mathcal{J} = \frac{1}{6} \int \frac{d\mathbf{k}_1 d\mathbf{k}_2 d\mathbf{k}_3}{(2\pi)^9} \mathcal{W}_{\text{M}}(k_1) \mathcal{W}_{\text{M}}(k_2) \mathcal{W}_{\text{M}}(k_3) \langle \mathcal{R}(\mathbf{k}_1) \mathcal{R}(\mathbf{k}_2) \mathcal{R}(\mathbf{k}_3) \rangle, \quad (4.13)$$

$$= -\frac{1}{5} \int \frac{d\mathbf{k}_1 d\mathbf{k}_2 d\mathbf{k}_3}{(4\pi)^2 \prod_i \mathcal{W}_{\text{M}}^{-1}(k_i)} \delta\left(\sum_i \mathbf{k}_i\right) f_{\text{NL}} \left[\frac{\mathcal{P}(k_1)\mathcal{P}(k_2)}{k_1 k_2} + \{\text{perms}\} \right]. \quad (4.14)$$

This last equation is valid at tree level in the expansion of $\langle \mathcal{R}\mathcal{R}\mathcal{R} \rangle$. It is justified as long as the loop contributions to the three-point function, generated by the convolution of \mathcal{R} -modes, are sub-dominant. This requirement is met when the second order contribution to \mathcal{R} in Eq. (4.9) does not exceed the linear contribution. This requirement is met if we demand that

$$f_{\text{NL}} \leq 1/\sqrt{\mathcal{P}(k)}. \quad (4.15)$$

The complete derivation of the PDF in Eq. (4.12) was already provided in Chapter 3. Here it is sufficient to say that the time-dependence of this probability is eliminated when the averaging scale is $k_{\text{M}} \leq a(t)H(t)$ providing the growing mode of the perturbation \mathcal{R} is constant on superhorizon scales. This is true in particular for perturbations \mathcal{R} considered in the radiation era, when the PBHs considered here are formed (see Chapter 1).

In order to adapt the PDF in Eq. (4.14) to the computation of PBH formation probabilities, this expression is integrated between the limits k_{min} and k_{max} defined to cover the relevant perturbation modes for PBH formation. PBHs are formed long before today, so in the large-box (small wavenumber) limit of integral (4.14), the present Hubble horizon $k_{\text{min}} = H_0$ is a reasonable lower limit for PBH formation [Lyth, 1992]. At the other end of the spectrum, the smallest PBHs have the size of the Hubble horizon at the end of inflation. A suitable upper limit in this case is the wavenumber associated with the comoving horizon at the end of inflation, $k_{\text{max}} = a(t_{\text{end}})H_{\text{end}}$. It is important to mention that, even though the integral in Eq. (4.14) should include all k -modes, finite limits are imposed to avoid loga-

rithmic divergences. Due to the window function factors $\mathcal{W}_M(k)$, the dominant part of the integral is independent of the choice of integration limits as long as they remain finite.

The integral (4.14) is considered only at the limit of equilateral configurations of the three-point correlator, that is, considering correlations for which $k_1 = k_2 = k_3$. This is not merely a computational simplification. In the integral, each perturbation mode has a filter factor $\mathcal{W}_M(k)$ which, upon integration, picks dominant contributions from the smoothing scale k_M common to all perturbation modes. In this case \mathcal{J} can be written in the suggestive way:

$$\mathcal{J} = -\frac{1}{8} \int_{k_{\min}}^{k_{\max}} \frac{dk}{k} [\mathcal{W}_M(k)\mathcal{P}(k)]^2 \left(\frac{6}{5} f_{\text{NL}} \right). \quad (4.16)$$

With the complete non-Gaussian PDF at hand, it is possible to characterise its effects on the probability of PBH formation. In the next section, \mathcal{J} is computed numerically for inflationary perturbations generated in a single-field slow-roll inflationary epoch. The results in this case are shown to be consistent with previous works on non-Gaussian computations of the probability of PBH formation. In Section 4.4, the non-Gaussian PDF is generated for the case of constant f_{NL} . This will be used to test the magnitude of the effects of non-Gaussianity on the probability of PBH formation.

4.3 Non-Gaussian modifications to the probability of PBH formation

The simplest models of structure formation within the inflationary paradigm are those where a single scalar field drives the accelerated expansion of the spacetime and its quantum fluctuations evolve into the observed structure in subsequent stages of the universe. Although small in magnitude, the non-Gaussianity of the fluctuations generated in this simple model provide a qualitative hint to the consequences that non-Gaussianity has for the probability of PBH formation.

In fact, for single-field inflationary models, the effects of non-Gaussianity on PBHs have been explored in the past but with inconclusive results. Bullock & Primack [1997] studied the probability of formation of PBHs numerically for non-Gaussian perturbations with a blue spectrum ($n_s > 0$). The motivation for this was that any inflationary model with a constant

tilt and a normalisation consistent with the perturbations at the CMB scale must have a blue spectrum to produce a significant number of PBHs [Carr et al., 1994; Green & Liddle, 1997]. Their analysis is based on the stochastic generation of perturbations on superhorizon scales, together with a Langevin equation for computing the PDF. For all the cases tested, the non-Gaussian PDF is skewed towards small fluctuations. In consequence, the probability of PBH formation, which integrates the high amplitude tail, is suppressed with respect to the Gaussian case. An example of the kind of potential studied by Bullock & Primack [1997] is

$$V_1(\phi) = V_0 \begin{cases} 1 + \arctan\left(\frac{\phi}{m_P}\right), & \phi > 0, \\ 1 + (4 \times 10^{33}) \left(\frac{\phi}{m_P}\right)^{21}, & \phi < 0. \end{cases} \quad (4.17)$$

where V_0 is the amplitude of the potential at $\phi = 0$. This potential features a plateau for $\phi < 0$. This produces an increase in the power of matter fluctuations corresponding to the production of PBHs of mass 10^{32} gr.

Another way of generating large perturbations in the inflationary scenario is to consider localised features in the potential dominating the dynamics regardless of the tilt of the spectrum. As one can see from Eq. (4.6), an abrupt change in the potential would generate a spike in the spectrum of perturbations. This is valid as long as we avoid a 'flat' or 'static' potential in which $dV/d\phi = 0$. In such case $\dot{\phi} = 0$ and Eq. (4.6) is invalid (for a treatment of this particular case, also known as 'ultra-slow roll' inflation, see Kinney [2005]).

The description of a model of inflation with large amplitude in the power spectrum is incomplete if we do not take on account the effects of nonlinear fluctuations. The effects of non-Gaussianity for an inflationary model producing features in an otherwise red spectrum ($n_s < 0$) were explored by Ivanov [1998], using the toy model

$$V_2(\phi) = \begin{cases} \lambda \frac{\phi^4}{4} & \text{for } \phi < \phi_1, \\ A(\phi_2 - \phi) + \lambda \frac{\phi^4}{4} & \text{for } \phi_2 > \phi > \phi_1, \\ \tilde{\lambda} \frac{\phi^4}{4} & \text{for } \phi > \phi_2. \end{cases} \quad (4.18)$$

where λ and $\tilde{\lambda}$ are coupling constants. Through a stochastic computation of the PDF, Ivanov found that the non-Gaussian PDF is skewed towards large perturbations. This result goes in the opposite direction to that of Bullock & Primack [1997].

To understand this difference and generalise the effects of non-Gaussianity, it is convenient to look at the fractional difference of the Gaussian and non-Gaussian PDFs:

$$\frac{\mathbb{P}_{\text{NG}} - \mathbb{P}_{\text{G}}}{\mathbb{P}_{\text{G}}} = \left[\left(\frac{\vartheta_0^3}{\Sigma_{\mathcal{R}}^3} - 3 \frac{\vartheta_0}{\Sigma_{\mathcal{R}}} \right) \frac{\mathcal{J}}{\Sigma_{\mathcal{R}}^3} \right]. \quad (4.19)$$

Both Bullock & Primack [1997] and Ivanov [1998] use perturbations generated in a piecewise slow-roll inflationary potential for which inflation is controlled by keeping the slow-roll parameters, defined in Eq. (2.93), smaller than one. Here the slow-roll approximation is used to explore the qualitative effects of Eq. (4.19).

To linear order, there is a straightforward expression for the spectral index in terms of these parameters [Stewart & Lyth, 1993],

$$n_s - 1 = 2(\eta_{\text{SR}} - 3\epsilon_{\text{SR}}). \quad (4.20)$$

On the other hand, by using a first order expansion in slow-roll parameters, Maldacena [2003] provides an expression for the nonlinear factor f_{NL} in terms of these parameters [Maldacena, 2003]:

$$f_{\text{NL}} = \frac{5}{12} (n_s + \mathcal{F}(k)n_t) = \frac{5}{6} (\eta_{\text{SR}} - 3\epsilon_{\text{SR}} + 2\mathcal{F}(k)\epsilon_{\text{SR}}), \quad (4.21)$$

where $n_t = 2\epsilon_{\text{SR}}$ is the scalar-tensor perturbation tilt and $\mathcal{F}(k)$ is a number depending on the triangulation used. For the case of equilateral configurations, when $\mathcal{F} = 5/6$,

$$f_{\text{NL}} = \frac{5}{6} \left(\eta_{\text{SR}} - \frac{4}{3}\epsilon_{\text{SR}} \right)_{\text{eq}}. \quad (4.22)$$

This last expression is used to evaluate the integral (4.16) for \mathcal{J} . The non-Gaussian effect on the PDF is illustrated in Fig. 4.1 for the potentials given by Eqs. (4.17) and (4.18) in terms of the fractional difference (4.19). This difference represents the skewness of the non-Gaussian PDF. The non-Gaussian contribution encoded in the factor \mathcal{J} is the integral of f_{NL} over all scales relevant for PBH formation. Consequently the sign of f_{NL} is what determines the enhancement or suppression of the probability for large amplitudes ϑ_0 in the non-Gaussian PDF. For the two cases illustrated, the scalar tilt n_s dominates over the tensor tilt n_t , so that

the sign of f_{NL} coincides with that of n_s . This result is illustrated in Fig. 4.1.

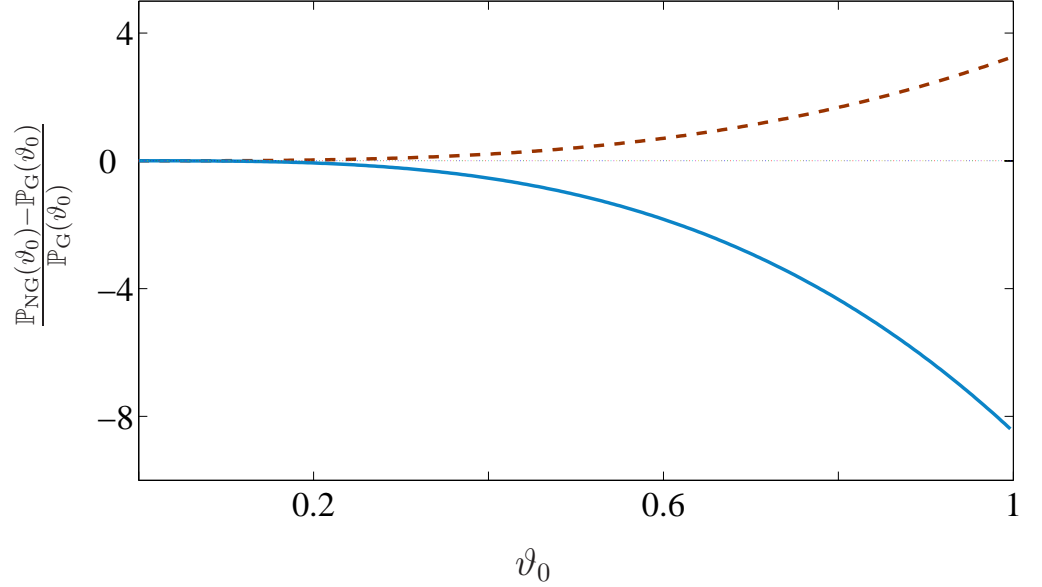


Figure 4.1: The fractional departure from the Gaussian PDF is plotted for two types of non-Gaussian distributions \mathbb{P}_{NG} , as defined in Eq. (4.12). For the potential in Eq. (4.17), $f_{\text{NL}} > 0$ and the departure is plotted with a solid line. For the potential in Eq. (4.18), $f_{\text{NL}} < 0$ and the departure is shown by a dashed line.

4.4 Constraints on non-Gaussian perturbations of PBH range

A standard practise in calculating the PBH mass fraction is to use the Press-Schechter formalism [Press & Schechter, 1974]. As described in Chapter 1, this involves integrating the probability of PBH formation over the relevant matter perturbation amplitudes, δ , measured at horizon epoch [Carr, 1975] and gives

$$\beta_{\text{PBH}}(\gtrsim M) = 2 \int_{\delta_{\text{th}}}^{\infty} \mathbb{P}(\delta_{\rho}(M)) d\delta_{\rho}(M). \quad (4.23)$$

For the large ratio $\delta_{\text{th}}/\Sigma_{\rho}$ this can be approximated as

$$\beta_{\text{PBH}}(\gtrsim M) \approx \frac{\Sigma_{\rho}(M)}{\delta_{\text{th}}} \exp \left[-\frac{\delta_{\text{th}}^2}{2\Sigma_{\rho}^2(M)} \right], \quad (4.24)$$

where $\Sigma_{\delta}^2(M)$ is the variance corresponding to the mass scale M and δ_{th} is the threshold amplitude of the perturbation necessary to form a PBH. When the relevant amplitudes of

a smoothed perturbation are integrated, β_{PBH} represents the mass fraction of PBHs with $M \geq w^{3/2} M_H \approx w^{3/2} k_M / (2\pi)$ [Carr, 1975], where w is the equation of state at the time of formation. Note that the approximation (4.24) is valid only for a Gaussian PDF.

The integral β_{PBH} establishes a direct relation between the mass fraction of PBHs and the variance of perturbations. The set of observational constraints on the abundance of PBHs is listed in Table I and has been used to place a bound to the mean amplitude δ in a variety of cosmological models (e.g. Carr et al. [1994]; Green & Liddle [1997]; Clancy et al. [2003]; Sendouda et al. [2006]). The Press-Schechter formula has also been tested against other estimations of the probability of PBH formation, such as peaks theory [Green et al., 2004].

The threshold value δ_{th} used in Eq. (4.23) has been modified with the improvement of gravitational collapse studies [Carr, 1975; Niemeyer & Jedamzik, 1998; Shibata & Sasaki, 1999; Hawke & Stewart, 2002]. A more appropriate approach has been noted recently, where simulations have addressed the problem using curvature fluctuations [Shibata & Sasaki, 1999; Musco et al., 2005; Polnarev & Musco, 2007]. The corresponding threshold value of the curvature perturbation can be deduced from the relation [Liddle & Lyth, 2000]

$$\delta_k(t) = \frac{2(1+w)}{5+3w} \left(\frac{k}{aH} \right)^2 \mathcal{R}_k, \quad (4.25)$$

which at horizon-crossing during the radiation-dominated era gives, $\mathcal{R}_{\text{th}} = 1.01$ for $\delta_{\text{th}} = 0.3$. This value has been also confirmed in the numerical simulations of Shibata & Sasaki [1999], Green et al. [2004] and Musco et al. [2005]. We will make use of it throughout.

The threshold value \mathcal{R}_{th} indicates the minimum amplitude of an inhomogeneity required to form a PBH. Consequently, the probability of PBH formation is best described by a non-linear treatment and this is the major motivation for our analysis. In the following we adapt the Press-Schechter formalism to derive the non-Gaussian abundance of PBHs. The use of the Press-Schechter integral for distributions of the curvature perturbation is not new. Zamballa et al. [2007] use it to estimate the PBH formation from the curvature perturbations which never exit the cosmological horizon. We apply the integral formula in Eq. (4.23) to the non-Gaussian probability distribution (4.12). The result of the integral is the sum of

incomplete Gamma functions Γ_{inc} and an exponential:

$$\beta(M) = \int_{\vartheta_{\text{th}}}^{\infty} \mathbb{P}_{\text{NG}}(\vartheta_0) d\vartheta_0 = \frac{1}{\sqrt{4\pi}} \Gamma_{\text{inc}} \left(1/2, \frac{\vartheta_{\text{th}}^2}{2\Sigma_{\mathcal{R}}^2(M)} \right) - \frac{1}{\sqrt{2\pi}} \frac{\mathcal{J}}{\Sigma_{\mathcal{R}}^3(M)} \left[2 \Gamma_{\text{inc}} \left(2, \frac{\vartheta_{\text{th}}^2}{2\Sigma_{\mathcal{R}}^2(M)} \right) - 3 \exp \left(-\frac{\vartheta_{\text{th}}^2}{2\Sigma_{\mathcal{R}}^2(M)} \right) \right]. \quad (4.26)$$

The Taylor series expansion of these functions around the limit $\Sigma_{\mathcal{R}}/\vartheta_0 = 0$ gives

$$\beta(M) \approx \frac{\Sigma_{\mathcal{R}}(M)}{\vartheta_{\text{th}} \sqrt{2\pi}} \exp \left[-\frac{1}{2} \frac{\vartheta_{\text{th}}^2}{\Sigma_{\mathcal{R}}^2(M)} \right] \times \left\{ 1 - 2 \left(\frac{\Sigma_{\mathcal{R}}}{\vartheta_{\text{th}}} \right)^2 + \frac{\mathcal{J}}{\Sigma_{\mathcal{R}}^3} \left[\left(\frac{\Sigma_{\mathcal{R}}}{\vartheta_{\text{th}}} \right)^{-2} - 1 \right] \right\}. \quad (4.27)$$

For the mass fraction shown in Eq. (4.27), the observational limits of Table I could in principle constrain the values of the variance $\Sigma_{\mathcal{R}}^2$ and of f_{NL} . However, when the mean amplitude of perturbations, $\Sigma_{\mathcal{R}}$, is normalised to the value at CMB scales, the obtained limits for f_{NL} are of order 10^4 . This is inconsistent with the analysis presented here because in such régime higher order contributions are expected to dominate non-Gaussianity. In fact, the expansion in Eq. (4.9) shows that when

$$|f_{\text{NL}}| \leq \frac{5}{3} \frac{1}{\mathcal{R}_{\text{RMS}}} = \frac{5}{3\Sigma_{\mathcal{R}}}, \quad (4.28)$$

the quadratic term of Eq. (4.9) dominates over the linear term, and in the computation of the three-point function Eq. (4.10), the loop contributions to the correlators become dominant. For the values of \mathcal{R}_{RMS} required to form a significant number of PBHs, the limit on $|f_{\text{NL}}|$ is of order 10. The computation of non-Gaussianities in this case goes beyond the scope of the present work. (For discussions on the loop corrections to the correlation functions, see Weinberg [2005], Zaballa et al. [2006], Byrnes et al. [2007] and Seery [2008].)

It is interesting to look at the values allowed for f_{NL} from WMAP and test the modifications that large non-Gaussianities bring to the amplitude of \mathcal{R} at the PBH scale. Fig. 4.2 presents the set of bounds on the initial mass fraction of PBHs listed in Table I. The corresponding limits to the variance of the curvature $\Sigma_{\mathcal{R}}$ are shown in Fig. 4.3 for the Gaussian and non-Gaussian cases. Independently of the model of cosmological perturbations adopted,

one can use the observational limits on f_{NL} to modify the bounds for $\Sigma_{\mathcal{R}}$ on small wavelengths. For the non-Gaussian case we choose to plot the central value of the present limits to $f_{\text{NL}}^{\text{equil.}} = 51$ [Komatsu et al., 2008] and the limit value $f_{\text{NL}} = 5/(3\Sigma_{\mathcal{R}}) \approx -66$ mentioned in Eq. (4.28). The tightest constraints on $\Sigma_{\mathcal{R}}$ come from perturbations of initial mass $M \approx 10^{15}$ g. With the non-Gaussian modification the limit is $\log(\Sigma_{\mathcal{R}}) \leq -1.2$, compared to the Gaussian case $\log(\Sigma_{\mathcal{R}}) \leq -1.15$. As shown in Fig. 4.3, the modification to $\Sigma_{\mathcal{R}}$ cannot be much larger if instead the limit value of Eq. (4.28) is used.

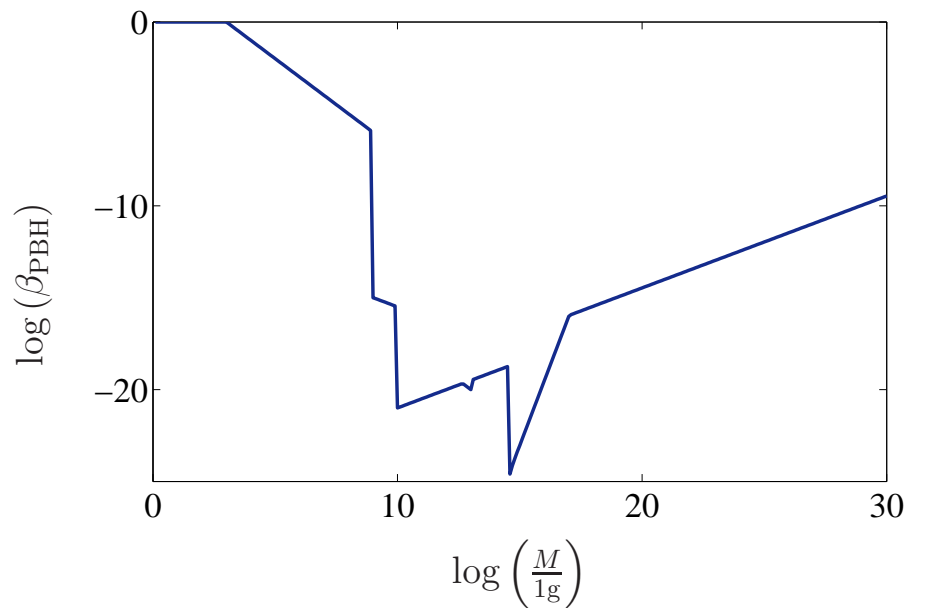


Figure 4.2: The constraints on β_{PBH} in Table I are plotted together with the smallest value considered for each mass.

4.5 Closing remarks

The present chapter shows, to lowest order in the contribution of the bispectrum, the effects of non-Gaussian perturbations on PBHs formation. Using curvature perturbations with a non-vanishing three-point correlation, an explicit form of the non-Gaussian PDF is presented, which features a direct contribution from the non-Gaussian parameter f_{NL} . Furthermore, it is shown how the sign of this parameter determines the enhancement or suppression of probability for large-amplitude perturbations. Using the simple slow-roll expression for f_{NL} in the context of single field inflation, a previous discrepancy in the literature regarding

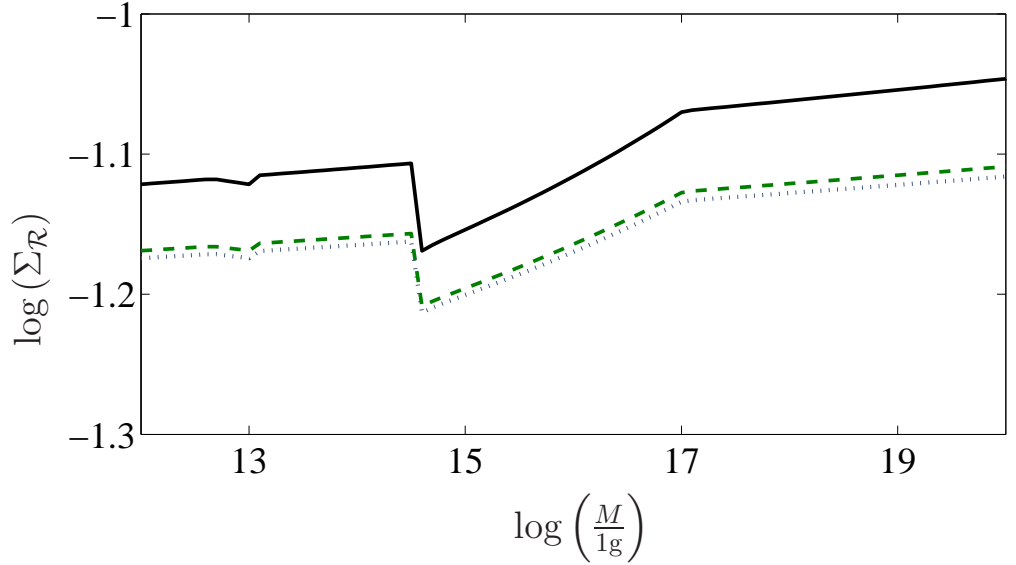


Figure 4.3: A subset of the constraints on $\Sigma_{\mathcal{R}}$ from overproduction of PBHs is plotted for a Gaussian and non-Gaussian correspondence between β and $\Sigma_{\mathcal{R}}$, Eqs. (4.24) and (4.27) respectively. The dashed line assumes a constant $f_{\text{NL}} = 51$ and the dotted line a value $f_{\text{NL}} = -1/\Sigma_{\mathcal{R}}^2 \approx -66$. The solid line represents the constraints for in the Gaussian case

effects of non-Gaussianity on the abundance of PBHs has been solved.

As a second application of the non-Gaussian PDF presented here is to use the Press-Schechter formalism of structure formation to determine the non-Gaussian effects on PBH abundance. In section 4.4 it is shown how the PBH constraints on the amplitude of perturbations can be modified when a non-Gaussian distribution is considered. As an example, it is shown that the limit $\Sigma_{\mathcal{R}}(M = 10^{15}\text{g}) < 6.3 \times 10^{-2}$ is reached for the marginal value $f_{\text{NL}} = -66.35$ modifying the known bounds for \mathcal{R} at the end of inflation [Carr et al., 1994]. This limit is, however, much larger than the observed amplitude at CMB scales, where $\Sigma_{\mathcal{R}} \approx 4.8 \times 10^{-5}$. The order of magnitude gap between the mean amplitude observed in cosmological scales and that required for significant PBH formation remains almost intact and, as a consequence, non-Gaussian perturbations do not modify significantly the standard picture of formation of PBHs.

Chapter 5

Curvature profiles of large overdensities

5.1 Introduction

As mentioned in Chapter 1, previous studies of PBH formation take the amplitude of the matter density or curvature inhomogeneities as the only parameter determining the probability density of PBH formation. Also the mass fraction in the form of PBHs is usually calculated with the aid of the Press-Schechter formula. Here we argue that this rough estimation is incomplete and that a different approach should be taken to evaluate the threshold value δ_{th} , or the equivalent curvature inhomogeneity \mathcal{R}_{th} , in the investigations of PBH formation.

From the first numerical simulations of PBH formation, it was evident that the process of PBH formation depends on the pressure gradients in the collapsing configuration as well as their amplitude. Nadezhin et al. [1978] found that such pressure gradients can modify the value of δ_{th} significantly. This has been confirmed in more recent works, which describe the configuration in terms of the curvature inhomogeneity $\mathcal{R}(\mathbf{r})$ (note that in this chapter we work with spherical coordinates $\{\mathbf{r}\}$ and not any set of coordinates $\{\mathbf{x}\}$). As we will show below, the Einstein equations relate the curvature profiles directly with the internal pressure gradients. This is the main motivation for considering the probability of curvature configurations.

We extend here the Press-Schechter formalism to consider a two-parameter probability. We include here for the first time a parameter related to the slope of curvature profile at the edge of the configuration. We start by calculating the probability of finding a spherically symmetric curvature configuration with a given radial profile. We can justify the sphericity

assumption using the argument of Zabotin et al. [1987]: PBH formation takes place only from nearly spherical configurations. In our analysis, we describe the radial profiles by introducing two parameters: the central amplitude of the curvature inhomogeneity $\mathcal{R}(\mathbf{r} = 0)$ and the central second radial derivative $\mathcal{R}''(\mathbf{r} = 0)$. The introduction of these parameters is a first step towards the full parametrisation of profiles in terms of all even derivatives at the centre of configurations. (The odd derivatives are all zero due to the assumed spherical symmetry.)

The method presented to derive a multiple-parameter probability enables us to compute the probability of any number of parameters describing the curvature profile. However, only families of curvature profiles described by two parameters are currently available, so we limit ourselves to a two-parametric description. More accurate future codes will simulate PBHs formation with a larger number of parameters. The number of parameters required for the complete description of these profiles and their probability distribution will be the same ¹⁰.

The central amplitude $\mathcal{R}(0)$ has been used in previous calculations of gravitational collapse and the probability of PBH formation, as illustrated in the previous chapter. Here we compute the probability to find a given configuration as a function of the two parameters $[\mathcal{R}(0), \mathcal{R}''(0)]$. We subsequently illustrate how this two-parametric probability is used to correct the probability of PBH formation. For this purpose we use the results of the latest numerical simulation of PBH formation Polnarev & Musco [2007]. Such an exercise shows how the corrections to β_{PBH} are potentially significant and they will be considered in more detail in future studies of PBH formation.

5.2 Probability of profile parameters of cosmological perturbations

Formally, the high amplitude inhomogeneous profiles describing configurations which collapse into PBHs are not perturbations. However, such regions are included in the statistics of random primordial curvature perturbations in the sense that the statistics of random fields can be used to estimate the probability of finding high-amplitude inhomogeneities. To describe such inhomogeneities, we consider the nonlinear curvature field $\mathcal{R}(t, r)$, as first described

¹⁰In the context of dark matter haloes, the profile of the initial inhomogeneity is effectively irrelevant because galaxies are formed from pressureless configurations. The density profiles and shapes of virialised haloes result from the evolution of the initial high peaks and are not linked to the profile of initial configurations that we investigate here

by Salopek & Bond [1990]. The nonlinear curvature $\mathcal{R}(t, r)$, defined in terms of the metric in the following equation, represents the relative expansion of a given local patch of the universe with respect to its neighboring patches. It is described by the metric

$$ds^2 = -N^2(t, \mathbf{r}) dt^2 + a^2(t) e^{2\mathcal{R}(t, \mathbf{r})} \tilde{\gamma}_{ij} (dr^i + N^i(t, \mathbf{r}) dt)(dr^j + N^j(t, \mathbf{r}) dt), \quad (5.1)$$

where $a(t)$ and $\tilde{\gamma}$ are the usual scale factor and the intrinsic metric of the spatial hypersurfaces. The gauge-dependent functions N and N^i are the lapse function and shift vector, respectively. These variables are determined by algebraic constraint equations in terms of the matter density ρ , pressure p and metric variables \mathcal{R} , a and $\tilde{\gamma}_{ij}$.

Here we consider the nonlinear configurations which correspond to large \mathcal{R} inside some restricted volume and zero \mathcal{R} outside, where the expansion of the universe follows the background FRW solution. There are several advantages of working with metric (5.1). First, as shown in Chapter 2, \mathcal{R} is defined as a gauge-invariant combination of the metric and matter variables [Wands et al., 2000]. Second, with the aid of the gradient expansion of the metric quantities, $\mathcal{R}(\mathbf{r}, t)$ appears in the Einstein equations in a non-perturbative way [Starobinsky, 1986; Salopek & Bond, 1990; Deruelle & Langlois, 1995; Rigopoulos & Shellard, 2005]. Third, \mathcal{R} does not depend on time for scales larger than the cosmological horizon, as proved by Lyth et al. [2005] and Langlois & Vernizzi [2005a]. In the present chapter we work in the superhorizon régime, where the field $\mathcal{R}(\mathbf{r})$ can be assumed to be time-independent.

The primordial field of random perturbations we consider presents a Gaussian probability distribution. The expressions for the PDF of the parameter $\mathcal{R}(0)$ in Chapter 3 are recovered here. For convenience we use a different notation, replacing ϱ in Section 3.3.1 with the amplitude $\vartheta_0 \equiv \mathcal{R}(0)$ and the variance with $\Sigma_{(2)} \equiv \Sigma_{\mathcal{R}}$. The PDF for the central amplitude ϑ is identical to that in Eq.(3.53):

$$\mathbb{P}[\vartheta_0] = \frac{1}{\sqrt{2\pi\Sigma_{(2)}}} \exp\left[-\frac{\vartheta_0^2}{2\Sigma_{(2)}}\right]. \quad (5.2)$$

We now derive the density of the probability for the central second derivative to have

amplitude

$$\vartheta_2 \equiv \mathcal{R}''(0) = \left[\frac{\partial^2}{\partial r^2} \mathcal{R}(r) \right]_{r=0}. \quad (5.3)$$

In order to compute the probability of a specific property of $\mathcal{R}(\mathbf{r})$, we integrate the original PDF, which encodes all the information about the field, weighted with the Dirac δ -functions of relevant arguments. Hereafter we assume $\mathcal{R}(0)$ and $\mathcal{R}''(0)$ as statistically independent parameters. The validity of this assumption is not explored here but is left for future investigations. Following this assumption, the probability of having $\mathcal{R}''(0) = \vartheta_2$ is given by the integral

$$\mathbb{P}(\vartheta_2) = \int [d\mathcal{R}] \mathbb{P}(\mathcal{R}) \delta[\mathcal{R}''(0) - \vartheta_2], \quad (5.4)$$

where $[d\mathcal{R}]$ indicates integration over all possible configurations $\mathcal{R}(\mathbf{k})$ in Fourier space. In order to compute this integral, we expand the smoothed curvature perturbation profile $\bar{\mathcal{R}}(\mathbf{r})$ in terms of spherical harmonic functions:

$$\bar{\mathcal{R}}(\mathbf{r}) = \int \frac{d^3k}{(2\pi)^3} \bar{\mathcal{R}}(\mathbf{k}) \exp(\mathbf{i}\mathbf{k} \cdot \mathbf{r}), \quad (5.5)$$

with

$$\bar{\mathcal{R}}(\mathbf{k}) = \sum_{\ell=0}^{\infty} \sum_{m=-\ell}^{\ell} \sum_{n=1}^{\infty} \mathcal{R}_{\ell|n}^m Y_{\ell m}(\theta, \phi) \psi_n(k). \quad (5.6)$$

Here $Y_{\ell m}$ are the usual spherical harmonics on the unit 2-sphere and $\psi_n(k)$ are a complete and orthogonal set of functions in an arbitrary finite interval $0 < k < \Lambda$. (The explicit expression for $\psi(k)$ and the value of Λ are given by Eq. (3.37) of Chapter 3.) The coefficients in the expansion are generically complex, so we separate the real and imaginary parts by introducing $\mathcal{R}_{\ell|n}^m = a_{\ell|n}^m + ib_{\ell|n}^m$. The reality condition for the curvature field, $\mathcal{R}^*(\mathbf{k}) = \mathcal{R}(-\mathbf{k})$, is met when

$$a_{\ell|n}^{-m} = (-1)^{\ell+m} a_{\ell|n}^m, \quad (5.7)$$

$$b_{\ell|n}^{-m} = (-1)^{\ell+m+1} b_{\ell|n}^m. \quad (5.8)$$

In particular, the $m = 0$ modes require $a_{\ell|n}^0$ and $b_{\ell|n}^0$ to be zero for odd and even ℓ , respectively. To integrate (5.4) we use the Fourier expansion (5.5) so that

$$\mathcal{R}''(0) = \int \frac{d^3k}{(2\pi)^3} \mathcal{R}(k) (\mathbf{i}k)^2 \exp(\mathbf{i}\mathbf{k} \cdot \mathbf{r})|_{r=0}. \quad (5.9)$$

Furthermore, we use (5.6) and the orthogonality of the spherical harmonics

$$\int Y_\ell^m(\theta, \phi) \sin\theta \, d\theta d\phi = \sqrt{4\pi} \delta^{m0} \delta_{\ell 0}, \quad (5.10)$$

to obtain

$$\mathcal{R}''(0) = - \sum_{n=1}^{\infty} \left(a_{0|n}^0 + \sqrt{\frac{4}{5}} a_{2|n}^0 \right) \int \frac{dk}{\sqrt{\pi}(2\pi)^2} \psi_n(k) k^4 \equiv \vartheta_2. \quad (5.11)$$

To compute the probability (5.4) we proceed by integrating over all configurations in Fourier space. With the aid of the expansion (5.6) we can express the measure of the integral in terms of the expansion coefficients satisfying the reality conditions (5.7) and (5.8), as shown in Eq. (3.34) this is

$$\int \Psi[\mathcal{R}] [d\mathcal{R}] = \left[\prod_{\ell=0}^{\infty} \prod_{m=1}^{\ell} \prod_{n=1}^{\infty} \mu \int_{-\infty}^{\infty} \Psi[\mathcal{R}] da_{\ell|n}^m \int_{-\infty}^{\infty} \Psi[\mathcal{R}] db_{\ell|n}^m \right] \times \left[\prod_{p=0}^{\infty} \prod_{q=1}^{\infty} \tilde{\mu} \int_{-\infty}^{\infty} \Psi[\mathcal{R}] da_{2p|q}^0 \int_{-\infty}^{\infty} \Psi[\mathcal{R}] db_{2p+1|q}^0 \right], \quad (5.12)$$

for any given functional Ψ of $\mathcal{R}(\mathbf{k})$. The constants μ and $\tilde{\mu}$ are weight factors to be included in the final normalisation of the joint probability.

The Gaussian PDF we are restricted to is written in terms of the spherical harmonic coefficients as (cf. Eq. (3.49))

$$\mathbb{P}[\mathcal{R}] = \exp \left(- \frac{1}{2\pi^2(2\pi)^3} \sum_{\ell=0}^{\infty} \sum_{m=0}^{\ell} \sum_{n=1}^{\infty} [|a_{\ell|n}^m|^2 + |b_{\ell|n}^m|^2] - \frac{1}{4\pi^2(2\pi)^3} \sum_{p=0}^{\infty} \sum_{q=1}^{\infty} [|a_{2p|q}^0|^2 + |b_{2p+1|q}^0|^2] \right). \quad (5.13)$$

In order to obtain the probability in Eq. (5.4), we use the standard representation of the Dirac

δ -function

$$\delta(x) = \int_{-\infty}^{\infty} dz \exp[izx]. \quad (5.14)$$

This allows us to write the δ -function in Eq. (5.4) in terms of the spherical harmonic coefficients as

$$\delta[\mathcal{R}''(0) - \vartheta_2] = \int dz \exp \left[iz \left(\sum_{n=1}^{\infty} \left(a_{0|n}^0 + \sqrt{\frac{4}{5}} a_{2|n}^0 \right) \int \frac{dk}{\sqrt{\pi}(2\pi)^2} \psi_n(k) k^4 + \vartheta_2 \right) \right]. \quad (5.15)$$

We now have all the elements required to integrate probability density of finding $\mathcal{R}''(0)$ with amplitude ϑ_2 . Substituting expressions (5.13) and (5.15) into Eq. (5.4), we perform the functional integral with the aid of the decomposition (5.12). For this case we have

$$\mathbb{P}(\vartheta_2) \propto \int [d\mathcal{R}] \int dz \mathbb{P}[\mathcal{R}] \exp \left[iz \left(\frac{3(2\pi)^3 \vartheta_2}{\sqrt{4\pi}} + \sum_n \Sigma_n^{(4)} \left(\sqrt{\frac{4}{5}} a_{2|n}^0 + a_{0|n}^0 \right) \right) \right], \quad (5.16)$$

where we have simplified the expression by defining the factor

$$\Sigma_n^{(4)} = \int dk k^4 \psi_n(k). \quad (5.17)$$

In the process of integration, we discard all the Gaussian integrals because they contribute to the probability only with a multiplicative constant which will be included in the final normalisation. On the other hand, the Dirac δ -function contributes to the integral with exponential functions of $a_{0|n}^0$ and $a_{2|n}^0$. The integrals of these parameters are computed by completing squares of the exponential arguments. First, we collect the terms of the integral with factors of $a_{0|n}^0$, that is,

$$\exp \left[-\frac{1}{4\pi^2(2\pi)^3} \sum_{n=1}^{\infty} |a_{0|n}^0| + iz \sum_{n=1}^{\infty} |a_{0|n}^0| \Sigma_n^{(4)} \right]. \quad (5.18)$$

Completing the squares, this last expression becomes

$$\exp \left[-\frac{1}{4\pi^2(2\pi)^3} \sum_{n=1}^{\infty} (|a_{0|n}^0| - i(2\pi)^3 2\pi^2 z \Sigma_n^{(4)})^2 - (2\pi)^3 \pi^2 z^2 \Sigma_{(4)}^2 \right]. \quad (5.19)$$

In the same way we can complete the squares for the expansion factors $a_{2|n}^0$:

$$\begin{aligned} \exp \left[-\frac{1}{4\pi^2(2\pi)^3} \sum_{n=1}^{\infty} |a_{2|n}^0| + iz \frac{4}{5} \sum_{n=1}^{\infty} |a_{2|n}^0| \Sigma_n^{(4)} \right] = \\ \exp \left[-\frac{1}{4\pi^2(2\pi)^3} \sum_{n=1}^{\infty} \left(|a_{2|n}^0| - i(2\pi)^3 \frac{4\pi^2}{\sqrt{5}} z \Sigma_n^{(4)} \right)^2 - (2\pi)^3 \pi^2 \frac{4}{5} z^2 \Sigma_{(4)}^2 \right]. \end{aligned} \quad (5.20)$$

Finally we can complete the squares for the terms containing the variable z , these being independent of $a_{0|n}^0$ and $a_{2|n}^0$:

$$\begin{aligned} \exp \left[-(2\pi)^3 \pi^2 \left(\frac{9}{5} \right) z^2 \Sigma_{(4)}^2 + i \frac{3(2\pi)^3}{\sqrt{4\pi}} \vartheta_2 z \right] = \\ \exp \left[-(2\pi)^3 \pi^2 \left(\frac{9}{5} \right) \Sigma_{(4)}^2 \left(z - i \frac{5}{12\sqrt{\pi^5}} \frac{\vartheta_2}{\Sigma_{(4)}^2} \right)^2 - \frac{5}{2} \frac{\vartheta_2^2}{\Sigma_{(4)}^2} \right], \end{aligned} \quad (5.21)$$

where for simplification we have written

$$\Sigma_{(4)}^2 \equiv \sum_{n=1}^{\infty} (\Sigma_n^{(4)})^2. \quad (5.22)$$

So by making the change of variables

$$\begin{aligned} a_{0|n}^0 &\mapsto a_{0|n}^0 + i2\pi^2(2\pi)^3 \Sigma_n^{(4)} z, \\ a_{2|n}^0 &\mapsto a_{2|n}^0 + i \frac{4\pi^2}{\sqrt{5}} (2\pi)^3 \Sigma_n^{(4)} z \\ z &\mapsto z + i \frac{5}{12\sqrt{\pi^5}} \frac{\vartheta_2}{\Sigma_{(4)}^2}, \end{aligned}$$

we can perform all the integrals and eliminate the Gaussian ones which contribute only up to an overall numerical factor subsequently absorbed by normalisation. The remaining factor expresses the probability of finding a perturbation \mathcal{R} with a central second derivative of value

ϑ_2 :

$$\mathbb{P}[\mathcal{R}''(\mathbf{r} = 0) = \vartheta_2] \propto \exp\left(-\frac{5\vartheta_2^2}{2\Sigma_{(4)}^2}\right). \quad (5.23)$$

The quantity $\Sigma_{(4)}^2$ represents the ‘variance’ of the PDF for $\mathcal{R}''(0)$. To evaluate this variance we integrate Eq. (5.22) and use the property (3.38) in Chapter 3 to integrate the complete sum and obtain

$$\Sigma_{(4)}^2 = \int_0^\Lambda d \ln k \mathcal{W}^2(k, k_H) \mathcal{P}(k) k^4. \quad (5.24)$$

The final probability density for the pair of parameters $\mathcal{R}(0)$ and $\mathcal{R}''(0)$ is the product of Eqs. (5.2) and (5.23)

$$\mathbb{P}(\mathcal{R}(0) = \vartheta_0, \mathcal{R}''(0) = \vartheta_2) = A \exp\left(-\frac{\vartheta_0^2}{2\Sigma_{(2)}^2} - \frac{5\vartheta_2^2}{2\Sigma_{(4)}^2}\right). \quad (5.25)$$

Here $\Sigma_{(2)}$ and $\Sigma_{(4)}$ are the dispersion of the amplitude and the second derivative respectively, and A is a normalisation factor obtained from the condition that the integral of the joint PDF over all possible values of the two independent parameters equals unity. The final normalised joint probability density is

$$\mathbb{P}(\vartheta_0, \vartheta_2) = \frac{4\sqrt{12}}{2\pi} \Sigma_{(2)}^{-1} \Sigma_{(4)}^{-1} \exp\left(-\frac{\vartheta_0^2}{2\Sigma_{(2)}^2} - \frac{5\vartheta_2^2}{2\Sigma_{(4)}^2}\right). \quad (5.26)$$

It is worth mentioning that the standard PDF containing only amplitudes ϑ_0 , Eq. (5.2), is recovered from Eq. (5.25) when we set all gradients in the Hubble scale equal to zero, i.e. $\nabla\mathcal{R}|_{r=r_H} = 0$. The Fourier transform of this expression demands $|k_H| \rightarrow \infty$. Using this in Eq. (5.24) means that $\Sigma_{(4)} \rightarrow \infty$ and the argument ϑ_2 goes to zero in the probability density of Eqs. (5.25) and (5.26).

According to the Press-Schechter formalism [Press & Schechter, 1974], the PDF is integrated over all perturbations which collapse to form the astrophysical objects under consideration. In this way we calculate the mass fraction of the universe in the form of such objects. To apply this formalism and calculate the probability of PBH formation and integrate the PDF (5.26), we require the range of values $\mathcal{R}(0)$ and $\mathcal{R}''(0)$ which correspond to PBH forma-

tion. In the next section we will obtain this range with the help of the results of numerical computations presented by Polnarev & Musco [2007].

5.3 The link between perturbation parameters and the curvature profiles used in numerical calculations

5.3.1 Initial conditions

As demonstrated by the first numerical simulations of PBH formation [Nadezhin et al., 1978], whether or not an initial configuration with given curvature profile leads to PBH formation predominantly depends on two factors:

- The ratio of the size of the initial configuration r_0 to the size of the extrapolated closed universe $r_k = a(t) \int_0^1 dr / \sqrt{1 - r^2}$, which is a measure of the strength of gravitational field within the configuration.
- The smoothness of the transition from the region of high curvature to the spatially flat FRW universe, which is characterised by the width of the transition region at the edge of the initial configuration and is inversely proportional to the pressure gradients there, strong pressure gradients inhibiting PBH formation (This is an argument beyond the Jeans' stability criterion and applies to configurations beyond the linear regime).

The numerical computations presented in Polnarev & Musco [2007] (hereafter PM) give the time evolution of the configurations with initial curvature profiles accounting for the above-mentioned factors. In that paper the initial conditions are obtained with the help of a quasi-homogeneous asymptotic solution valid in the limit $t \rightarrow 0$. This solution to the Einstein equations was first introduced by Lifshitz & Khalatnikov [1963]; see also Zeldovich & Novikov [1983] and Landau & Lifshitz [1975]. Following Nadezhin et al. [1978], PM used this asymptotic solution to set self-consistent initial conditions for curvature inhomogeneities, the initial curvature inhomogeneity being described by the spherically symmetric curvature profile $K(\hat{r})$. This sets the initial conditions for the process of black hole formation. Asymptotically, the metric can be presented in terms of $K(\hat{r})$ as

$$ds^2 = -d\hat{\eta}^2 + s^2(\hat{\eta}) \left[\frac{1}{1 - K(\hat{r})\hat{r}^2} d\hat{r}^2 + \hat{r}^2 \left(d\theta^2 + \sin^2 \theta d\phi^2 \right) \right], \quad (5.27)$$

where η is the conformal time, $s(\eta)$ is the scale factor for this metric. As we will show in the paragraph after Eq. (5.42), this is identical to the usual scale factor $a(\eta)$ of a flat Friedmann universe, only here we use a different notation to distinguish between metrics. Also, we write \hat{r} for the radial coordinate to distinguish it from the coordinate of the metric (5.1).

An advantage of working with this metric is that it contains the curvature profile $K(\hat{r})$ explicitly. We choose a set of coordinates with the origin at the centre of spherical symmetry and fix $K(0) = 1$. The condition that $K(\hat{r})$ is a local inhomogeneity requires that $K(\hat{r}) = 0$ for radii \hat{r} larger than the scale \hat{r}_0 where the metric matches the homogeneous FRW background.

In PM the profiles $K(\hat{r})$ are presented in two forms, one of which is characterised by two independent parameters α and Δ as

$$K(\hat{r}) = \left[1 + \alpha \frac{\hat{r}^2}{2\Delta^2} \right] \exp \left(-\frac{\hat{r}^2}{2\Delta^2} \right). \quad (5.28)$$

The parameter Δ describes the width of the Gaussian profile, while α parametrises linear deviations from this profile. The results of the numerical simulations in PM indicate that PBHs are formed in the region of the parameter space $[\alpha, \Delta]$ shown in Fig. 5.1a.

5.3.2 Physical criteria for the identification of parameters

We proceed to find the correspondence between the two sets of parameters, $[\mathcal{R}(0), \mathcal{R}''(0)]$ and $[\alpha, \Delta]$, both of which describe the initial curvature profiles. First let us note that the sets of coordinates $\{t, r\}$ and $\{\hat{\eta}, \hat{r}\}$ are those of the metrics (5.1) and (5.27), respectively. Thus we require a relationship between these set of coordinates too. Assuming that the size of the configuration, r_0 , is much larger than the Hubble radius, $r_H = H^{-1}$, we can use the gradient expansion of the functions in metrics (5.1) and (5.27). In this case, the time derivative of any function $f(t, r)$ is of order $f/t \sim Hf$ and significantly exceeds the spatial gradient which is of order f/r_0 . Hence the small parameter in the gradient expansion is

$$\varepsilon \equiv \frac{r_H}{r_0} = \frac{k}{aH}, \quad (5.29)$$

where k is the wave-number corresponding to the scale of the configuration.

For the metric (5.1), using the coordinate freedom to set $N^i = 0$ and ignoring any tensor

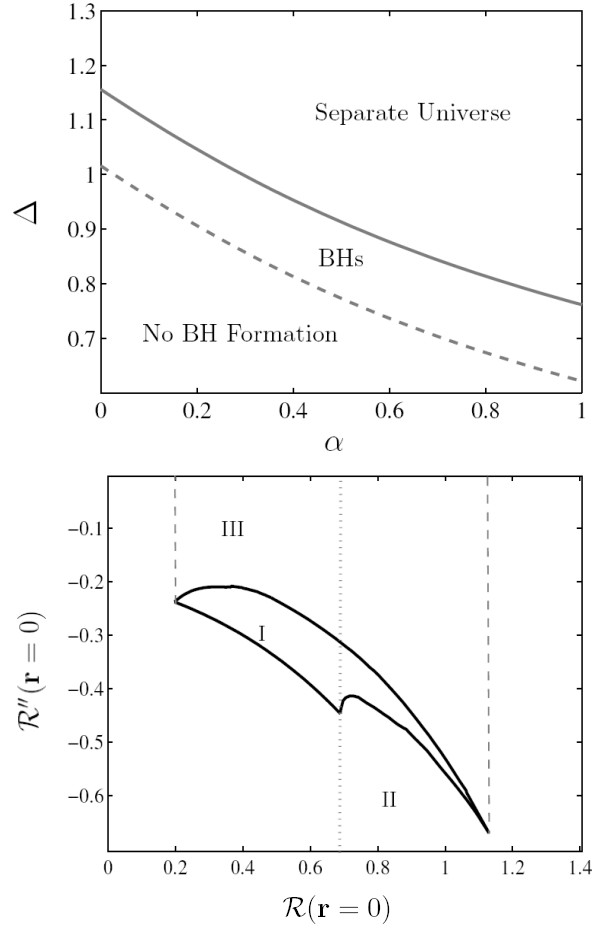


Figure 5.1: (a) The top plot shows the parameter values for initial configurations which collapse to form black holes according to Polnarev & Musco [2007]. (b) In the $[\mathcal{R}(0), \mathcal{R}''(0)]$ plane three regions of integration are considered to compute the probability of PBH formation. Area I is the region enclosed by the solid curves and corresponds to the area denoted by BH in Fig. 1a. Area II is the region to the right of the grey dotted line, representing the area of integration considered in previous studies where only the amplitude is taken into account. Area III is the region above the solid line and between the dashed lines. This contains those configurations which have a smooth profile in the centre and present the amplitudes $\mathcal{R}(0)$ that are found to form PBHs in [Polnarev & Musco, 2007]. The complete description of the physical characteristics of profiles with values in this region is given in Section 5.3.

contributions (i.e. $\tilde{\gamma}_{ij} = \delta_{ij}$), the expansion of the Einstein equation $G_0^0 = 8\pi GT_0^0$ to order ε^2 can be written as,¹¹

$$\frac{1}{2} \left(\frac{6\dot{a}^2}{a^2} + {}^{(3)}R - \frac{4\dot{a}^2}{a^2}(N-1) \right) + \mathcal{O}(\varepsilon^4) = 8\pi G(\rho_0 + \delta\rho) + \mathcal{O}(\varepsilon^4), \quad (5.30)$$

where ${}^{(3)}R$ is the spatial curvature, or the Ricci scalar for the spatial metric g_{ij} . To zero order

¹¹For the complete second order expansion of the metric quantities, see Lyth et al. [2005] and Langlois & Vernizzi [2005b].

in ε , we have

$$\frac{3\dot{a}^2}{a^2} = 8\pi G \rho_0, \quad (5.31)$$

which corresponds to the homogeneous part of Eq. (5.30). The time-slicing can be taken to be the uniform expansion gauge in which

$$N - 1 = -\frac{1 + 3w}{1 + w} \delta_\rho + \mathcal{O}(\varepsilon^4), \quad (5.32)$$

where w is the equation of state [Shibata & Asada, 1995; Shibata & Sasaki, 1999; Tanaka & Sasaki, 2007]. Using (5.30), (5.31) and (5.32), we find the equivalence between the spatial curvature and the matter overdensity:

$${}^{(3)}\mathbf{R} = \frac{8\pi G}{3} \delta_\rho \left(\frac{7 + 3w}{3 + 3w} \right). \quad (5.33)$$

In consequence, the gradients of this quantity relates to the pressure gradient:

$$\nabla {}^{(3)}\mathbf{R} = \frac{8\pi G}{3} \frac{7 + 3w}{3(w + 1)} \nabla (\delta_\rho) = \frac{8\pi G}{3} \left(\frac{7 + 3w}{3w(w + 1)} \right) \nabla p, \quad (5.34)$$

where $\nabla = (g_{rr})^{-1/2} d/dr$. Hence, subject to the two physical conditions at the edge of the configuration listed at the beginning of Section 5.3, we relate the profiles $\mathcal{R}(r)$ and $\mathbf{K}(\hat{r})$ by equating the spatial curvature and its gradient for the metrics (5.1) and (5.27). That is,

$${}^{(3)}\mathbf{R} = - \left[2\mathcal{R}''(r) + (\mathcal{R}'(r))^2 \right] \exp(-2\mathcal{R}(r)) = 3\mathbf{K}(\hat{r}) + \hat{r}\mathbf{K}'(\hat{r}), \quad (5.35)$$

and

$$\begin{aligned} & \frac{1}{\sqrt{g_{rr}}} \frac{d}{dr} ({}^{(3)}\mathbf{R}) = \\ & - [\mathcal{R}'\mathcal{R}'' + \mathcal{R}'''] \exp(-3\mathcal{R}(r)) = \left[\frac{1 - \mathbf{K}\hat{r}^2}{\hat{r}^2} \right]^{1/2} \left(2\hat{r}\mathbf{K}'(\hat{r}) + \frac{1}{2}\hat{r}^2\mathbf{K}''(\hat{r}) \right). \end{aligned} \quad (5.36)$$

By definition, the 3-curvature must vanish at the edge of the configuration, so Eq. (5.35)

implies

$$2\mathcal{R}''(r_0) + (\mathcal{R}'(r_0))^2 = 0 \quad (5.37)$$

and

$$3\mathbf{K}(\hat{r}_0) + \hat{r}_0\mathbf{K}'(\hat{r}_0) = 0. \quad (5.38)$$

Thus the gradient relation (5.36) can be written as

$$[\mathcal{R}'(r_0)^3 - 2\mathcal{R}'''(r_0)] \exp(-3\mathcal{R}(r_0)) = \left[\frac{1 - \mathbf{K}\hat{r}_0^2}{\hat{r}_0^2} \right]^{1/2} [-12\mathbf{K}(\hat{r}_0) + \hat{r}_0^2\mathbf{K}''(\hat{r}_0)]. \quad (5.39)$$

This establishes a relation between $\mathcal{R}(r)$ and $\mathbf{K}(\hat{r})$ at the edge points r_0 and \hat{r}_0 . The configuration $\mathbf{K}(\hat{r})$ is parametrised by $[\alpha, \Delta]$, as shown in Eq. (5.28). As follows from condition (5.38), the radius r_0 can be written in terms of those parameters as

$$\hat{r}_0^2 = \left(\frac{5\alpha - 2 + \sqrt{(5\alpha - 2)^2 - 24\alpha}}{2\alpha} \right) \Delta^2. \quad (5.40)$$

Then we use two more equations obtained from the conformal transformation of coordinates at zero order in ε :

$$a^2(\tau)e^{2\mathcal{R}(r)} dr^2 = s^2(\eta) \frac{d\hat{r}^2}{1 - \mathbf{K}(\hat{r})\hat{r}^2} \quad (5.41)$$

and

$$a^2(\tau) e^{2\mathcal{R}(r)} r^2 d\Omega^2 = s^2(\eta) \hat{r}^2 d\Omega^2. \quad (5.42)$$

Asymptotically, in the limit $[r, \hat{r}] \rightarrow \infty$, the homogeneous Einstein equations are identical in both metrics, therefore, the homogeneous scale factors $a(\tau)$ and $s(\eta)$ can be identified. Thus we find a relation between the radial coordinates,

$$e^{\mathcal{R}(r)} r = \hat{r}, \quad (5.43)$$

and an integral relation between the configurations,

$$\int_0^r e^{\mathcal{R}(x)} dx = \int_0^{\hat{r}} \frac{dx}{\sqrt{1 - \mathcal{K}(x)x^2}}. \quad (5.44)$$

One can verify that Eqs. (5.35), (5.36) and (5.44) are not independent. For example, Eq. (5.36) follows from (5.35) and (5.44).

In the previous section we have developed a method to account for the probability of any set of parameters describing the curvature profile. For simplicity we have chosen the pair $[\mathcal{R}(0), \mathcal{R}''(0)]$. We now illustrate how to relate $[\mathcal{R}(0), \mathcal{R}''(0)]$ and $[\alpha, \Delta]$ by considering the parabolic profile

$$\mathcal{R}(r) = \mathcal{R}(0) + \frac{1}{2}\mathcal{R}''(0)r^2. \quad (5.45)$$

This parametrisation meets the minimal requirement of covering the $[\alpha, \Delta]$ parameter space in Fig. 5.1 (a).

Eqs. (5.37), (5.44) and (5.43) are now reduced to the following system of algebraic equations:

$$r_0^2 = -\frac{2}{\mathcal{R}''(0)}, \quad (5.46)$$

$$\mathcal{R}(0) = 2 \log \left(\frac{2}{\text{erf}(1)} [\pi \exp(1)\hat{r}_0]^{-1/2} \int_0^{\hat{r}_0} \frac{dx}{(1 - \mathcal{K}(x)x^2)^{1/2}} \right), \quad (5.47)$$

$$\mathcal{R}''(0) = -2 \frac{\exp(2\mathcal{R}(0) - 2)}{\hat{r}_0^2}, \quad (5.48)$$

where \hat{r}_0 is given in terms of $[\alpha, \Delta]$ by Eq. (5.40).

5.3.3 Parameter values leading to PBH formation

The numerical computations of PM, which used the parametrisation (5.28), show that PBHs are formed in the $[\alpha, \Delta]$ region shown in Fig. 5.1(a). Eqs. (5.47) and (5.48) map this region to Area I in the $[\mathcal{R}(0), \mathcal{R}''(0)]$ plane shown in Fig. 5.1b. The Jacobian of the transformation corresponding to this mapping is non-vanishing, which guarantees a one-to-one correspondence of the ‘BH’ region in Fig. 5.1a with Area I in Fig. 5.1b. Each point here corresponds

to a parabolic profile which leads to PBH formation.

For each one of these parabolic profiles, there is a family of non-parabolic profiles with the same central amplitude $\mathcal{R}(0)$, the same configuration size r_0 , and the same behaviour near the edge, as shown in Fig. 5.2. In this figure, the profiles lying below the parabola correspond to larger absolute magnitudes of $\mathcal{R}''(0)$ and do not form PBHs because they have lower average gravitational field strength and higher average pressure gradient. The non-parabolic profiles which lie above the parabolic one (with smaller absolute magnitude $\mathcal{R}''(0)$) should also collapse to form PBHs because they correspond to higher average gravitational field strength and lower pressure gradient.

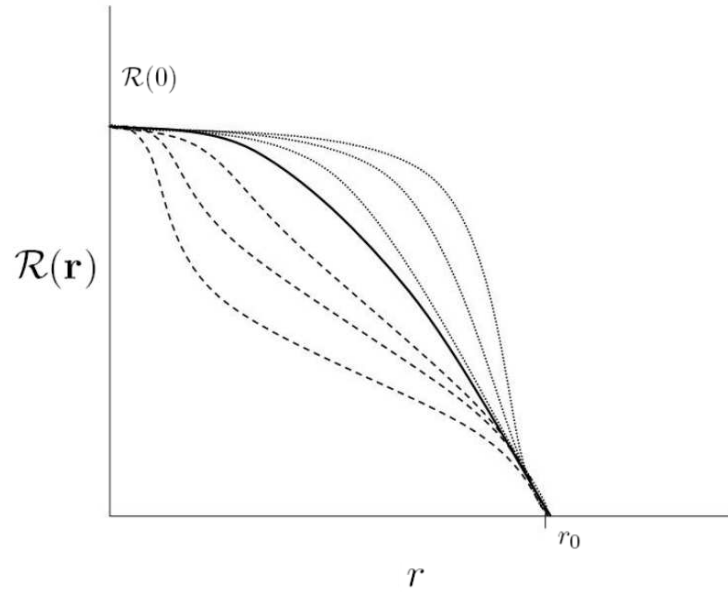


Figure 5.2: The curvature profile for three different families of configurations with common central amplitude $\mathcal{R}(0) = 1$. The configurations shown by the dashed lines have values of $\mathcal{R}''(0)$ larger in absolute magnitude than the parabolic one shown in black. The configurations shown by the dotted lines have values of $\mathcal{R}''(0)$ smaller than the parabolic one. All profiles satisfy conditions (5.37) and (5.39).

In the parameter space $[\mathcal{R}(0), \mathcal{R}''(0)]$, this last set of profiles corresponds to Area III in Fig. 5.1b. This region will be included in the calculation of the probability of PBH formation in the next section.

5.4 Two-parametric probability of PBH formation

To calculate the probability of PBH formation, which is equivalent to the mass fraction of the universe going into PBHs of given mass, it is customary to use the standard Press-Schechter formalism [Press & Schechter, 1974]. This has been widely used in previous calculations of the one parametric probability of PBH formation [Carr, 1975; Carr et al., 1994; Liddle & Green, 1998; Carr, 2005; Chongchitnan & Efstathiou, 2007; Zaballa et al., 2007]. When the probability depends on a single amplitude parameter, this method reduces to the integration of the corresponding PDF over the relevant perturbation amplitudes. The final integral is equivalent to the mass fraction of PBHs of mass [Carr, 1975]

$$M \sim w^{3/2} M_H \approx w^{3/2} k_M / (2\pi) \quad (5.49)$$

with the equation of state w measured at their formation time. Here we extend the standard Press-Schechter formalism to include for the first time an additional parameter accounting for the radial pressure in the initial configuration. When the $[\mathcal{R}'(0), \mathcal{R}''(0)]$ area is a square $[\mathcal{R}_1 < \mathcal{R}(0) < \mathcal{R}_2, \mathcal{R}_1'' < \mathcal{R}''(0) < \mathcal{R}_2'']$, the integrated two-parametric probability is

$$\begin{aligned} \beta_{\text{PBH}}(M) = 2 \int_{\mathcal{R}_1}^{\mathcal{R}_2} d\vartheta_0 \int_{\mathcal{R}_1''}^{\mathcal{R}_2''} d\vartheta_2 \mathbb{P}(\vartheta_0, \vartheta_2) = \\ \frac{1}{2} \left[\text{erf} \left(\frac{\mathcal{R}_2}{\sqrt{2}\Sigma_{(2)}(M)} \right) - \text{erf} \left(\frac{\mathcal{R}_1}{\sqrt{2}\Sigma_{(2)}(M)} \right) \right] \times \\ \left[\text{erf} \left(\frac{\mathcal{R}_2''}{\sqrt{2}\Sigma_{(4)}(M)} \right) - \text{erf} \left(\frac{\mathcal{R}_1''}{\sqrt{2}\Sigma_{(4)}(M)} \right) \right]. \end{aligned} \quad (5.50)$$

We use this result to integrate numerically over a mesh of small squares covering each of the areas of the plane $[\mathcal{R}(0), \mathcal{R}''(0)]$ shown in Fig. 5.1b. The results of this integration for two different power-law spectra $\mathcal{P}_{\mathcal{R}}(k) \propto k^{n-1}$ are shown in Fig. 5.3.

From that figure we note that the probability function $\beta_{\text{PBH}}(M)$ has a maximum at a value of M_{max} that changes with the of the spectral index. This can be easily derived by computing the solution of $d\beta_{\text{PBH}}/dM = 0$. We find that this equation provides a formula for the value M_{max} which indeed depends sensitively on the spectral index n_s . Assuming

$n_s > 1$ we have:

$$M_{\max} = M_{\text{eq}} \frac{3\gamma}{2} \frac{P_{\text{eq}}}{\mathcal{R}_{\text{th}}^2} \exp\left(-\frac{2}{n_s - 1}\right), \quad (5.51)$$

where M_{eq} and P_{eq} are the Hubble mass and the power spectrum at the time of matter-radiation equivalence ($k_{\text{eq}} = 8.9 \times 10^{-2} \text{Mpc}^{-1}$), and γ is a factor of order unity that changes slightly with the value of n_s .

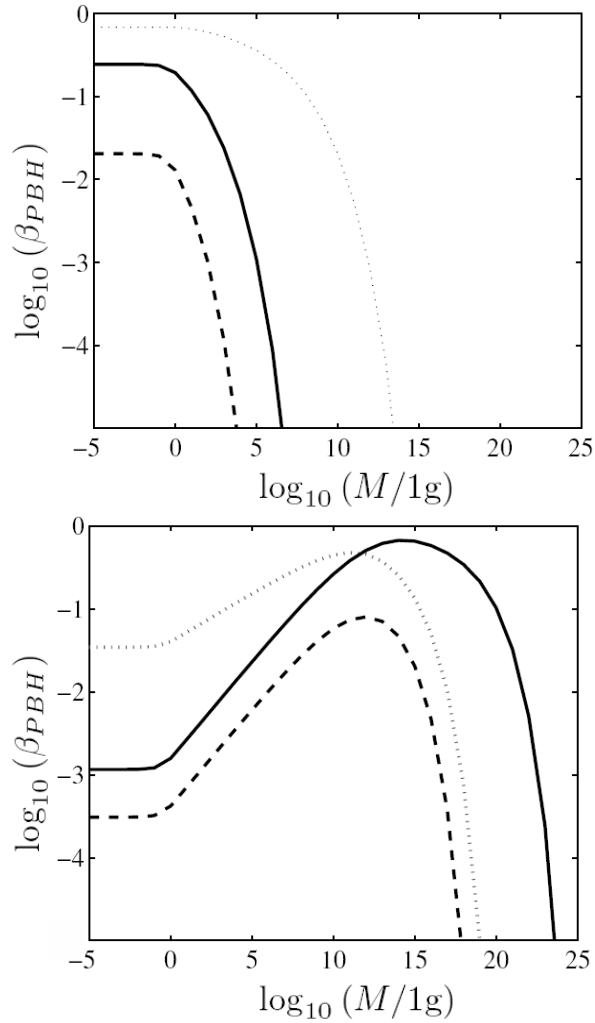


Figure 5.3: The logarithmic probability of PBHs for two tilts in the power spectrum ($n_s = 1.23$ on the top figure, $n_s = 1.47$ on the bottom figure), integrated for the three different regions sketched in Fig. 5.1. The integrals over Areas I and II correspond to the dashed and solid lines, respectively. The probability integrated over Area III is represented by the dotted lines in both figures.

We contrast the case of parabolic profiles described by Eq. (5.45) with the non-parabolic set presented in Fig. 5.2 by plotting the probability β_{PBH} for different values of $\mathcal{P}_{\mathcal{R}}$. This is

presented in Fig. 5.4. The figure shows that the probability of PBH formation can be larger than the one-parameter probability computed in previous studies from the integration of Area II [Green et al., 2004]. This important result requires confirmation from more detailed numerical simulations of PBH formation in this parameter area. The uncertainty is explained by the fact that the two-parametric calculation of the probability of PBH formation is still incomplete. This should be complemented in the future by the introduction of all relevant higher-order derivative parameters and the higher-order correlations in the PDF.

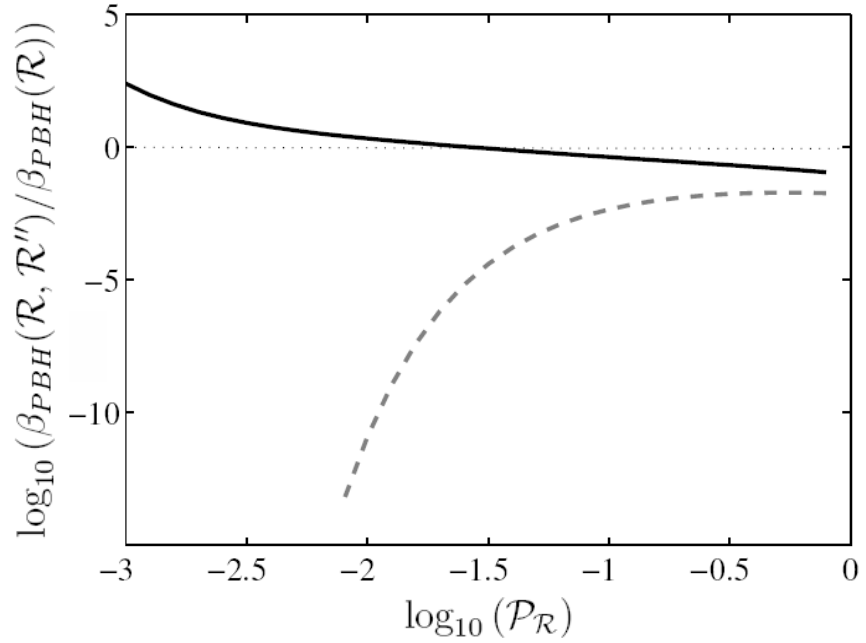


Figure 5.4: The grey dashed line shows the ratio of the total probability β_{PBH} which results from integrating over Area I on the $[\mathcal{R}(0), \mathcal{R}''(0)]$ parameter space of Fig. 1b to the probability which results from the integrating over Area II. The black line is the ratio of the probability integrated over Area III to the probability integrated over Area II.

5.5 Discussion

We have developed a method for calculating the two-parametric probability of PBH formation, taking into account the radial profiles of nonlinear curvature cosmological inhomogeneities. This is the first step towards calculating the N -parametric probability, which takes into account the radial profiles more precisely than studies using the amplitude as the only relevant parameter. We have incorporated the derived contribution to the total probability of

PBH formation by considering the range of values of $\mathcal{R}''(0)$ that will form PBHs, using the results of the numerical computations presented by Polnarev & Musco [2007]. Finally, we have provided an example of the consequences of this probability for the statistics of PBHs.

The results obtained show that, if we restrict ourselves to PBH formation from parabolic profiles (as described in Section 5.3), then the total PBH probability is orders of magnitude below previous estimates! On the other hand, if non-parabolic configurations are also included (see Fig. 5.2), the total probability of PBH formation is higher than the single-parametric probability estimated in previous works. In this case, we can impose new bounds on the power spectrum in the scales relevant for PBH formation. Analysing the uncertainty of our results, we have demonstrated how much we still have to understand about the formation and statistics of PBHs. The physical arguments supporting our results should be verified by numerical hydrodynamical simulations of PBH formation, which would provide a valuable feedback to the initial motivation of this work.

The main argument of this chapter is that the amplitude of initial inhomogeneities is not the only parameter which determines the probability of PBH formation. The ultimate solution of the problem requires a greater set of parameters and a larger range of their values to determine all high curvature configurations that form PBHs. This is a huge task for future research. In the meantime, we have a method to operate with the statistics of all these parameters.

Chapter 6

Conclusions and future work

In this thesis we have presented a study of large inhomogeneities in the early universe. Such large concentrations of matter may collapse to form primordial black holes (PBHs). The number of PBHs in our universe is calculated by integrating the probability distribution function (PDF) of primordial inhomogeneities, this encoding all the statistical information of primordial inhomogeneities. The main objective of this thesis is to quantify the probability of PBH formation in the context of nonlinear perturbation theory. This represents a significant improvement in the study of large-amplitude inhomogeneities since, by definition, these are nonlinear.

The statistics of inhomogeneities are the point of contact between theory and observations. In theoretical studies the statistics of primordial fluctuations are studied in the framework of cosmological perturbation theory. Until recently, perturbation theory was restricted to consider only linear departures from the homogeneous background. Linear perturbations are Gaussian due to the independence of the perturbation modes. This is an excellent approximation to describe the structures observed in the universe. Indeed, observationally, only the variance, or second statistical moment, has been measured. However, the detailed observations of large-scale structure (LSS) and the cosmic microwave background (CMB) now allow us to test for corrections to the linear approximation. This motivates the study of extensions of linear perturbation theory. In particular, the non-Gaussianity of curvature fluctuations has been a subject of intense investigation.

6.1 Summary of results

In Chapter 2 we presented a brief introduction to cosmological perturbation theory within general relativity. We reviewed the basic results of this theory for the cosmological inflation paradigm. From the evolution equations, we identified the conditions under which curvature fluctuations can grow significantly at superhorizon scales. As shown in Eqs. (2.87) and (2.88), these conditions are mainly the presence of a non-adiabatic component in the matter field fluctuations. This has motivated several previous studies of non-Gaussianity resulting from the second-order perturbations of an isocurvature (non-adiabatic) field χ . The conditions for inflation show that a non-adiabatic field is only a subdominant component of the total matter during inflation. The cosmological model in which χ is responsible for the curvature perturbations is called the curvaton model.

In Section 2.5 we calculated non-Gaussian correlators for some special cases of the curvaton model. The lowest order non-Gaussian signature is a non-vanishing skewness or third moment of the PDF. In perturbation theory this is equivalent to the correlation of three copies of the curvature perturbation field. This correlator itself is only present when we consider nonlinear perturbations. In order to derive the three-point correlator we have considered nonlinear field fluctuations $\delta\chi$. We have calculated the second order perturbations of a single isocurvature field during inflation and radiation domination. We have done this by solving the Klein-Gordon equation of the perturbation $\delta\chi$ to second order. For simplicity we consider only the matter fluctuations, assuming a large contribution from the third derivative of the potential $d^3W(\chi)/d\chi^3$. We find that an effectively massless field does not generate a large nonlinear contribution to the perturbation $\delta\chi$. Conversely, a slightly massive field allows an exponential growth of the nonlinear perturbation. With the aid of a new method to compute non-Gaussian correlators, we derived the field bispectrum $F(\mathbf{k}_i)$ given by Eq. (2.169). We then derived the curvature perturbation bispectrum $B(\mathbf{k}_i)$, considering a dominant contribution from the field bispectrum $F(\mathbf{k}_i)$. Equation (2.188) expresses the non-Gaussian parameter f_{NL} in terms of the elements of the potential $W(\chi)$. Chapter 2 closed with a brief discussion of the observational limits to the curvaton.

One of the main objectives of this thesis is to present the modified probability of structure formation from the non-Gaussian PDF. From the central limit theorem, we know that the non-Gaussian PDF produces non-trivial moments of order higher than two. To determine the shape of the distribution uniquely, one requires the *a priori* knowledge of all moments. From studies of non-Gaussianity in perturbation theory, however, we only know the skewness (third moment) and kurtosis (fourth moment) of some models of structure formation. Finding a PDF which encodes the contribution of only these two higher order moments is not trivial. In Chapter 3 we have constructed, in the context of quantum field theory, the general non-Gaussian PDF for curvature perturbations \mathcal{R} . Formally, this is a probability functional for the ensemble of realisations of $\mathcal{R}(\mathbf{x})$ at some specified time t . We refer to this probability as $\mathbb{P}_t[\mathcal{R}]$. We first derived a mathematical expression of the above statement by writing $\mathbb{P}_t[\mathcal{R}]$ in terms of the n -point correlation functions (see Eqs. (3.12) and (3.15)). We then constructed an explicit expression for the PDF using only the first three statistical moments.

We found that, in order to calculate the PDF, it is necessary to consider a regularised function $\bar{\mathcal{R}}(\mathbf{k})$. We must therefore consider a field sufficiently smooth on small scales, with a smoothing scale customarily set as the horizon scale at time t . We also require an upper limit for the k -numbers in order to avoid divergences in the integrations required to construct the PDF. This is achieved by artificially compactifying the momentum space over a scale $\Lambda > k$. This regularisation is a common requirement of calculations in the theory of perturbations and in the statistics of LSS. The results of this chapter are important because the final expression is an explicit functional probability $\mathbb{P}_t[\mathcal{R}(\mathbf{k})]$. This means that the probability of any parameter appearing in the function $\mathcal{R}(\mathbf{k})$, or equivalently $\mathcal{R}(\mathbf{x})$, can be retrieved from this PDF. We rely on this property to study two important modifications of the probability of PBH formation in the subsequent Chapter 4 and Chapter 5.

In the last two chapters of this thesis we revisit the calculation of the probability of PBH formation, taking into account two important effects which are characteristic of nonlinear inhomogeneities. In Chapter 4 we calculate the probability of PBHs using a non-Gaussian PDF we considered the non-Gaussian PDF of curvature perturbations \mathcal{R} . The featured PDF

includes a linear contribution from the three-point correlation function as derived in Chapter 3. In Section 4.2, this PDF was adapted to curvature configurations $\mathcal{R}(\mathbf{r})$ that give rise to PBHs. As previous works show, the amplitude at the centre of the curvature configuration $\mathcal{R}(\mathbf{r} = \mathbf{0})$ is a good parameter to determine the formation of PBHs. Eq. (4.12) gives the non-Gaussian PDF for the mentioned parameter. With the aid of this PDF we have reproduced qualitatively the effects of the non-Gaussian contribution considered in two previous works. We first identified the source of inconsistencies in previous works studying non-Gaussian effects in the probability of PBH formation. We showed that the fundamental difference in the inflationary models considered by Bullock & Primack [1997] and by Ivanov [1998] is the spectral index. In the first work, perturbations involve a blue power spectrum (for which the spectral index accomplishes $n_s - 1 > 0$), while the power spectrum is red ($n_s - 1 < 0$) in the second. Noting that, in single-field inflation, the non-Gaussian parameter f_{NL} is directly related to the spectral index $n_s - 1$, we have shown the source of the discrepancy. The main effect on the non-Gaussian PDF is the respective suppression and enhancement of the probability for large values of \mathcal{R} .

Chapter 4 also presented the non-Gaussian modifications to the probability of PBH formation (or the mass fraction of PBHs). In Section 4.4 we have shown how the new PDF can modify the bounds to the variance of curvature fluctuations $\Sigma_{\mathcal{R}}$. This comes from the observational limits to the abundance of PBH for each mass scale. Such modifications are illustrated in Fig. 5.4. Note that in this figure we have used the maximum value of the parameter f_{NL} allowed by perturbation theory. In the future, greater values could be considered by constructing PDFs with the techniques described here.

In Chapter 5 we have studied the probability of configurations $\mathcal{R}(\mathbf{x})$ from another perspective: We compute the probability of a parameter describing the curvature profile in addition to the probability of $\mathcal{R}(\mathbf{0})$. Specifically, we compute the probability of the second radial derivative at the centre of the configuration, $\mathcal{R}''(\mathbf{0}) = d^2\mathcal{R}/dr^2|_{\mathbf{r}=\mathbf{0}}$. As studied in that chapter, the consideration of additional parameters describing curvature profiles is a significant improvement in the study of gravitational collapse. In other words, the choice of initial

configurations collapsing to form PBHs relies on two sets of parameters. Parameters of the profile $\mathcal{R}(\mathbf{r})$ are required in addition to the amplitude parameters customarily used. We used the results of the latest simulations of PBH formation to integrate all the allowed configurations parametrised with the pair $[\mathcal{R}(0), \mathcal{R}''(0)]$. The result shows, heuristically, how the probability of PBH formation can be drastically changed by considering curvature profiles in the PDF.

6.2 Future research

The non-Gaussian signatures of cosmological inhomogeneities offer good prospects for model discrimination. An example of this is given at the end of Chapter 2, where we were able to limit special cases of the curvaton model with the observed constraints on the parameter f_{NL} . A number of extensions to this work are possible. First, the curvaton model can be adapted, with pertinent modifications, to describe models of modulated reheating [Zaldarriaga, 2004]. In such models, the auxiliary field modifies the expansion in different patches of the universe during the reheating process. The present work can be extended to cover such models by modifying the scales of the mass and expectation values of the auxiliary field χ . In this way one can search for feasible models of modulated reheating which satisfy the observational limits of non-Gaussianity.

Another application of our study is to compute higher-order correlations from the derived solutions to the nonlinear Klein-Gordon equation. Future probes of non-Gaussianity could detect the ‘trispectrum’ of curvature perturbations, which is a higher order discriminator between models of inflation. Computing the corresponding four-point function is thus crucial for a characterisation of the hypothetical detection of non-Gaussianity at this level.

An important complement of the work presented in Chapter 2 is the computation of the solutions to the Klein-Gordon equation allowing for metric perturbations. This has been ignored here because we assumed that the field fluctuations dominate over all other sources, as applies in the slow roll limit of the Klein-Gordon equation. As mentioned in Section 2.5, however, the curvature perturbation contribution (often called backreaction) may entail im-

portant corrections for $\delta\chi$ [see e.g. Malik [2007]]. It is important to compute such contributions because, on the one hand, they could be the dominating component in the growth of the fluctuations and, on the other hand, the curvature back-reaction could cancel large f_{NL} values. This could prompt reconsideration of models previously excluded by observations. Which case applies is an open question that should be addressed in the near future.

There is another set of problems where the methods of Chapter 3 find an important application. This is the determination stochastic sources in the evolution equations of classical fields. A functional probability is written in terms of products of the n -point correlation functions with n copies of the field configuration in Fourier space (see Eq.(3.15) for the case of curvature perturbations). This can be used, in particular, to derive and extend the stochastic equations of inflation by Starobinsky & Yokoyama [1994]. This seminal work presents a Fokker-Planck equation for the probability of the configuration $\phi(\mathbf{x})$ on small scales and for a single-field inflationary field. A first connection between the stochastic framework and the work presented here has been given by Seery [2009]. In that paper, a wave-functional similar to Eq. (3.13) is considered and the governing Hamiltonian operator for the scalar field ϕ is recovered from its action. The Fokker-Planck equation suggested by Starobinsky can be deduced easily from the Schrödinger equation for that wave-functional. Such a method can be extended to calculate PDFs of multi-scalar or non-canonical models of inflation. The construction of the probability distribution for configurations $\phi(\mathbf{x})$ and other possible fields allows for the consideration of full non-Gaussian distributions. This is clearly the way to go beyond approximations like the one considered in Chapter 3.

Regarding the probability of PBH formation, the results of Chapter 5 cannot be conclusive because we do not have at hand the complete set of collapsing configurations. Determining the set of all configurations collapsing to form PBHs is a huge task to be explored elsewhere. We can assert, however, that if PBHs are to be used as a tool for cosmology, the curvature profile parameters have to be taken into account in the derivation of the PDF. A less ambitious task is to have an estimate of how severe the modifications to the single-parameter approximation are. This would require the determination of more appropriate parameters

describing curvature profiles, a topic currently under investigation.

From the results of Chapter 4 we are able to set constraints on inflationary models. Specifically one can look at models with an enhancement of the power spectrum at small scales. In such cases, the constraints from PBHs can be more or less stringent, depending on the values and the sign of the non-Gaussian parameter f_{NL} . Here we have provided a tool for testing those models. Such tool can also be improved as more constraints are derived from observational tests to the abundance of PBHs.

References

- ACQUAVIVA, V., BARTOLO, N., MATARRESE, S. & RIOTTO, A., 2003. Second-order cosmological perturbations from inflation. *Nucl. Phys.*, **B667**, 119–148. [arXiv:astro-ph/0209156].
- ALABIDI, L. & LIDSEY, J. E., 2008. Single-Field Inflation After WMAP5. *Phys. Rev.*, **D78**, 103519. [arXiv:0807.2181].
- ALABIDI, L. & LYTH, D. H., 2006a. Inflation models after WMAP year three. *JCAP*, **0608**, 013. [arXiv:astro-ph/0603539].
- ALABIDI, L. & LYTH, D. H., 2006b. Inflation models and observation. *JCAP*, **0605**, 016. [arXiv:astro-ph/0510441].
- ALBEVERIO, S., JOST, J., PAYCHA, S. & SCARLATTI, S., 1997. *A Mathematical Introduction to String Theory*. Microgravity Science and Technology, Cambridge University Press.
- ALISHAHIHA, M., SILVERSTEIN, E. & TONG, D., 2004. DBI in the sky. *Phys. Rev.*, **D70**, 123505. [arXiv:hep-th/0404084].
- ALLEN, L. E., GUPTA, S. & WANDS, D., 2006. Non-Gaussian perturbations from multi-field inflation. *JCAP*, **0601**, 006. [arXiv:astro-ph/0509719].
- ALLEN, T. J., GRINSTEIN, B. & WISE, M. B., 1987. Non-gaussian density perturbations in inflationary cosmologies. *Phys. Lett.*, **B197**, 66.
- ARKANI-HAMED, N., CREMINELLI, P., MUKOHYAMA, S. & ZALDARRIAGA, M., 2004. Ghost inflation. *JCAP*, **0404**, 001. [arXiv:hep-th/0312100].
- ASTIER, P. ET AL., 2006. The Supernova Legacy Survey: Measurement of Ω_M , Ω_Λ and w from the First Year Data Set. *Astron. Astrophys.*, **447**, 31–48. [arXiv:astro-ph/0510447].
- BABICH, D., 2005. Optimal Estimation of Non-Gaussianity. *Phys. Rev.*, **D72**, 043003. [arXiv:astro-ph/0503375].
- BABICH, D., CREMINELLI, P. & ZALDARRIAGA, M., 2004. The shape of non-Gaussianities. *JCAP*, **0408**, 009. [arXiv:astro-ph/0405356].
- BABICH, D. & ZALDARRIAGA, M., 2004. Primordial Bispectrum Information from CMB Polarization. *Phys. Rev.*, **D70**, 083005. [arXiv:astro-ph/0408455].

- BARDEEN, J. M., 1980. Gauge Invariant Cosmological Perturbations. *Phys. Rev.*, **D22**, 1882–1905.
- BARDEEN, J. M., BOND, J. R., KAISER, N. & SZALAY, A. S., 1986. The Statistics of Peaks of Gaussian Random Fields. *Astrophys. J.*, **304**, 15–61.
- BARTOLO, N. & LIDDLE, A. R., 2002. The simplest curvaton model. *Phys. Rev.*, **D65**, 121301. [arXiv:astro-ph/0203076].
- BARTOLO, N., MATARRESE, S. & RIOTTO, A., 2004. Evolution of second-order cosmological perturbations and non-Gaussianity. *JCAP*, **0401**, 003. [arXiv:astro-ph/0309692].
- BENNETT, C. L. ET AL., 1996. 4-Year COBE DMR Cosmic Microwave Background Observations: Maps and Basic Results. *Astrophys. J.*, **464**, L1–L4. [arXiv:astro-ph/9601067].
- BERNARDEAU, F. & UZAN, J.-P., 2002. Non-Gaussianity in multi-field inflation. *Phys. Rev.*, **D66**, 103506. [arXiv:hep-ph/0207295].
- BERNARDEAU, F. & UZAN, J.-P., 2003. Inflationary models inducing non-gaussian metric fluctuations. *Phys. Rev.*, **D67**, 121301. [arXiv:astro-ph/0209330].
- BIRRELL, N. D. & DAVIES, P. C. W., 1984. *Quantum Fields in Curved Space*.
- BOUBEKEUR, L. & LYTH, D. H., 2006. Detecting a small perturbation through its non-Gaussianity. *Phys. Rev.*, **D73**, 021301. [arXiv:astro-ph/0504046].
- BUCHMULLER, W., DI BARI, P. & PLUMACHER, M., 2005. Leptogenesis for pedestrians. *Ann. Phys.*, **315**, 305–351. [arXiv:hep-ph/0401240].
- BUGAEV, E. & KLIMAI, P., 2006. Constraints on power spectrum of density fluctuations from PBH evaporations. [arXiv:astro-ph/0612659].
- BUGAEV, E. & KLIMAI, P., 2008. Large curvature perturbations near horizon crossing in single-field inflation models. [arXiv:0806.4541].
- BUGAEV, E. V. & KONISHCHEV, K. V., 2001. Extragalactic neutrino background from PBHs evaporation. [arXiv:astro-ph/0103265].
- BULLOCK, J. S. & PRIMACK, J. R., 1997. Non-Gaussian fluctuations and primordial black holes from inflation. *Phys. Rev.*, **D55**, 7423–7439. [arXiv:astro-ph/9611106].
- BUNCH, T. S. & DAVIES, P. C. W., 1988. *Quantum Field Theory in de Sitter Space: Renormalization by Point Splitting*, 673–+.
- BYRNES, C. T., KOYAMA, K., SASAKI, M. & WANDS, D., 2007. Diagrammatic approach to non-Gaussianity from inflation. *JCAP*, **0711**, 027. [arXiv:0705.4096].
- CABELLA, P. ET AL., 2006. The integrated bispectrum as a test of CMB non-Gaussianity: detection power and limits on f_{NL} with WMAP data. *MNRAS*, **369**, 819–824. [arXiv:astro-ph/0512112].

- CALCAGNI, G., 2005. Non-Gaussianity in braneworld and tachyon inflation. *JCAP*, **0510**, 009. [arXiv:astro-ph/0411773].
- CALDWELL, R. R. & CASPER, P., 1996. Formation of Black Holes from Collapsed Cosmic String Loops. *Phys. Rev.*, **D53**, 3002–3010. [arXiv:gr-qc/9509012].
- CALZETTA, E. & HU, B. L., 1987. Closed Time Path Functional Formalism in Curved Space- Time: Application to Cosmological Back Reaction Problems. *Phys. Rev.*, **D35**, 495.
- CARR, B. J., 1975. The Primordial black hole mass spectrum. *Astrophys. J.*, **201**, 1–19.
- CARR, B. J., 1976. Some cosmological consequences of primordial black-hole evaporations. *ApJ*, **206**, 8–25.
- CARR, B. J., 2003. Primordial black holes as a probe of cosmology and high energy physics. *Lect. Notes Phys.*, **631**, 301–321. [arXiv:astro-ph/0310838].
- CARR, B. J., 2005. Primordial black holes - recent developments. [arXiv:astro-ph/0504034].
- CARR, B. J., GILBERT, J. H. & LIDSEY, J. E., 1994. Black hole relics and inflation: Limits on blue perturbation spectra. *Phys. Rev.*, **D50**, 4853–4867. [arXiv:astro-ph/9405027].
- CARR, B. J. & HAWKING, S. W., 1974. Black holes in the early Universe. *MNRAS*, **168**, 399–415.
- CARR, B. J. & LIDSEY, J. E., 1993. Primordial black holes and generalized constraints on chaotic inflation. *Phys. Rev.*, **D48**, 543–553.
- CHONGCHITNAN, S. & EFSTATHIOU, G., 2007. Accuracy of slow-roll formulae for inflationary perturbations: Implications for primordial black hole formation. *JCAP*, **0701**, 011. [arXiv:astro-ph/0611818].
- CHRISTOPHERSON, A. J. & MALIK, K. A., 2009. The non-adiabatic pressure in general scalar field systems. *Phys. Lett.*, **B675**, 159–163. [arXiv:0809.3518].
- CLANCY, D., GUEDENS, R. & LIDDLE, A. R., 2003. Primordial black holes in braneworld cosmologies: Astrophysical constraints. *Phys. Rev.*, **D68**, 023507. [arXiv:astro-ph/0301568].
- CRAWFORD, M. & SCHRAMM, D. N., 1982. Spontaneous generation of density perturbations in the early universe. *nature*, **298**, 538–540.
- CREMINELLI, P., 2003. On non-gaussianities in single-field inflation. *JCAP*, **0310**, 003. [arXiv:astro-ph/0306122].
- CREMINELLI, P., NICOLIS, A., SENATORE, L., TEGMARK, M. & ZALDARRIAGA, M., 2006. Limits on non-Gaussianities from WMAP data. *JCAP*, **0605**, 004. [arXiv:astro-ph/0509029].
- CREMINELLI, P. & ZALDARRIAGA, M., 2004. Single field consistency relation for the 3-point function. *JCAP*, **0410**, 006. [arXiv:astro-ph/0407059].

- DERUELLE, N. & LANGLOIS, D., 1995. Long wavelength iteration of Einstein's equations near a space-time singularity. *Phys. Rev.*, **D52**, 2007–2019. [arXiv:gr-qc/9411040].
- DEWITT, B., 2003. *The Global Approach to Quantum Field Theory*. Oxford University Press.
- ENQVIST, K., JOKINEN, A., MAZUMDAR, A., MULTAMAKI, T. & VAIHKONEN, A., 2005a. Non-gaussianity from instant and tachyonic preheating. *JCAP*, **0503**, 010. [arXiv:hep-ph/0501076].
- ENQVIST, K., JOKINEN, A., MAZUMDAR, A., MULTAMAKI, T. & VAIHKONEN, A., 2005b. Non-Gaussianity from Preheating. *Phys. Rev. Lett.*, **94**, 161301. [arXiv:astro-ph/0411394].
- ENQVIST, K. & NURMI, S., 2005. Non-gaussianity in curvaton models with nearly quadratic potential. *JCAP*, **0510**, 013. [arXiv:astro-ph/0508573].
- ENQVIST, K. & SLOTH, M. S., 2002. Adiabatic CMB perturbations in pre big bang string cosmology. *Nucl. Phys.*, **B626**, 395–409. [arXiv:hep-ph/0109214].
- FALK, T., RANGARAJAN, R. & SREDNICKI, M., 1993. The Angular dependence of the three point correlation function of the cosmic microwave background radiation as predicted by inflationary cosmologies. *Astrophys. J.*, **403**, L1. [arXiv:astro-ph/9208001].
- FREEDMAN, W. L., MADORE, B. F., GIBSON, B. K., FERRARESE, L., KELSON, D. D., SAKAI, S., MOULD, J. R., KENNICUTT, JR., R. C., FORD, H. C., GRAHAM, J. A., HUCHRA, J. P., HUGHES, S. M. G., ILLINGWORTH, G. D., MACRI, L. M. & STETSON, P. B., 2001. Final Results from the Hubble Space Telescope Key Project to Measure the Hubble Constant. *ApJ*, **553**, 47–72. [arXiv:astro-ph/0012376].
- GANGUI, A., LUCCHIN, F., MATARRESE, S. & MOLLERACH, S., 1994. The Three point correlation function of the cosmic microwave background in inflationary models. *Astrophys. J.*, **430**, 447–457. [arXiv:astro-ph/9312033].
- GARRIGA, J. & SAKELLARIADOU, M., 1993. Effects of friction on cosmic strings. *Phys. Rev.*, **D48**, 2502–2515. [arXiv:hep-th/9303024].
- GREEN, A. M. & LIDDLE, A. R., 1997. Constraints on the density perturbation spectrum from primordial black holes. *Phys. Rev.*, **D56**, 6166–6174. [arXiv:astro-ph/9704251].
- GREEN, A. M., LIDDLE, A. R., MALIK, K. A. & SASAKI, M., 2004. A new calculation of the mass fraction of primordial black holes. *Phys. Rev.*, **D70**, 041502. [arXiv:astro-ph/0403181].
- GROSSI, M. ET AL., 2009. Large-scale non-Gaussian mass function and halo bias: tests on N-body simulations. [arXiv:0902.2013].
- GUTH, A. H., 1981. The Inflationary Universe: A Possible Solution to the Horizon and Flatness Problems. *Phys. Rev.*, **D23**, 347–356.
- GUTH, A. H. & PI, S. Y., 1982. Fluctuations in the New Inflationary Universe. *Phys. Rev. Lett.*, **49**, 1110–1113.

- HAJICEK, P., 1979. Time-loop formalism in quantum field theory. (TALK). In *Trieste 1979, Proceedings, General Relativity, Part A*, 483-491.
- HANANY, S., ADE, P., BALBI, A., BOCK, J., BORRILL, J. ET AL., 2000. MAXIMA-1: A Measurement of the Cosmic Microwave Background Anisotropy on Angular Scales of $10' - 5\text{deg}$. *Astrophys. J. Letters*, **545**, L5-L9. [arXiv:astro-ph/0005123].
- HARADA, T. & CARR, B. J., 2005. Upper limits on the size of a primordial black hole. *Phys. Rev.*, **D71**, 104009. [arXiv:astro-ph/0412134].
- HARRISON, E. R., 1970. Fluctuations at the threshold of classical cosmology. *Phys. Rev.*, **D1**, 2726-2730.
- HAWKE, I. & STEWART, J. M., 2002. The dynamics of primordial black hole formation. *Class. Quant. Grav.*, **19**, 3687-3707.
- HAWKING, S., 1971. Gravitationally collapsed objects of very low mass. *MNRAS*, **152**, 75-+.
- HAWKING, S. W., 1974. Black hole explosions. *Nature*, **248**, 30-31.
- HAWKING, S. W., 1977. Zeta Function Regularization of Path Integrals in Curved Space-Time. *Commun. Math. Phys.*, **55**, 133.
- HAWKING, S. W., 1982. The Development of Irregularities in a Single Bubble Inflationary Universe. *Phys. Lett.*, **B115**, 295.
- HAWKING, S. W., 1989. Black holes from cosmic strings. *Physics Letters B*, **231**, 237-239.
- HEAVENS, A., 2006. The quest for non-Gaussianity. In *CTC Workshop: Non-Gaussianity from inflation*.
- HIDALGO, J. C., 2007. The effect of non-Gaussian curvature perturbations on the formation of primordial black holes. [arXiv:0708.3875].
- HIDALGO, J. C. & POLNAREV, A. G., 2009. Probability of primordial black hole formation and its dependence on the radial profile of initial configurations. *Physical Review D (Particles, Fields, Gravitation, and Cosmology)*, **79**(4), 044006. [arXiv:0806.2752].
- HINSHAW, G. ET AL., 2007. Three-year Wilkinson Microwave Anisotropy Probe (WMAP) observations: Temperature analysis. *Astrophys. J. Suppl.*, **170**, 288. [arXiv:astro-ph/0603451].
- HU, W., 2001. Angular trispectrum of the cosmic microwave background. *Phys. Rev.*, **D64**, 083005. [arXiv:astro-ph/0105117].
- HU, W., SELJAK, U., WHITE, M. J. & ZALDARRIAGA, M., 1998. A Complete Treatment of CMB Anisotropies in a FRW Universe. *Phys. Rev.*, **D57**, 3290-3301. [arXiv:astro-ph/9709066].
- HU, W. & SUGIYAMA, N., 1995. Toward understanding CMB anisotropies and their implications. *Phys. Rev.*, **D51**, 2599-2630. [arXiv:astro-ph/9411008].

- IVANOV, P., 1998. Non-linear metric perturbations and production of primordial black holes. *Phys. Rev.*, **D57**, 7145–7154. [arXiv:astro-ph/9708224].
- JAFFE, A. H. ET AL., 2001. Cosmology from Maxima-1, Boomerang and COBE/DMR CMB Observations. *Phys. Rev. Lett.*, **86**, 3475–3479. [arXiv:astro-ph/0007333].
- JEDAMZIK, K., 1997. Primordial black hole formation during the QCD epoch. *Phys. Rev.*, **D55**, 5871–+. [arXiv:astro-ph/9605152].
- JOKINEN, A. & MAZUMDAR, A., 2006. Very Large Primordial Non-Gaussianity from multi-field: Application to Massless Preheating. *JCAP*, **0604**, 003. [arXiv:astro-ph/0512368].
- JORDAN, R. D., 1986. Effective Field Equations for Expectation Values. *Phys. Rev.*, **D33**, 444–454.
- JOSAN, A. S., GREEN, A. M. & MALIK, K. A., 2009. Generalised constraints on the curvature perturbation from primordial black holes. *ArXiv e-prints*. [arXiv:0903.3184].
- KHLOPOV, M. Y. & POLNAREV, A. G., 1980. PRIMORDIAL BLACK HOLES AS A COSMOLOGICAL TEST OF GRAND UNIFICATION. *Phys. Lett.*, **B97**, 383–387.
- KIM, H. I., LEE, C. H. & MACGIBBON, J. H., 1999. Diffuse gamma-ray background and primordial black hole constraints on the spectral index of density fluctuations. *Phys. Rev.*, **D59**, 063004. [arXiv:astro-ph/9901030].
- KINNEY, W. H., 2005. Horizon crossing and inflation with large eta. *Phys. Rev.*, **D72**, 023515. [arXiv:gr-qc/0503017].
- KLEINERT, H., 2004. *Path integrals in quantum mechanics, statistics polymer physics, and financial markets*.
- KODAMA, H. & SASAKI, M., 1984. Cosmological Perturbation Theory. *Prog. Theor. Phys. Suppl.*, **78**, 1–166.
- KOGO, N. & KOMATSU, E., 2006. Angular Trispectrum of CMB Temperature Anisotropy from Primordial Non-Gaussianity with the Full Radiation Transfer Function. *Phys. Rev.*, **D73**, 083007. [arXiv:astro-ph/0602099].
- KOLB, E. W. & TURNER, M. S., 1990. The Early universe. *Front. Phys.*, **69**, 1–547.
- KOMATSU, E. & SPERGEL, D. N., 2001. Acoustic signatures in the primary microwave background bispectrum. *Phys. Rev.*, **D63**, 063002. [arXiv:astro-ph/0005036].
- KOMATSU, E. ET AL., 2008. Five-Year Wilkinson Microwave Anisotropy Probe (WMAP) Observations: Cosmological Interpretation. [arXiv:0803.0547].
- LANDAU, L. D. & LIFSHITZ, E. M., 1975. *The classical theory of fields*. Course of theoretical physics - Pergamon International Library of Science, Technology, Engineering and Social Studies, Oxford: Pergamon Press, 1975, 4th rev.engl.ed.

- LANGLOIS, D. & VERNIZZI, F., 2004. Mixed inflaton and curvaton perturbations. *Phys. Rev.*, **D70**, 063522. [arXiv:astro-ph/0403258].
- LANGLOIS, D. & VERNIZZI, F., 2005a. Conserved non-linear quantities in cosmology. *Phys. Rev.*, **D72**, 103501. [arXiv:astro-ph/0509078].
- LANGLOIS, D. & VERNIZZI, F., 2005b. Evolution of non-linear cosmological perturbations. *Phys. Rev. Lett.*, **95**, 091303. [arXiv:astro-ph/0503416].
- LE BELLAC, M., 2000. *Thermal Field Theory*. Cambridge University Press.
- LIDDLE, A. R. & GREEN, A. M., 1998. Cosmological constraints from primordial black holes. *Phys. Rept.*, **307**, 125–131. [arXiv:gr-qc/9804034].
- LIDDLE, A. R. & LYTH, D. H., 1993. The Cold dark matter density perturbation. *Phys. Rept.*, **231**, 1–105. [arXiv:astro-ph/9303019].
- LIDDLE, A. R. & LYTH, D. H., 2000. *Cosmological Inflation and Large-Scale Structure*. Cambridge University Press.
- LIFSHITZ, E., 1946. On the Gravitational stability of the expanding universe. *J. Phys. (USSR)*, **10**, 116.
- LIFSHITZ, E. M. & KHALATNIKOV, I. M., 1963. Investigations in relativistic cosmology. *Adv. Phys.*, **12**, 185–249.
- LIGUORI, M., HANSEN, F. K., KOMATSU, E., MATARRESE, S. & RIOTTO, A., 2006. Testing Primordial Non-Gaussianity in CMB Anisotropies. *Phys. Rev.*, **D73**, 043505. [arXiv:astro-ph/0509098].
- LINDE, A. D. & MUKHANOV, V. F., 1997. Nongaussian isocurvature perturbations from inflation. *Phys. Rev.*, **D56**, 535–539. [arXiv:astro-ph/9610219].
- LOVERDE, M., MILLER, A., SHANDERA, S. & VERDE, L., 2008. Effects of Scale-Dependent Non-Gaussianity on Cosmological Structures. *JCAP*, **0804**, 014. [arXiv:0711.4126].
- LU, T. H.-C., ANANDA, K. & CLARKSON, C., 2008. Vector modes generated by primordial density fluctuations. *Phys. Rev.*, **D77**, 043523. [arXiv:0709.1619].
- LUKASH, V. N., 1980. Production of phonons in an isotropic universe. *Sov. Phys. JETP*, **52**, 807–814.
- LUO, X.-C. & SCHRAMM, D. N., 1993. Kurtosis, skewness, and nonGaussian cosmological density perturbations. *Astrophys. J.*, **408**, 33–42.
- LYTH, D. H., 1985. Large Scale Energy Density Perturbations and Inflation. *Phys. Rev.*, **D31**, 1792–1798.
- LYTH, D. H., 1992. Axions and inflation: Sitting in the vacuum. *Phys. Rev.*, **D45**, 3394–3404.

- LYTH, D. H., 2004. Can the curvaton paradigm accommodate a low inflation scale. *Phys. Lett.*, **B579**, 239–244. [arXiv:hep-th/0308110].
- LYTH, D. H., 2006. Non-gaussianity and cosmic uncertainty in curvaton-type models. *JCAP*, **0606**, 015. [arXiv:astro-ph/0602285].
- LYTH, D. H., MALIK, K. A. & SASAKI, M., 2005. A general proof of the conservation of the curvature perturbation. *JCAP*, **0505**, 004. [arXiv:astro-ph/0411220].
- LYTH, D. H., MALIK, K. A., SASAKI, M. & ZABALLA, I., 2006. Forming sub-horizon black holes at the end of inflation. *Journal of Cosmology and Astro-Particle Physics*, **1**, 11–+. [arXiv:astro-ph/0510647].
- LYTH, D. H. & RODRIGUEZ, Y., 2005a. Non-gaussianity from the second-order cosmological perturbation. *Phys. Rev.*, **D71**, 123508. [arXiv:astro-ph/0502578].
- LYTH, D. H. & RODRIGUEZ, Y., 2005b. The inflationary prediction for primordial non-gaussianity. *Phys. Rev. Lett.*, **95**, 121302. [arXiv:astro-ph/0504045].
- LYTH, D. H. & WANDS, D., 2002. Generating the curvature perturbation without an inflaton. *Phys. Lett.*, **B524**, 5–14. [arXiv:hep-ph/0110002].
- LYTH, D. H. & ZABALLA, I., 2005. A Bound Concerning Primordial Non-Gaussianity. *JCAP*, **0510**, 005. [arXiv:astro-ph/0507608].
- MACGIBBON, J. H. & CARR, B. J., 1991. Cosmic rays from primordial black holes. *Astrophys. J.*, **371**, 447–469.
- MACK, K. J. & WESLEY, D. H., 2008. Primordial black holes in the Dark Ages: Observational prospects for future 21cm surveys. [arXiv:0805.1531].
- MALDACENA, J. M., 2003. Non-Gaussian features of primordial fluctuations in single field inflationary models. *JHEP*, **05**, 013. [arXiv:astro-ph/0210603].
- MALIK, K. A., 2001. Cosmological perturbations in an inflationary universe. [arXiv:astro-ph/0101563].
- MALIK, K. A., 2007. A not so short note on the Klein-Gordon equation at second order. *JCAP*, **0703**, 004. [arXiv:astro-ph/0610864].
- MALIK, K. A. & LYTH, D. H., 2006. A numerical study of non-gaussianity in the curvaton scenario. *JCAP*, **0609**, 008. [arXiv:astro-ph/0604387].
- MALIK, K. A. & WANDS, D., 2004. Evolution of second order cosmological perturbations. *Class. Quant. Grav.*, **21**, L65–L72. [arXiv:astro-ph/0307055].
- MALIK, K. A. & WANDS, D., 2008. Cosmological perturbations. [arXiv:0809.4944].

- MARTIN, J., 2008. Quintessence: a mini-review. *Mod. Phys. Lett.*, **A23**, 1252–1265. [arXiv:0803.4076].
- MATARRESE, S., VERDE, L. & JIMENEZ, R., 2000. The Abundance of High-Redshift Objects as a Probe of Non-Gaussian Initial Conditions. *ApJ*, **541**, 10–24. [arXiv:astro-ph/0001366].
- MATSUDA, T., 2006. Primordial black holes from cosmic necklaces. *JHEP*, **04**, 017. [arXiv:hep-ph/0509062].
- MIYAMA, S. & SATO, K., 1978. THE UPPER BOUND OF THE NUMBER DENSITY OF PRIMORDIAL BLACK HOLES FROM THE BIG BANG NUCLEOSYNTHESIS. *Prog. Theor. Phys.*, **59**, 1012.
- MOLLERACH, S., 1990. Isocurvature baryon perturbations and inflation. *Phys. Rev.*, **D42**, 313–325.
- MOLLERACH, S., MATARRESE, S. & LUCCHIN, F., 1994. Blue perturbation spectra from inflation. *Phys. Rev.*, **D50**, 4835–4841. [arXiv:astro-ph/9309054].
- MOROI, T. & TAKAHASHI, T., 2001. Effects of cosmological moduli fields on cosmic microwave background. *Phys. Lett.*, **B522**, 215–221. [arXiv:hep-ph/0110096].
- MORSE, P. M. & FESHBACH, H., 1953. *Methods of theoretical physics*. International Series in Pure and Applied Physics, New York: McGraw-Hill, 1953.
- MUKHANOV, V. F., 1988. Quantum Theory of Gauge Invariant Cosmological Perturbations. *Sov. Phys. JETP*, **67**, 1297–1302.
- MUSCO, I., MILLER, J. C. & REZZOLLA, L., 2005. Computations of primordial black hole formation. *Class. Quant. Grav.*, **22**, 1405–1424. [arXiv:gr-qc/0412063].
- MUSSO, M., 2006. A new diagrammatic representation for correlation functions in the in-in formalism. [arXiv:hep-th/0611258].
- NADEZHIN, D. K., NOVIKOV, I. D. & POLNAREV, A. G., 1978. The hydrodynamics of primordial black hole formation. *Soviet Astronomy*, **22**, 129–138.
- NETTERFIELD, C. B. ET AL., 2002. A measurement by BOOMERANG of multiple peaks in the angular power spectrum of the cosmic microwave background. *Astrophys. J.*, **571**, 604–614. [arXiv:astro-ph/0104460].
- NIEMEYER, J. C. & JEDAMZIK, K., 1998. Near-Critical Gravitational Collapse and the Initial Mass Function of Primordial Black Holes. *Phys. Rev. Lett.*, **80**, 5481–5484. [arXiv:astro-ph/9709072].
- NIEMEYER, J. C. & JEDAMZIK, K., 1999. Dynamics of Primordial Black Hole Formation. *Phys. Rev.*, **D59**, 124013. [arXiv:astro-ph/9901292].
- NOVIKOV, I. D., POLNAREV, A. G., STAROBINSKII, A. A. & ZELDOVICH, I. B., 1979. Primordial black holes. *AA*, **80**, 104–109.

- OKAMOTO, T. & HU, W., 2002. The Angular Trispectra of CMB Temperature and Polarization. *Phys. Rev.*, **D66**, 063008. [arXiv:astro-ph/0206155].
- PAGE, D. N. & HAWKING, S. W., 1976. Gamma rays from primordial black holes. *Astrophys. J.*, **206**, 1–7.
- PEACOCK, J. A. & HEAVENS, A. F., 1990. Alternatives to the Press-Schechter cosmological mass function. *MNRAS*, **243**, 133–143.
- PEEBLES, P. J. E., 1980. *The large-scale structure of the universe*.
- PEEBLES, P. J. E. & YU, J. T., 1970. Primeval adiabatic perturbation in an expanding universe. *Astrophys. J.*, **162**, 815–836.
- PEIRIS, H. V. & EASTHER, R., 2008. Primordial Black Holes, Eternal Inflation, and the Inflationary Parameter Space after WMAP5. *JCAP*, **0807**, 024. [arXiv:0805.2154].
- PENZIAS, A. A. & WILSON, R. W., 1965. A Measurement of excess antenna temperature at 4080-Mc/s. *Astrophys. J.*, **142**, 419–421.
- PERCIVAL, W. J. ET AL., 2007. Measuring the Baryon Acoustic Oscillation scale using the SDSS and 2dFGRS. *Mon. Not. Roy. Astron. Soc.*, **381**, 1053–1066. [arXiv:0705.3323].
- PESKIN, M. E. & SCHROEDER, D. V., 1995. *An Introduction to Quantum Field Theory*. Westview Press.
- PINA AVELINO, P., 2005. Primordial black hole constraints on non-gaussian inflation models. *Phys. Rev.*, **D72**, 124004. [arXiv:astro-ph/0510052].
- POLCHINSKI, J., 1998. *String Theory*. Cambridge, UK: Cambridge University Press.
- POLNAREV, A. & ZEMBOWICZ, R., 1991. Formation of primordial black holes by cosmic strings. *Phys. Rev. D*, **43**(4), 1106–1109.
- POLNAREV, A. G. & MUSCO, I., 2007. Curvature profiles as initial conditions for primordial black hole formation. *Class. Quant. Grav.*, **24**, 1405–1432. [arXiv:gr-qc/0605122].
- PRESS, W. H. & SCHECHTER, P., 1974. Formation of galaxies and clusters of galaxies by selfsimilar gravitational condensation. *Astrophys. J.*, **187**, 425–438.
- PYNE, T. & CARROLL, S. M., 1996. Higher-Order Gravitational Perturbations of the Cosmic Microwave Background. *Phys. Rev.*, **D53**, 2920–2929. [arXiv:astro-ph/9510041].
- RIESS, A. G. ET AL., 2007. New Hubble Space Telescope Discoveries of Type Ia Supernovae at $z > 1$: Narrowing Constraints on the Early Behavior of Dark Energy. *Astrophys. J.*, **659**, 98–121. [arXiv:astro-ph/0611572].
- RIGOPOULOS, G. I. & SHELLARD, E. P. S., 2005. Non-linear inflationary perturbations. *JCAP*, **0510**, 006. [arXiv:astro-ph/0405185].

- RIGOPOULOS, G. I., SHELLARD, E. P. S. & VAN TENT, B. J. W., 2006a. Large non-Gaussianity in multiple-field inflation. *Phys. Rev.*, **D73**, 083522. [arXiv:astro-ph/0506704].
- RIGOPOULOS, G. I., SHELLARD, E. P. S. & VAN TENT, B. J. W., 2006b. Non-linear perturbations in multiple-field inflation. *Phys. Rev.*, **D73**, 083521. [arXiv:astro-ph/0504508].
- RIGOPOULOS, G. I., SHELLARD, E. P. S. & VAN TENT, B. J. W., 2007. Quantitative bispectra from multifield inflation. *Phys. Rev.*, **D76**, 083512. [arXiv:astro-ph/0511041].
- RIVERS, R. J., 1988. *Path Integral Methods in Quantum Field Theory*. Cambridge, UK: Cambridge University Press.
- RUBIN, S. G., SAKHAROV, A. S. & KHLOPOV, M. Y., 2001. The Formation of Primary Galactic Nuclei during Phase Transitions in the Early Universe. *Soviet Journal of Experimental and Theoretical Physics*, **92**, 921–929. [arXiv:hep-ph/0106187].
- SACHS, R. K. & WOLFE, A. M., 1967. Perturbations of a cosmological model and angular variations of the microwave background. *Astrophys. J.*, **147**, 73–90.
- SALOPEK, D. S. & BOND, J. R., 1990. Nonlinear evolution of long wavelength metric fluctuations in inflationary models. *Phys. Rev.*, **D42**, 3936–3962.
- SASAKI, M., 1986. Large Scale Quantum Fluctuations in the Inflationary Universe. *Prog. Theor. Phys.*, **76**, 1036.
- SASAKI, M. & STEWART, E. D., 1996. A General analytic formula for the spectral index of the density perturbations produced during inflation. *Prog. Theor. Phys.*, **95**, 71–78. [arXiv:astro-ph/9507001].
- SASAKI, M. & TANAKA, T., 1998. Super-horizon scale dynamics of multi-scalar inflation. *Prog. Theor. Phys.*, **99**, 763–782. [arXiv:gr-qc/9801017].
- SASAKI, M., VALIVIITA, J. & WANDS, D., 2006. Non-gaussianity of the primordial perturbation in the curvaton model. *Phys. Rev.*, **D74**, 103003. [arXiv:astro-ph/0607627].
- SCHWINGER, J. S., 1961. Brownian motion of a quantum oscillator. *J. Math. Phys.*, **2**, 407–432.
- SCOCCIMARRO, R., SEFUSATTI, E. & ZALDARRIAGA, M., 2004. Probing Primordial Non-Gaussianity with Large-Scale Structure. *Phys. Rev.*, **D69**, 103513. [arXiv:astro-ph/0312286].
- SEERY, D., 2008. One-loop corrections to the curvature perturbation from inflation. *JCAP*, **0802**, 006. [arXiv:0707.3378].
- SEERY, D., 2009. A parton picture of de Sitter space during slow-roll inflation. [arXiv:0903.2788].
- SEERY, D. & HIDALGO, J. C., 2006. Non-Gaussian corrections to the probability distribution of the curvature perturbation from inflation. *JCAP*, **0607**, 008. [arXiv:astro-ph/0604579].

- SEERY, D. & LIDSEY, J. E., 2005a. Primordial non-gaussianities from multiple-field inflation. *JCAP*, **0509**, 011. [arXiv:astro-ph/0506056].
- SEERY, D. & LIDSEY, J. E., 2005b. Primordial non-gaussianities in single field inflation. *JCAP*, **0506**, 003. [arXiv:astro-ph/0503692].
- SEERY, D., MALIK, K. A. & LYTH, D. H., 2008. Non-gaussianity of inflationary field perturbations from the field equation. *JCAP*, **0803**, 014. [arXiv:0802.0588].
- SENDOUDA, Y., NAGATAKI, S. & SATO, K., 2006. Mass spectrum of primordial black holes from inflationary perturbation in the Randall-Sundrum braneworld: A limit on blue spectra. *JCAP*, **0606**, 003. [arXiv:astro-ph/0603509].
- SHIBATA, M. & ASADA, H., 1995. PostNewtonian equations of motion in the flat universe. *Prog. Theor. Phys.*, **94**, 11–31.
- SHIBATA, M. & SASAKI, M., 1999. Black hole formation in the Friedmann universe: Formulation and computation in numerical relativity. *Phys. Rev.*, **D60**, 084002. [arXiv:gr-qc/9905064].
- SLOTH, M. S., 2006. On the one loop corrections to inflation and the CMB anisotropies. *Nucl. Phys.*, **B748**, 149–169. [arXiv:astro-ph/0604488].
- SMITH, K. M., SENATORE, L. & ZALDARRIAGA, M., 2009. Optimal limits on $f_{\text{NL}}^{\text{local}}$ from WMAP 5-year data. *ArXiv e-prints*. [arXiv:0901.2572].
- SMOOT, G. F. E. A., 1992. Structure in the COBE differential microwave radiometer first year maps. *Astrophys. J.*, **396**, L1–L5.
- SPERGEL, D. N. ET AL., 2007. Wilkinson Microwave Anisotropy Probe (WMAP) three year results: Implications for cosmology. *Astrophys. J. Suppl.*, **170**, 377. [arXiv:astro-ph/0603449].
- STAROBINSKY, A. A., 1982. Dynamics of Phase Transition in the New Inflationary Universe Scenario and Generation of Perturbations. *Phys. Lett.*, **B117**, 175–178.
- STAROBINSKY, A. A., 1985. Multicomponent de Sitter (Inflationary) Stages and the Generation of Perturbations. *JETP Lett.*, **42**, 152–155.
- STAROBINSKY, A. A., 1986. Stochastic de Sitter (inflationary) Stage in the Early Universe. In H. J. de Veta & N. Sánchez, eds., *Field Theory, Quantum Gravity and Strings*, vol. 246 of *Lecture Notes in Physics*, Berlin Springer Verlag, 107–+.
- STAROBINSKY, A. A. & YOKOYAMA, J., 1994. Equilibrium state of a selfinteracting scalar field in the De Sitter background. *Phys. Rev.*, **D50**, 6357–6368. [arXiv:astro-ph/9407016].
- STEWART, E. D. & LYTH, D. H., 1993. A More accurate analytic calculation of the spectrum of cosmological perturbations produced during inflation. *Phys. Lett.*, **B302**, 171–175. [arXiv:gr-qc/9302019].

- STREATER, R. & WIGHTMAN, A., 2000. *PCT, Spin and Statistics and All That*. Princeton University Press.
- TABENSKY, R. & TAUB, A. H., 1973. Plane symmetric self-gravitating fluids with pressure equal to energy density. *Commun. Math. Phys.*, **29**, 61–77.
- TANAKA, Y. & SASAKI, M., 2007. Gradient expansion approach to nonlinear superhorizon perturbations. *Prog. Theor. Phys.*, **117**, 633–654. [arXiv:gr-qc/0612191].
- TAYLOR, A. & WATTS, P., 2000. Evolution of the cosmological density distribution function. [arXiv:astro-ph/0001118].
- VERDE, L. & HEAVENS, A. F., 2001. On the trispectrum as a gaussian test for cosmology. [arXiv:astro-ph/0101143].
- VERDE, L., JIMENEZ, R., KAMIONKOWSKI, M. & MATARRESE, S., 2001. Tests for primordial non-Gaussianity. *MNRAS*, **325**, 412. [arXiv:astro-ph/0011180].
- VERDE, L., WANG, L., HEAVENS, A. F. & KAMIONKOWSKI, M., 2000. Large-scale structure, the cosmic microwave background and primordial non-Gaussianity. *Mon. Not. Roy. Astron. Soc.*, **313**, 141–147. [arXiv:astro-ph/9906301].
- VERDE, L., WANG, L.-M., HEAVENS, A. & KAMIONKOWSKI, M., 2000. Large-scale structure, the cosmic microwave background, and primordial non-gaussianity. *MNRAS*, **313**, L141–L147. [arXiv:astro-ph/9906301].
- VERNIZZI, F. & WANDS, D., 2006. Non-Gaussianities in two-field inflation. *JCAP*, **0605**, 019. [arXiv:astro-ph/0603799].
- VISSER, M., 1996. *Lorentzian Wormholes*. From Einstein to Hawking, 412 pp. AIP Press.
- WALD, R. M., 1984. *General relativity*.
- WANDS, D., MALIK, K. A., LYTH, D. H. & LIDDLE, A. R., 2000. A new approach to the evolution of cosmological perturbations on large scales. *Phys. Rev.*, **D62**, 043527. [arXiv:astro-ph/0003278].
- WEINBERG, S., 2005. Quantum contributions to cosmological correlations. *Phys. Rev.*, **D72**, 043514. [arXiv:hep-th/0506236].
- WEINBERG, S., 2006. Quantum contributions to cosmological correlations. II: Can these corrections become large? *Phys. Rev.*, **D74**, 023508. [arXiv:hep-th/0605244].
- WYMAN, M., POGOSIAN, L. & WASSERMAN, I., 2005. Bounds on cosmic strings from WMAP and SDSS. *Phys. Rev.*, **D72**, 023513. [arXiv:astro-ph/0503364].
- YOKOYAMA, J., 1999. Formation of primordial black holes in inflationary cosmology. *Prog. Theor. Phys. Suppl.*, **136**, 338–352.

- ZABALLA, I., GREEN, A. M., MALIK, K. A. & SASAKI, M., 2007. Constraints on the primordial curvature perturbation from primordial black holes. *JCAP*, **0703**, 010. [arXiv:astro-ph/0612379].
- ZABALLA, I., RODRIGUEZ, Y. & LYTH, D. H., 2006. Higher order contributions to the primordial non- gaussianity. *JCAP*, **0606**, 013. [arXiv:astro-ph/0603534].
- ZABOTIN, N. A., NASELSKII, P. D. & POLNAREV, A. G., 1987. High-Amplitude Peaks of Density Disturbances and the Formation of Primordial Black-Holes in the Dust like Universe. *Soviet Astronomy*, **31**, 353–+.
- ZALDARRIAGA, M., 2004. Non-Gaussianities in models with a varying inflaton decay rate. *Phys. Rev.*, **D69**, 043508. [arXiv:astro-ph/0306006].
- ZELDOVICH, I. B. & NOVIKOV, I. D., 1983. *Relativistic astrophysics. Volume 2 - The structure and evolution of the universe /Revised and enlarged edition/*. Chicago, IL, University of Chicago Press, 1983, 751 p. Translation.
- ZELDOVICH, Y. B., 1972. A Hypothesis, unifying the structure and the entropy of the universe. *Mon. Not. Roy. Astron. Soc.*, **160**, 1P–3P.
- ZEL'DOVICH, Y. B. & NOVIKOV, I. D., 1966. The Hypothesis of Cores Retarded during Expansion and the Hot Cosmological Model. *azh*, **43**, 758–+.